

Ministry of Water Resources



Bangladesh Water Development Board

Coastal Embankment Improvement Project, Phase-I (CEIP-I)

Long Term Monitoring, Research and Analysis of Bangladesh Coastal Zone (Sustainable Polders Adapted to Coastal Dynamics)

Baleswar River: Meso scale bank erosion modelling - current situation & future projections



Joint Venture of



The expert in WATER ENVIRONMENTS

&



in association with IWM, Bangladesh and University of Colorado, Boulder and Columbia University

May 2022





**Ministry of Water Resources**



**Bangladesh Water Development Board**

Coastal Embankment Improvement Project, Phase-I (CEIP-I)

**Long Term Monitoring, Research and Analysis of Bangladesh Coastal Zone (Sustainable Polders Adapted to Coastal Dynamics)**

**Baleswar River: Meso scale bank erosion modelling - current situation & future projections**

May 2022

Joint Venture of



The expert in **WATER ENVIRONMENTS**

&



in association with



University of Colorado, Boulder, USA  
Columbia University, USA



## Long Term Monitoring, Research and Analysis of Bangladesh Coastal Zone

Office: Flat #3/B, House #4, Road #23/A, Banani, Dhaka 1213, BANGLADESH

Phone +880 1307 693299

Memo No: CEIP/LTMRA/0622/173

5 June 2022

Project Management Unit  
Coastal Embankment Improvement Project, Phase-I (CEIP-I)  
Pani Bhaban, Level-10  
72, Green Road, Dhaka-1205

**Attn: Mr. Syed Hasan Imam, Project Director**

Dear Mr Imam,

**Subject: Submission of the Baleswar River: Meso Scale Bank Erosion Modelling – current situation and future projections (D-4A-2:1,2&3)**

It is our pleasure to submit herewith five copies of the Report Titled “**Baleswar River: Meso Scale Bank Erosion Modelling – Current situation & future projections**”. According to the World Bank Tracker, this report falls under component **D-4A-2:1,2&3**.

This report includes both model development and applications. The model development report titled “Meso scale bank erosion modelling – current situation – interim report” was submitted earlier and was reviewed by the World Bank. DHI revised the interim report to address the review and extended to include future projections.

There are five chapters in this report. Chapter 1 is the introduction chapter describing the background, objective and approach. Chapter 2 gives an overview on the availability of measurement data and how the data was processed. The development and calibration/validation of the model are described in Chapter 3. Model applications are documented in chapter 4, while the report finalizes with conclusions in Chapter 5.

Thanking you,

Yours sincerely,



Dr Ranjit Galappatti  
Team Leader

Copies: Engineer Fazlur Rashid, Director General, BWDB  
Dr. Zia Uddin Baig, ADG (Planning), BWDB  
Dr Kim Wium Olesen, Project Manager, DHI  
Ms. Sonja Pans, Deltares Project Manager  
Mr Zahirul Haque Khan, Deputy Team Leader  
Mr AKM Bodruddoza, Procurement Specialist  
Swarna Kazi, Sr. Disaster Risk Management Specialist, World Bank



# CONTENTS

<b>1</b>	<b>Introduction.....</b>	<b>1</b>
1.1	Background .....	1
1.2	Objective and Approach.....	3
1.3	This report .....	4
1.4	General definitions .....	5
1.5	Important note regarding MIKE 21C version.....	5
<b>2</b>	<b>Data.....</b>	<b>7</b>
2.1	Bathymetry .....	7
2.2	Hydrometric time-series .....	9
2.3	Sediment bed samples.....	10
2.4	Suspended sediment data .....	14
2.5	Suspended sediment particle size distribution data.....	16
2.6	Historical bank lines from satellite imagery.....	17
2.7	Subsidence.....	21
<b>3</b>	<b>Model development .....</b>	<b>23</b>
3.1	Grid and bathymetry.....	23
3.1.1	2011 model grid and bathymetry.....	23
3.1.2	2019 model grid and bathymetry.....	26
3.2	Hydrodynamic boundary conditions .....	27
3.3	Hydrodynamic boundary conditions for scenario simulations .....	30
3.4	Hydrodynamic calibration and validation .....	31
3.4.1	Hydrodynamic model calibration for 2011 .....	32
3.4.2	Hydrodynamic model validation for 2015.....	34
3.4.3	Hydrodynamic model validation for 2016.....	36
3.5	Sediment model .....	37
3.6	Sediment transport boundary conditions .....	38
3.7	Calibration against observed bed level changes .....	38
3.8	Longitudinal validations.....	41
3.9	Bank erosion model .....	43
3.10	Comparison of observed and simulated bank lines 2011-2019.....	44
<b>4</b>	<b>Model applications .....</b>	<b>47</b>
4.1	Dredging the shoal opposite of the eroding bank at the downstream tip of Polder 35/1 .....	47
4.2	Bank erosion forecast 30 years into the future .....	50
4.3	Impact of climate change on future bank erosion .....	56
4.4	Impact of bank protection.....	58
4.5	Impact of protecting all banks .....	62
4.6	Dredging of a large shoal .....	65
<b>5</b>	<b>Conclusions .....</b>	<b>71</b>
5.1	Recommended future data collection .....	72
5.2	Recommended model improvements .....	73
5.3	Conclusions from the scenario simulations.....	73
<b>6</b>	<b>References .....</b>	<b>75</b>

## FIGURES

Figure 1-1	Revetment along Baleswar River (photo 11 February 2019).....	2
Figure 1-2	The five MIKE 21C models developed for the project. ....	3
Figure 2-1	Observed bathymetries of Baleswar River from 2009, 2011, 2015 and 2019. ....	8
Figure 2-2	Observed bathymetries and bed level changes 2011-2015-2019. From left: 1) 2011 bathymetry, 2) 2015 bathymetry, 3) 2019 bathymetry, 4) bed level changes 2011-2015, 5) bed level changes 2015-2019, 6) bed level changes 2011-2019. ....	9
Figure 2-3	Measured sediment fractions in the Baleswar River.....	12
Figure 2-4	Particle size distribution of Baleswar River for 2011, 2017 and 2019.....	13
Figure 2-5	Suspended sediment concentration stations in Baleswar River. ....	15
Figure 2-6	Correlation between discharge and sediment concentration for the all the stations in Baleswar River. ....	16
Figure 2-7	Particle size distribution of Bholgang River joining the Baleswar River at Shawrankhola (IWM, 2001) .....	17
Figure 2-8	Locations of the 17 characteristic eroding banks along the Baleswar River based on digitized bank lines 1988, 1995, 2001, 2011, 2019. The bathymetry is based on the 2011 survey. The chainage coordinates (km) are shown along the river. ....	18
Figure 2-9	Observed west bank erosion 2011-2019 along Baleswar River as a function of chainage.....	19
Figure 2-10	Observed east bank erosion 2011-2019 along Baleswar River as a function of chainage. ....	19
Figure 2-11	Accumulated area curves associated with bank erosion and accretion along each bank and total for the period 2011-2019. ....	20
Figure 2-12	Estimated bank erosion accumulated bulk volume curves for Baleswar River 2011-2019 compared to the observed bathymetry changes bulk volume curve for the same period. ....	20
Figure 2-13	Subsidence spatial map in the area where the four models are located. ....	21
Figure 2-14	Subsidence interpolated to the Baleswar 2019 model grid.....	22
Figure 3-1	Baleswar River 792x20 curvilinear grid conforming to the 2011 bank lines. ....	24
Figure 3-2	Baleswar River 2011 bathymetry contoured on the curvilinear grid with the 2011 Landsat image as background.....	25
Figure 3-3	Baleswar River 2019 bathymetry on the 2019 grid with the 2019 Landsat image as background.....	26
Figure 3-4	Illustration of the differences between the 2011 and 2019 grids, which cannot be identified without looking at the details. This is just upstream of the Gashiakali inflow where the eastern bank has been eroding consistently. The 2019 grid conforms to the 2019 bank line, as seen in the figure. The bank line moved roughly 100 m from 2011 to 2019. ....	27
Figure 3-5	Baleswar River 2011 bathymetry, boundaries and chainages used for showing longitudinal variations. ....	28
Figure 3-6	Daily minimum, maximum and mean flows 2011-2019 upstream boundary (Swarupkati) in the Baleswar River model. It is noted that the Baleswar River model repeated the 2011 SWRM results for the period 2011-2019. ....	29
Figure 3-7	Daily minimum, maximum and mean flows 2018-2019 upstream boundary in the Baleswar River model for the two cases Base and Sub+CC.....	30
Figure 3-8	Daily minimum, maximum and mean water levels 2018-2019 downstream boundary in the Baleswar River model for the two cases Base and Sub+CC.....	30
Figure 3-9	Discharge and water level calibration locations for 2011.....	32
Figure 3-10	Discharge calibration at Chardoani during 2011 monsoon.....	33
Figure 3-11	Water level calibration at Chardoani during 2011 monsoon. ....	33
Figure 3-12	Water level calibration of BWDB station at Umedpur 2011 (6-hourly data).....	33
Figure 3-13	Locations of discharge and water level stations used for 2015 validation. ....	34
Figure 3-14	Discharge validation at Charkhali for 2015 (August), also showing the SWRM 2015 results. ....	35
Figure 3-15	Water level calibration at Tele Khali Bazar for 2015 (August). ....	35
Figure 3-16	Water level validation at Tafalbari Lanchghat for 2015 (August). ....	35
Figure 3-17	Discharge validation at Rayenda (Sarmasi) for 2016. ....	36
Figure 3-18	Comparison of observed and simulated bathymetry development 2011-2015. From left: Observed bathymetry 2011, Observed bathymetry 2015, Simulated bathymetry 2015, Observed bed level changes 2011-2015, Simulated bed level changes 2011-2015.....	39



Figure 3-19 Comparison of observed and simulated bathymetry development 2011-2019. From left: Observed bathymetry 2011, Observed bathymetry 2019, Simulated bathymetry 2019, Observed bed level changes 2011-2019, Simulated bed level changes 2011-2019.....40

Figure 3-20 Comparison of observed and simulated width-integrated bed level changes 2011-2015. ....41

Figure 3-21 Comparison of observed and simulated width-integrated bed level changes 2011-2019. ....41

Figure 3-22 Comparison of observed and simulated bulk volume curves for 2011-2015. The bulk volume curve for 2011-2015 bank erosion was not calculated. ....42

Figure 3-23 Comparison of observed and simulated bulk volume curves for 2011-2019. ....42

Figure 3-24 Observed and simulated west bank erosion for the Baleswar River model 2011-2019. ....44

Figure 3-25 Observed and simulated east bank erosion for the Baleswar River model 2011-2019. ....44

Figure 3-26 Observed bank lines 2011 and 2019 with four local areas shown, which are zoomed in the following. ....45

Figure 3-27 Bank lines 2011 (observed) and 2019 (observed and simulated) for the Baleswar River model in the four sub-areas. ....46

Figure 4-1 Historical bathymetry around the ebb channel (west) and flood channel (east). ....47

Figure 4-2 Historical bank line and planform changes around Polder 35/1. ....48

Figure 4-3 Bed level and bed level changes for base and shoal dredging option around Polder 35/1 .....48

Figure 4-4 Maximum current speed for base and shoal dredging option around Polder 35/1 .....49

Figure 4-5 Erosion of both banks from 2011 to 2012 in the Baleswar River (baseline and option). ....49

Figure 4-6 Bathymetries from various years, from left: 2011 (observed), 2019 (observed), 2034 (simulated), 2049 (simulated).....50

Figure 4-7 Width-integrated bed levels as a function of chainage in the Baleswar River for 2011 (observed), 2019 (observed), 2034 (simulated) and 2049 (simulated).....52

Figure 4-8 Minimum bed levels in the area between Polder 35/1 and 39/1. The observed bed levels were extracted from cross-sections, while the simulated bed levels were extracted from model results. Hence the comparison is not completely valid. ....52

Figure 4-9 Bank lines 2019 (observed), 2034 (simulated), 2049 (simulated). ....53

Figure 4-10 Comparison of bank lines digitized from Landsat 1988-2005-2019 and model results 2019-2034-2049. The bank lines hence cover comparable timescales and are shown in the very sharp bend in the middle of the Baleswar model. ....54

Figure 4-11 Comparison of bank lines digitized from Landsat 1988-2005-2019 and model results 2019-2034-2049. The bank lines hence cover comparable timescales and are shown in the downstream end close to the Bogi channel. ....54

Figure 4-12 Bank erosion along the Baleswar River west bank for 2011-2019, 2019-2034 and 2019-2049. The arrow shows the location where the embanked west bank is projected to cease eroding due to the bend cut activating the eastern channel (currently a flood channel, then becoming an ebb channel). ....55

Figure 4-13 Bank erosion along the Baleswar River east bank for 2011-2019, 2019-2034 and 2019-2049. The arrow shows the eastern bank projected to erode up to 100 m during the next 30 years, and it can also be seen that the erosion starts after 2034. ....55

Figure 4-14 Width-integrated bed levels as a function of chainage in the Baleswar River for 2049 with and without climate change (subsidence included in both simulations). ....56

Figure 4-15 West bank eroded areas integrated along the river for the period 2019-2049 with and without climate change. ....57

Figure 4-16 East bank eroded areas integrated along the river for the period 2019-2049 with and without climate change. ....57

Figure 4-17 Bank protection added along the Polder 39/2 east bank. ....58

Figure 4-18 Bathymetries and induced bed level changes. From left: 1) observed 2019 bathymetry (initial condition), 2) simulated 2034 bathymetry, 3) simulated 2034 bathymetry with protected bank, 4) induced bed level changes in 2034 caused by bank protection. ....59

Figure 4-19 Simulated induced bed level changes 2019-2034 caused by bank protection shown in the black line along the bank. This zoom is used for discussing the impacts. ....60

Figure 4-20 Induced bed level changes along the east and west banks. ....61

Figure 4-21	Bank erosion integrated in eroded areas along the east and west bank as well as differences between the scenarios. ....	61
Figure 4-22	Induced bed level changes 2019-2034 caused by protecting all banks from erosion. ....	63
Figure 4-23	Simulated bed levels in 2034 along the east bank as well as the induced scour equal to the reduction in bed levels caused by protecting all banks from erosion. The induced bed level changes based on protecting one eroding bank are shown for reference. ....	64
Figure 4-24	Simulated bed levels in 2034 along the west bank as well as the induced scour equal to the reduction in bed levels caused by protecting all banks from erosion. ....	64
Figure 4-25	The large bar opposite of the east bank eroding Polder 39/2 was selected for dredging scenarios. Individual eroding banks in this reach are marked with numbers in brackets. ....	65
Figure 4-26	Scenario A initial (2019) bathymetry (left) and simulated bathymetry after 15 years (right). ....	67
Figure 4-27	Scenario B initial (2019) bathymetry (left) and simulated bathymetry after 15 years (right). ....	67
Figure 4-28	Scenario C initial (2019) bathymetry (left) and simulated bathymetry after 15 years (right). ....	68
Figure 4-29	Scenario D initial (2019) bathymetry (left) and simulated bathymetry after 15 years (right). ....	68
Figure 4-30	Simulated bank erosion along eastern bank 2019-2034 for existing conditions and dredging scenarios A, B, C, D. The numbers in brackets refer to the specific eroding banks shown in Figure 4-25. ....	70
Figure 4-31	Simulated bank erosion along western bank 2019-2034 for existing conditions and dredging scenarios A, B, C, D. The numbers in brackets refer to the specific eroding banks shown in Figure 4-25. ....	70

## TABLES

Table 2-1	Available bathymetry data for Baleswar River. The more recent datasets have similar spatial resolution with cross-sections typically spaced 500-1000 m longitudinally and with 3 m spacing across the river. ....	7
Table 2-2	Measured water level data for Baleswar River. ....	10
Table 2-3	Measured discharge data for Baleswar River. ....	10
Table 2-4	Bed samples in Baleswar River compiled from various data sources. The Krumbein (1934) scale for size classes has been used, i.e. VFS = very fine sand, FS = fine sand, MS = medium sand. The three bed samples collected in 2016 were only available as $d_{50}$ , while the particle size distribution curves were not known. ....	11
Table 2-5	Suspended sediment measurement locations In Baleswar River compiled from available sources. ....	14
Table 3-1	MIKE 21C model boundaries for 2011 and 2015. ....	29

## ACRONYMS AND ABBREVIATIONS

ADCP	Acoustic Doppler Current Profiler
BDP2100	Bangladesh Delta Plan 2100
BIWTA	Bangladesh Inland Water Transport Authority
BMD	Bangladesh Meteorological Department
BoB	Bay of Bengal
BWDB	Bangladesh Water Development Board
CBA	Coast Benefit Analysis
CCP	Chittagong Coastal Plain
CDMP	Comprehensive Disaster Management Program
CDSP	Char Development Settlement Project
CEA	Cost Effectiveness Analysis
CEGIS	Centre for Environmental and Geographic Information Services
CEIP	Coastal Embankment Improvement Project
CEP	Coastal Embankment Project
CERP	Coastal Embankment Rehabilitation Project
CPA	Chittagong Port Authority
CPP	Cyclone Protection Project
CSPS	Cyclone Shelter Preparatory Study
DDM	Department of Disaster Management
DEM	Digital Elevation Model
DOE	Department of Environment
EDP	Estuary Development Program
EHRM	Eastern Hilly Regional Model
FAP	Flood Action Plan
FM	Flexible Mesh
FFWC	Flood Forecasting and Warning Centre
GBM	Ganges Brahmaputra Meghna
GCM	General Circulation Model

GIS	Geographical Information System
GRRP	Gorai River Restoration Project
GTPE	Ganges Tidal Plain East
GTPW	Ganges Tidal Plain West
HD	Hydrodynamic
InSAR	Interferometric Synthetic Aperture Radar
IPCC	Intergovernmental Panel for Climate Change
IPSWAM	Integrated Planning for Sustainable Water Management
IWM	Institute of Water Modelling
LCC	Life Cycle Costs
LGED	Local Government Engineering Department
LGI	local Government Institute
LRP	Land Reclamation Project
MCA	Multi Criteria Analysis
MES	Meghna Estuary Study
MIKE 11	DHI's 1-dimensional hydraulic model
MIKE 21C	DHI's 2-dimensional model made specifically for river morphology
MIKE FM	DHI's 2-dimensional flexible mesh flow model
MoWR	Ministry of Water Resources
MPA	Mongla Port Authority
MSL	Mean Sea Level
NAM	Nedbor Afstromnings Model
PPMM	Participatory Polder Management Model
PSD	Particle Size Distribution
PWD	Public Works Datum
RCP	Representative Concentration Pathways
RTK	Real-Time Kinematic
SET-MH	Surface Elevation Tables – Marker Horizons
SLR	Sea Level Rise
SOB	Survey of Bangladesh
SSC	Suspended Sediment Concentration
SWMC	Surface Water Modelling Centre

SWRM	South West Region Model
TBM	Temporary Bench Mark
TRM	Tidal River Management
ToR	Terms of Reference
UTM	Universal Transverse Mercator
WARPO	Water Resources Planning Organization
WL	Water Level

Joint Venture of



The expert in **WATER ENVIRONMENTS**



in association with



University of Colorado, Boulder, USA  
Columbia University, USA



## EXECUTIVE SUMMARY

DHI and IWM studied five rivers in the coastal zone of Bangladesh as part of the project “Long Term Monitoring, Research and Analysis of Bangladesh Coastal Zone (Sustainable Polders Adapted to Coastal Dynamics)”.

This Executive Summary applies to all meso-scale bank erosion models and reports developed during the study. The same Executive Summary can be found in all five model reports.

The main objectives of the modelling study were to develop predictive bank erosion tools for selected rivers and to estimate future bank line changes under different scenarios.

The five rivers were studied with emphasis on meso-scale bank erosion, and the rivers listed from west to east are: Sibsa, Pussur, Baleswar, Bishkhali and Sangu. The four rivers in the SW region of Bangladesh are all tidally dominated, while the Sangu in morphological terms is dominated by the monsoon hydrograph.

One report was issued for each of the studied rivers. The same overall modelling approach was used for all five rivers, and therefore all the reports followed the same template.

The overall approach can be summarized into:

- Preliminary study of historical bank erosion in the larger tidal rivers by using satellite imagery
- Digitization of historical bank lines (Landsat) for the selected rivers
- Review of publications related to bank erosion with the emphasis on identifying the most suited bank erosion description for the tidal rivers in Bangladesh
- Setup, calibration, and validation of the model with field measurements and remote sensing data
- Morphological hindcast – reproduce historical bathymetric and bank line shifting
- Scenario runs - study future changes in the morphological processes based on possible scenarios, e.g. climate change, upstream development and subsidence
- Output - geospatial datasets of present erosion and sedimentation in the river system for various seasons and for possible scenarios

The following data were required for each model:

- Bathymetries
- Hydrometric data (water levels and discharges)
- Sediment bed samples
- Sediment bank material samples
- Suspended sediment concentrations
- Suspended sediment particle size distributions
- Historical bank lines from satellite imagery

All meso-scale bank erosion reports follow this template:

- Introduction
- Data
- Model development
- Model application
- Conclusions

### Bank erosion

Bank erosion patterns in Bangladesh vary significantly from the monsoon dominated fluvial rivers to the tidally dominated muddy rivers. Two main reasons were identified in the study:

Firstly, tidal flow: The monsoon dominated rivers exhibit large imbalances between the dry season and monsoon, while the tidally dominated rivers do not show this imbalance, but instead exhibit similar discharge amplitudes during the dry season and monsoon. Due to this, the monsoon dominated rivers will experience very high morphological activity during the monsoon, which will be followed by high bank erosion rates, while the tidal rivers are better adjusted morphologically to the hydraulic conditions all year. In practice, monsoon dominated rivers are morphologically inactive during the dry season.

Secondly, cohesion: The tidally dominated rivers have cohesive banks, which are erosion resistant, while the sandy banks in most inland fluvial rivers have much higher erodibility.

The difference between fluvial and tidal rivers is significant and can also be followed along the coastal zone with strong tidal dominance in the west and monsoon dominance in the east. The increase in erosion from west to east can even be followed gradually from the Baleswar to the Bishkhali and increases further in the Sangu River.

Bank erosion rates in the tidally dominated muddy rivers are typically 5-10 m/year, while the rivers are kilometres wide, hence annual erosion is less than 1% of the width. Further to the east, bank erosion increased markedly in the Bishkhali and increases dramatically in the Lower Meghna and Sangu when measured relatively to the width (the absolute erosion rates in Lower Meghna are measured in hundreds of meters per year, while Sangu is narrow).

#### The value of Landsat data in Bangladesh

In most countries, Landsat data (30 m satellite imagery) is of little use for determining bank line movements due to the lack of resolution in the images compared to bank erosion rates. However, in Bangladesh, Landsat imagery is extremely useful because bank erosion rates are high. Although annual bank erosion cannot be followed in the tidal rivers from Landsat images, bank erosion over 5-10 years can be tracked accurately in the Landsat imagery. The Landsat data hence became a prism through which bank erosion in the past could be identified accurately.

The relatively slow bank erosion in the tidally dominated rivers was also found through data analysis to be systematic, such that a bank eroding in 1988 is extremely likely also to be eroding in 2019, and more or less with the same rate.

#### Model development template

The model development followed this template:

- Select model extent
- Develop curvilinear grid
- Interpolate bathymetry data to the curvilinear grid
- Extract hydrometric boundary conditions from e.g. the South West Regional Model (SWRM)
- Develop sediment transport boundary conditions
- Calibrate hydrodynamic model to observed water levels
- Calibrate sediment transport and morphological model to observed bed level changes
- Calibrate bank erosion model to observed bank line changes

The models were developed as hydro-morphological models with bank erosion included and physically moving the curvilinear grids to account for bank line changes. Model calibration was performed in depth by using the period 2011-2019 as hindcast, which was found ideal due to the two bathymetry datasets typically collected in 2011 and 2019 by IWM with almost identical resolution and accuracy. The value of such data cannot be overstated, and by combining with bank erosion obtained from Landsat data in the same period, the models could be calibrated in depth. There are exceptions to this, namely that no 2011 bathymetry was available for Bishkhali River, while Sangu River was calibrated to 2018-2020 for which good data was available.

The calibration of the tidally dominated rivers resulted in very similar calibration parameters, especially the silt transport models and bank erosion formulas were almost identical in the rivers.



### Bank erosion mechanics and formula

The bank erosion formula is central to the simulated behaviour of the rivers. Several bank erosion descriptions were investigated in detail in the models, and the optimal choice was found to be a formula derived from Hasegawa (1989). The Hasegawa model is based on a near-bank excess velocity approach, which means that bank erosion occurs when the near-bank flow speed is higher than the cross-section average flow speed. This could in principle have been adopted in the model engine, but it was found to give some practical problems because the Hasegawa formula was developed for meandering rivers with an outer bend and associated bend scour, which is not always the layout for the tidal rivers. Hence, the formula was modified by estimating the excess flow speed from the near-bank flow speed and an estimated average flow depth using the Manning formula. This resulted in bank erosion derived from the near-bank flow speed and water depth, notably bank erosion is proportional to the near-bank flow speed and a function of the water depth, such that the water depth must exceed a characteristic average depth for bank erosion to occur and then it will increase with depth beyond this limit.

Several bank erosion expressions were found calibratable to observed bank erosion, even with significant variations in the described mechanics. The best calibration was obtained by simply using a critical bank height (Mosselman, 1995) beyond which bank erosion increases with the exceedance of the bank height beyond the critical height. However, this was found mechanistically problematic because it does not state anything about erosive fluid forces along the bank, and hence bank erosion would continue along any bank independent of the flow along the bank, if the bank height exceeded the critical limit.

Bank erosion calibration using the Hasegawa derived formula is only slightly less accurate than for the critical height formulation, and Hasegawa has a solid theoretical foundation in addition to its inclusion of the flow speed along the bank. Hence, all taken into consideration, there was no doubt that Hasegawa was the correct choice.

Several traditional bank erosion descriptions were tested without success. For instance, a simple bank erosion description is to derive bank erosion from near-bank scouring; however, this does not work in the tidal rivers because the description is only valid for sandy banks. Surprisingly, relating the bank erosion rate to the shear stress was initially found to give a bad description of bank erosion. This was also the case when relating bank erosion rate to the flow speed without considering water depth.

It is important to understand that in addition to being able to describe the bank line changes over time, the bank erosion formula also needs to describe the physical processes in a lumped manner. The adopted Hasegawa derived formula derives bank erosion from flow speed and water depth, which proved to be the two most important variables.

### Limitations in the models and data

In general, the models developed suffer from similar limitations, which are also related to the lack of specific types of data. The limitations are listed in the order of importance.

In particular, all models show that simulated bar formation is sensitive to flow resistance used in the models and that the flow resistance calibrations adopted in the models are only one variant in a calibration space. Detailed investigations were conducted to show that different resistance models can be developed to yield the same simulated water levels but resulting in different velocity distributions between bars and channels as well as different sediment transport patterns and hence different bar sizes. Essentially the models have calibration spaces where the true calibration cannot be identified solely by matching water levels. Consequently, the bathymetry and bank erosion behaviours can vary significantly. The best approach for reducing calibration uncertainties is to collect ADCP velocity profiles, but this was not done as part of the present project.

The sensitivity of bar development to the flow resistance model used is very pronounced. For instance, a constant resistance number applied in a model can cause bars to erode in a manner where the deep channel will be located where the bar should be located and vice versa. In turn, this will lead to a simulated bank erosion where the erosion pattern essentially becomes the opposite of the observed. Due to feedback in the river morphology, this can also cause other bars to behave incorrectly. The implication of this sensitivity is that when the model simulates the right morphological development, this is a strong indication that the right resistance model has been applied.

The models also suffer from uncertainties in the calibration of sediment concentrations. This comes back to the traditional way of collecting data in Bangladesh, namely the standard collection of total sediment concentrations (i.e. the combined concentration of clay, silt and (fine) sand). The tidal rivers contain significant clay concentrations, which do not contribute morphologically. In the tidal rivers only the silt transport contributes to the morphological development since the sand concentration is negligible. Hence, it is not possible to calibrate silt transport models to the observed concentrations, as the observations generally only show the total concentration. However, observed particle size distribution data was available only in a few cases.

Only a handful of bank sediment samples were available. The erosion resistance of banks depends on the sediment composition of the banks. Bank erosion plays an important role in the river morphology, in some of the rivers contributing significantly to sedimentation, but the particle size distributions in the banks is largely unknown.

Rivers with mixed sediments require many bed samples to identify the particle size distribution in the riverbed. All the tidally dominated rivers are probably characterized by a mixture of sand and silt (while clay is morphologically inactive), but it was only possible for some of the rivers to identify this mixture, and none of the rivers had enough bed samples to determine the spatial distribution of the bed sediment composition.

The limitations of the available dataset have probably impacted the quality of the calibration of the models. However, the fact that the models all predict the overall morphology of the rivers quite well, including bank line migration and erosion/deposition pattern of the riverbeds, gives some confidence that also flow distribution, sediment transport etc. are well represented in the final model calibrations. Further model improvements can be made at a later stage if/when additional data collection is carried out. IWM has the capacity to conduct the necessary data collection.

#### Model applications

Model applications included the following:

- Projection of bank lines 30 years into the future
- Impact of climate change
- Impacts of bank protection on bank erosion and bed levels
- Dredging of shoals to mitigate or eliminate bank erosion
- Access to Mongla Port

#### *Projection of bank lines 30 years into the future*

The most important deliverable of the project was projected bank lines 30 years into the future for the four tidally dominated rivers in the west (Sibsa, Pussur, Baleswar and Bishkhali). The future projections showed that most of the banks currently eroding will continue eroding in the future with more or less the same rates. Hence, the future development was essentially projected to be similar to the 1988-2019 development. This is a very important finding that can be utilized for planning and managing polders and embankments. There are deviations from the overall systematic behaviour, but these are few in numbers. The projected future bank lines were also submitted to the CEIP-2 feasibility study in digital format (line themes) in order to maximize the value to planners and decision makers. Projection of bank erosion 30 years into the future is not meaningful for the Sangu River because the erosion rates are too high compared to the river width for projections on such timescale and was therefore not conducted.

#### *Impact of climate change*

In most of the models, climate change increases the tidal flow amplitude slightly, leading to a small increase in bank erosion. However, the impact of climate change is small compared to the absolute future bank line changes. Hence, the impact of climate change on future bank lines is modest.

#### *Impacts of bank protection on bank erosion and bed levels*

Bank protection was also shown to induce scouring due to the removal of sediment sources associated with bank erosion. The effect on bed levels is not insignificant, while bank erosion impacts are small. The models do not suggest that local bank protection will cause significant changes to the erosion of other banks, which is an important conclusion to keep in mind for management purposes, i.e. eroding banks do not seem to significantly influence each other in the tidal rivers.

#### *Dredging of shoals to mitigate or eliminate bank erosion*

The use of dredging of shoals located opposite of eroding banks was tested in the Baleswar River. The model results suggest that shoal dredging is potentially very effective at reducing bank erosion, especially if combined with backfilling of dredged spoils in the deep channel along the eroding bank. Unfortunately, this cannot be conducted simply by dumping the spoils in the deep channel due to the settling length for the silt exceeding the length of the eroding bank. However, the impact of shoals dredging combined with filling the deep channel essentially eliminates bank erosion over a long timescale and should be studied further, assuming that the filling problem can be addressed. A simple approach using geotextile (e.g. jute) bags to secure sedimentation in the deep channels was proposed, but needs to be investigated further and tested.

#### *Access to Mongla Port*

A separate investigation was also carried out for Mongla Port. Several scenarios were tested using the model, including quantification of the impact of Ganges Barrage, bank protection, closing and/or regulating upstream connections to Sibsa, guide bunds at Mongla, and TRM applied to Pussur or Sibsa. The investigation confirmed that the fundamental problem with Mongla Port is that the Sibsa incoming flood tide occupies (captures) most of the tidal prism located upstream of Mongla Port, preventing the incoming slower tide in the shallower Pussur River from occupying the tidal prism. The Pussur flood tide hence stagnates at Mongla Port, making the port susceptible to sedimentation, and model results show that Mongla Port indeed has the highest sedimentation rate in the Pussur River. The only way to really fix the sedimentation problem is to prevent the Sibsa from capturing tidal prism from the Pussur, while other schemes do not really solve the underlying problem, although they can act to mitigate. Schemes involving attempts to add tidal prism to the Pussur are remarkably ineffective due to the always faster flood tide in Sibsa, which will occupy tidal storage before Pussur. In effect adding tidal basins to Pussur downstream of Mongla Port just causes the Sibsa to capture more of the upstream tidal prism.

#### Conclusions

The conclusions from the study can be summarized into the following.

Bank erosion in the tidally dominated rivers of Bangladesh is slow and systematic, and therefore the predictability is very good, even over decades. This is a very important finding that can be utilized for planning and managing polders and embankments, for instance, designing embankments in safe distance from the eroding rivers, planning future retirement of embankments or when to implement bank erosion measures. On the contrary, fluvial systems in Bangladesh are known to have good predictability only over relatively short timescale, if even that.

The five developed models reflect the bank erosion predictability. For the four tidally dominated rivers, the bank erosion model was applied for projections 30 years into the future, while this is not meaningful for the Sangu River.

Although one should never take morphological predictions as accurate, the project team is confident that the future bank lines projected 30 years into the future are reliable enough for decision-making purposes. The predictable planform development should be exploited when managing polders and banks.

Dredging of shoals located opposite of eroding banks shows promising results, although only tested conceptually. The best outcome is achieved by combining dredging with dumping of the spoils into the deep channel flowing along the eroding bank, which will give two synergizing effects, namely attracting flow to the dredged flow path through the shoal and attracting less flow to the deep outer channel. There is a major practical issue with the approach, namely that it is not easy to dump the spoils into the outer channel. One proposal for handling this is to fill the spoils into geotextile bags and dump them in the outer channel, which is similar to the approach followed in some meandering rivers for navigation purposes (by preventing deep bend scour), but here done to prevent bank erosion (by also preventing deep bend scour).

For the Sangu and other fluvial systems, managing polders via predictable future bank lines is not meaningful. However, a river like the Sangu has a meander belt, which has good predictability, even if the bank lines themselves are difficult to predict. However, this may require allowing the Sangu River to move within its meander belt, which means accepting a loss of land area behind polders.

The model shows that Mongla Port has the highest sedimentation rate in the Pussur River model. In other words, Mongla Port happens to be located at the worst possible location for a port.

The Pussur River model was also applied to scenario testing at Mongla Port. The fundamental problem with Mongla Port is that it is located just south of the tidal meeting point between the Pussur and Sibsa tides, which has been understood for decades, and indeed some of the scenarios addressing this problem have been tested before. Several mitigation schemes were tested, and it was found that the most effective solution is to increase the Pussur tidal prism located upstream of Mongla Port. Getting the Pussur flood tide to flow north from Mongla can only be done by preventing the faster Sibsa flood tide from occupying the prism. Closing the three upstream connections to the Sibsa River was proposed and tested almost 30 years ago by DHI (1993), and the present study reverified the validity of this scheme. However, the scheme can be further developed by using regulators on the connection rivers to enhance the outgoing tide (ebb) at Mongla Port, which is the driver for keeping the Mongla Port water depths sufficiently large. It was shown that closing the connections appears neutral in the Mongla Port bed levels, while significant scouring can be achieved with regulators, opening up for managing the Mongla Port bathymetry by using the regulators to adjust the hydraulic dredging driven by the ebb flows.

The use of guide bunds at Mongla Port, proposed before, was investigated by using the MIKE 21C model. It was found that this scheme can sustain deep channels at Mongla Port, but it will also induce sedimentation further downstream due to the slightly reduced tidal discharges associated with the added flow resistance from the guide bunds. This suggests that the guide bund scheme cannot stand alone in solving the Mongla Port problem.

Various other schemes were also investigated, in particular increasing the tidal prism of the Pussur downstream of the tidal meeting point located upstream of Mongla Port. Schemes involving an increase in the Pussur tidal prism downstream of the tidal meeting point are problematic because they ultimately leave more tidal prism for the Sibsa flood tide to occupy from the Pussur upstream of Mongla Port.

A real solution to the Mongla Port problem must address the ability of the faster Sibsa flood tide to capture (from the Pussur) tidal prism upstream of Mongla Port, which is the fundamental problem. Mitigation schemes that do not address the fundamental problem do not seem to be able to stand alone.

# 1 Introduction

## 1.1 Background

Bangladesh is situated at the confluence of three great trans-Himalayan rivers, the Ganges, the Brahmaputra or Jamuna, and the Meghna, which form the Bengal (or GBM) Delta. While over 90 percent of the catchment of the GBM system lies outside of Bangladesh, more than 200 rivers and tributaries and distributaries of the GBM system drain through the country via a constantly changing network of channels, tidal inlets and creeks, forming the most active large delta on the planet. The coastal land mass is shaped by the interaction of large volumes of sediment laden water with the moderate to high tides of the Bay of Bengal.

Land in the coastal zone is built up by the deposition of river sediments in the tidal delta, including the mangroves of the Sundarbans, the largest mangrove forest in the world. The deposits of sand, silt, clay, and organic material form the land mass which, despite subsidence due to continuous consolidation of layers many kilometres deep, is kept around the level of the highest tides by the continuing deposition of sediments.

The coastal zone of Bangladesh spans over 710 km of coastline and is subject to multiple threats. Sixty-two percent of the coastal land has an elevation less than 3 meters above mean sea level. With a sediment supply of 1 billion tons per year, this is the delta with the largest sediment supply in the world. This leads to continuing accretion of the land area in the coastal zone (5-10 km<sup>2</sup>/year), mainly in the Meghna Estuary, but also erosion of the coast farther west. It has been observed that the land subsidence rate may vary from place to place due to anthropogenic factors such as drainage and ground water extraction as well as the properties and depth of underlying strata. On top of this there are tectonic plate movements, particularly in the eastern delta, that give rise to other changes in ground level.

The coastal lands, particularly in SW Bangladesh, being subject to regular flooding by saline water during high tides, could not be used for normal agricultural production in a country with a very high demand for land. The Coastal Embankment Project (CEP) was initiated in the 1950s and 1960s to build polders surrounded by embankments preventing the spilling of saline water onto the land at high tides. These embankments were built along the larger rivers and across the smaller rivers and creeks which then formed the drainage system within each polder and connected to the peripheral rivers via appropriately sized flap gate regulators, that open at low tide to let the drainage water out.

The Coastal Embankment Project enabled the reclamation of large tracts of land for agriculture from 1960 onwards. Polder building proceeded continuously until today. Up till now, 1.2 million hectares have been reclaimed in 139 active polders in the coastal zone of Bangladesh.

In over half a century of its existence, a number of challenges have surfaced that threaten the long-term safety and even the very existence of the polder system as a viable and sustainable resource. These are:

- Sea level rise and changes in precipitation and water discharge due to climate change
- Threats of damming and diversion to the delivery of river sediments from upstream
- Subsidence of lands (except where it has been allowed to be rebuilt by tidal flooding) and structures founded on existing land
- Drainage congestion due to accumulation of silt in some peripheral waterways around polders
- Changes in tidal hydrodynamics and related river erosion and siltation in the peripheral rivers of polders
- Increasing vulnerability to cyclones and storm surges

The main objective of the “Long-term monitoring, research and analysis of Bangladesh coastal zone” project is to create a framework for polder design, based on understanding of the long-term and large-scale dynamics of the delta and sustainable polder concepts. The field and modelling work within the project is carried out to improve understanding of the long-term and large-scale dynamics of the Ganges-Brahmaputra-Meghna (GBM) delta. There is insufficient knowledge about sediment budget in the delta involving sediment transport within the estuaries, sediment sources and sediment distribution into the river system. Sediment and tidal dynamics are important for river and coastal erosion, land reclamation, and delta development. Subsidence of the land alters the topography and hydrodynamics and increases flooding, coastal erosion and salinization. The knowledge of sediment dynamics, distribution, subsidence, erosion-deposition processes, sediment management at present and in the future under climate change, land use changes and proposed interventions in the upstream reaches of the Ganges Brahmaputra River systems is essential for the framework of polder design.

In the coastal zone of Bangladesh – both in the major estuaries and in the peripheral rivers of the polders – bank erosion is a significant problem even though the erosion rates are normally smaller than those encountered further upstream in the non-tidal main rivers (e.g. Padma, Brahmaputra). Failure of embankments in the coastal zone during storms has not always been as the result of overtopping. There have been many failures as a result of undermining of the toes of the embankment due to riverbank erosion. In fact, unexpectedly high levels of bank erosion have already been encountered in the execution of CEIP-1. This matter was highlighted in the Inception Workshop of this project leading to the recommendation that a special meso-scale study of “Bank Erosion Hindcasting” should be undertaken to analyse the bank erosion processes that have taken place in the large tidal estuaries in the last 20 or more years in areas where large and often intensive data collection programmes have been mounted for various projects. Improved guidelines for predicting medium term bank erosion are supposed to emerge from this study.



Figure 1-1 Revetment along Baleswar River (photo 11 February 2019).

## 1.2 Objective and Approach

The main objective of the modelling presented in this report is to develop a predictive bank erosion tool for the Pussur River and to estimate future bank line changes under different scenarios.

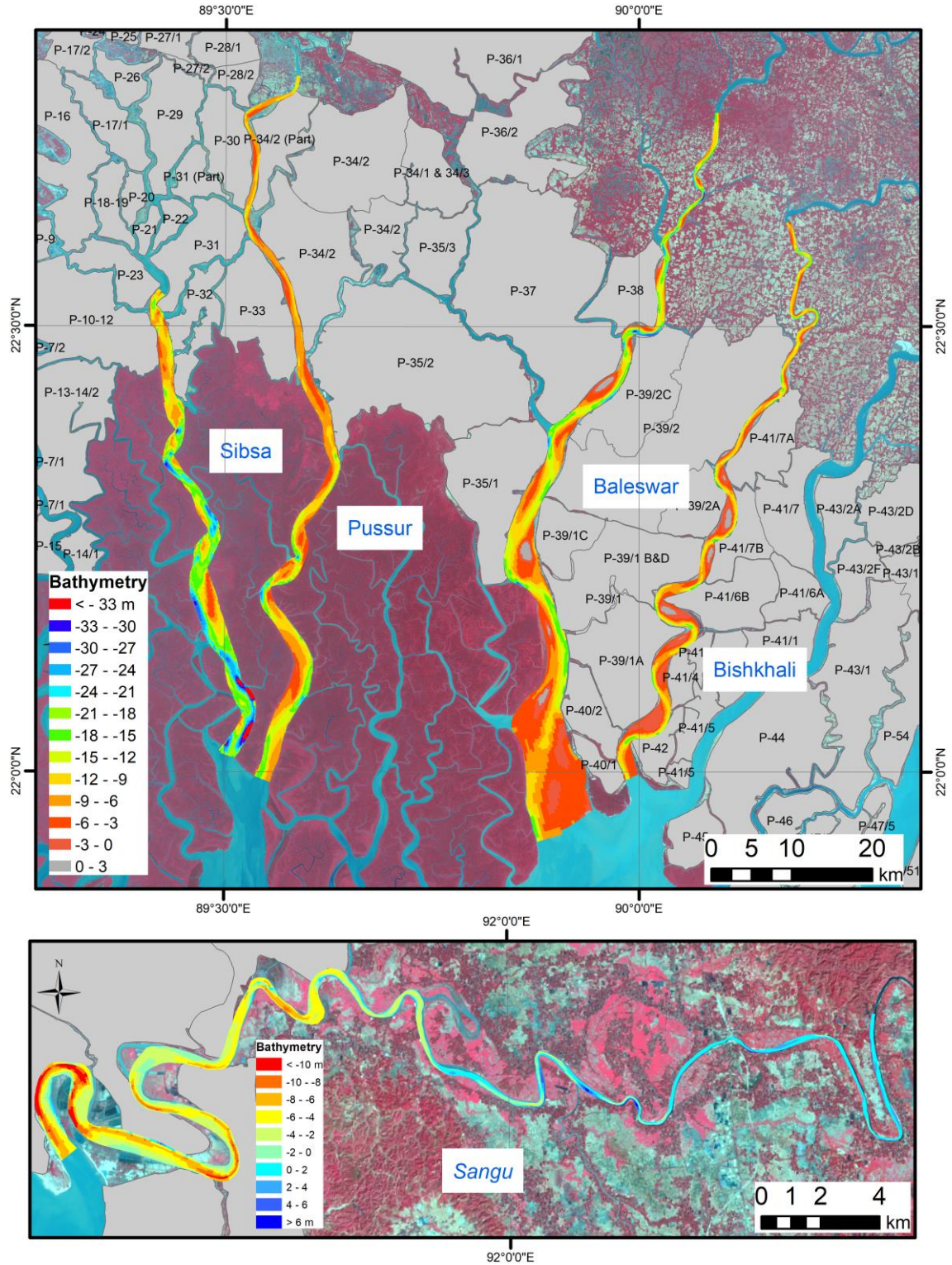


Figure 1-2 The five MIKE 21C models developed for the project.

The general approach for this modelling is the following:

- Preliminary study of historical bank erosion in the larger tidal rivers by using satellite imagery
- Digitization of historical bank lines (Landsat) for the selected rivers
- Review of publications related to bank erosion with the emphasis on identifying the most suited bank erosion description for the tidal rivers in Bangladesh
- Setup, calibration, and validation of the model with field measurements and remote sensing data
- Morphological hindcast – reproduce historical bathymetric and bank line shifting
- Scenario runs - study future changes in the morphological processes based on possible scenarios, e.g. climate change, upstream development and subsidence
- Output - geospatial datasets of present erosion and sedimentation in the river system for various seasons and for possible scenarios 25, 50 and 100 years from now, for various seasons and circumstances

The modelling is carried out using MIKE 21C. The key features of this modelling system are:

- Curvilinear boundary conforming grids allowing accurate representation of the river planform with relatively few grid points
- 2D Saint-Venant equations with a parallelized and optimized solver allowing time-true simulations covering several years
- Helical flow
- Multi-fraction sediment framework covering mixtures of clay, silt, sand, gravel
- Bed-load calculated with inclusion of helical flow and bed slope
- Suspended load calculated from advection-dispersion with helical flow included
- Morphological updating of the bed levels
- N-layer substrate model
- Bank erosion with optional inclusion of eroded material in the sediment budget
- Dynamic updating of the curvilinear grid to account for bank line changes

Waves are not included in any of the MIKE 21C models. The fetch is generally small within the estuaries of the delta, and the modelled rivers are very deep, usually at least 10 m and often up to 40 m water depth along eroding banks, which means that the small surface waves will not penetrate to the lower water column, hence it may be assumed that waves have little influence on the sediment transport in the areas modelled.

## 1.3 This report

An interim report describing the model development for the current situation was submitted earlier in the study and reviewed by the World Bank. The interim report was titled:

“Meso scale bank erosion modelling - current situation - interim report”

DHI revised the interim report to address the review, and the report was extended to include future projections. The final report was titled:

“Meso scale bank erosion modelling – current situation & future projections”

The interim report is included already in the final report and not submitted separately.

The five modelling reports are organised in a similar manner with the following chapters: Chapter 2 gives an overview on the availability of measurement data, as well as how the data was processed. These data are used in Chapter 3, which describes the development and calibration/validation of the model used to study the river morphology and bank erosion. Model applications are documented in Chapter 4, while the report finalizes with conclusions in Chapter 5.



## 1.4 General definitions

It is useful to provide some general definitions and explanations for the terminology used in this report.

The projection is always BTM, and the vertical datum is always mPWD. In some cases, data was made available in UTM and MSL, but they were converted.

All MIKE 21C models were developed with the grid direction going in the direction of the river from upstream. This means that the discharge sign convention is that ebb flow is positive and flood flow is negative in all models.

The term “mud” is defined as a mixture of mainly fine-grained sediments, organic matter and water where the cohesive properties of the clay fraction, enhanced by the properties of the organic matter, dominate the overall behaviour of the sediment mixture.

Several figures present results in ways that can seem confusing if the reader is not aware:

- Some figures show Baleswar River divided into upstream and downstream
- Some figures show several Baleswar River maps side-by-side

The MIKE 21C models are very long, and to avoid narrow graphics, the 2D figures are made by splitting the river into upstream and downstream parts shown side by side, with the upstream part to the left and the downstream part to the right. Grids and bathymetries are shown in this manner.

The plots with several Baleswar River 2D maps shown next to each other are useful for showing several results together because they belong together. Examples include bathymetries that need to be compared as well as bed level changes shown together with the bathymetries. When showing these, the 2D maps are displaced 10 km in eastern direction (to the right), and the easting coordinates are hence only correct for the first 2D maps shown to the left. When showing more 2D variations together in this manner, there can be several colour scales in a figure, and the reader is notified in the caption.

For one-dimensional variations it is necessary to introduce a chainage coordinate. Although the river runs generally north to south, the northing cannot be used as unique coordinate along the river. The chainage coordinate was calculated along the grid centreline of the river, starting from 0 at the upstream end, and these chainages do not align to the SWRM. All one-dimensional variations are shown as functions of this chainage.

## 1.5 Important note regarding MIKE 21C version

The developed MIKE 21C models take advantage of the most recent developments of the modelling software, hence it is important that MIKE 21C version 2022.1 or later is used. This version is installed on the project computers.



## 2 Data

This section documents all the data that was used for the model development.

The projection is BTM, and the vertical datum is mPWD.

### 2.1 Bathymetry

A very detailed bathymetry survey was conducted in 2011 for the Baleswar River as part of the Gorai River Restoration Project (GRRP). For the present project, a similarly detailed survey was conducted in 2019. A bathymetry dataset was also available for 2015 with sufficient density for 2D contouring, but also with some gaps in the downstream end of the river. Finally, there is a bathymetry survey from 2009 with too sparse cross-sections for 2D contouring.

Table 2-1 Available bathymetry data for Baleswar River. The more recent datasets have similar spatial resolution with cross-sections typically spaced 500-1000 m longitudinally and with 3 m spacing across the river.

Bathymetry data collection year	Sources
2009 (dates not available)	IWM (FFWC)
2011 (dates not available)	IWM (GRRP)
2015 (dates not available)	IWM (CEIP-I)
2019 (March)	Primary data (present project)

The available bathymetries are shown in Table 2-1.

The 2009, 2011, 2015 and 2019 bathymetries were contoured, see Figure 2-1. The 2009 bathymetry was not interpolated due to too few data points, but a cross-section analysis showed that erosion took place in 2009-2011. The contoured bathymetry (excluding 2009) is shown in Figure 2-2 along with observed bed level changes.

Figure 2-1 and Figure 2-2 In combination show that there was erosion in 2009-2011 (based on cross-sections), while significant deposition took place in the period 2011-2015. Deposition continued at a slow pace in 2015-2019. Of interest is that the 2015 and 2019 bathymetries were very similar.

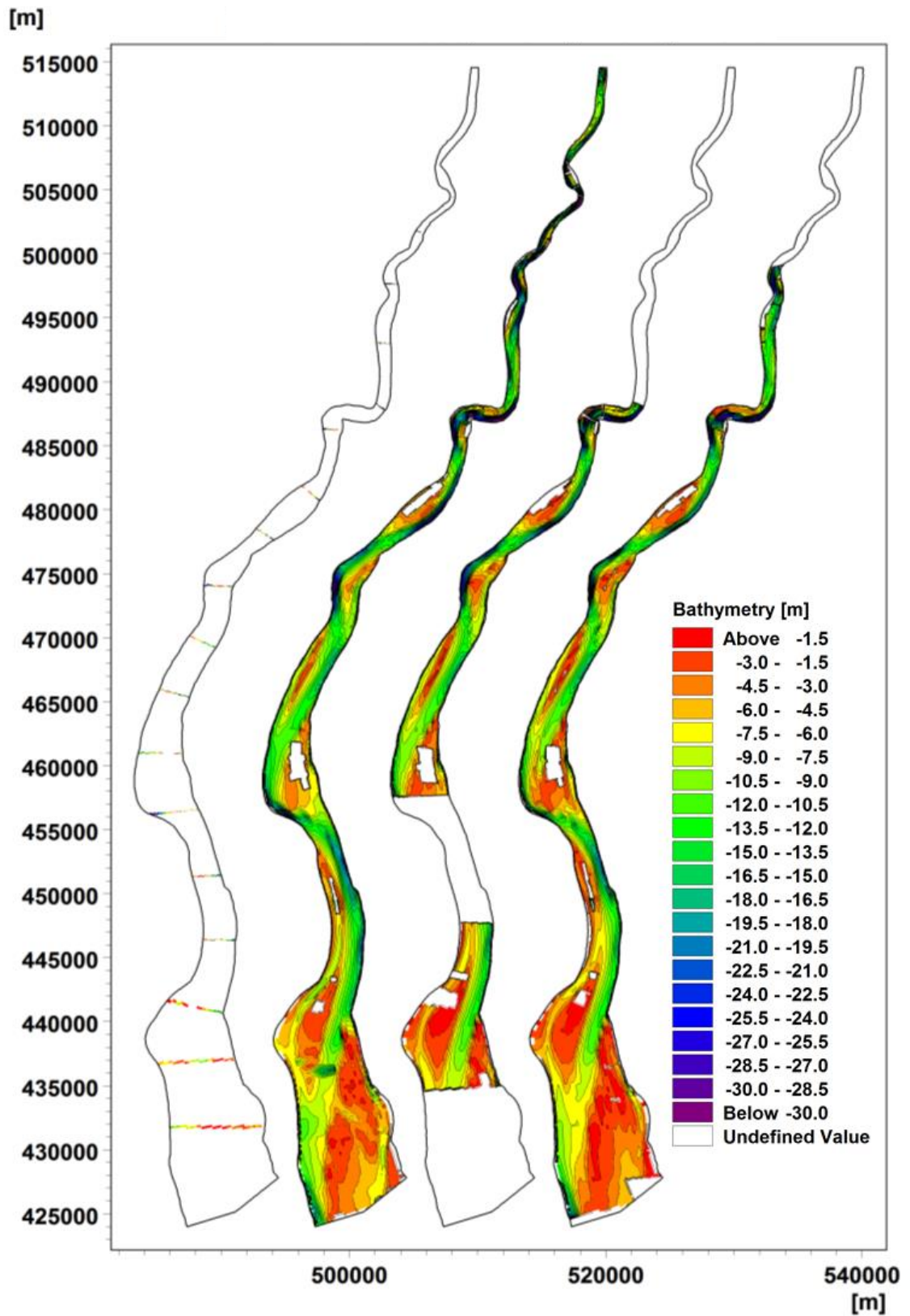


Figure 2-1 Observed bathymetries of Baleswar River from 2009, 2011, 2015 and 2019.

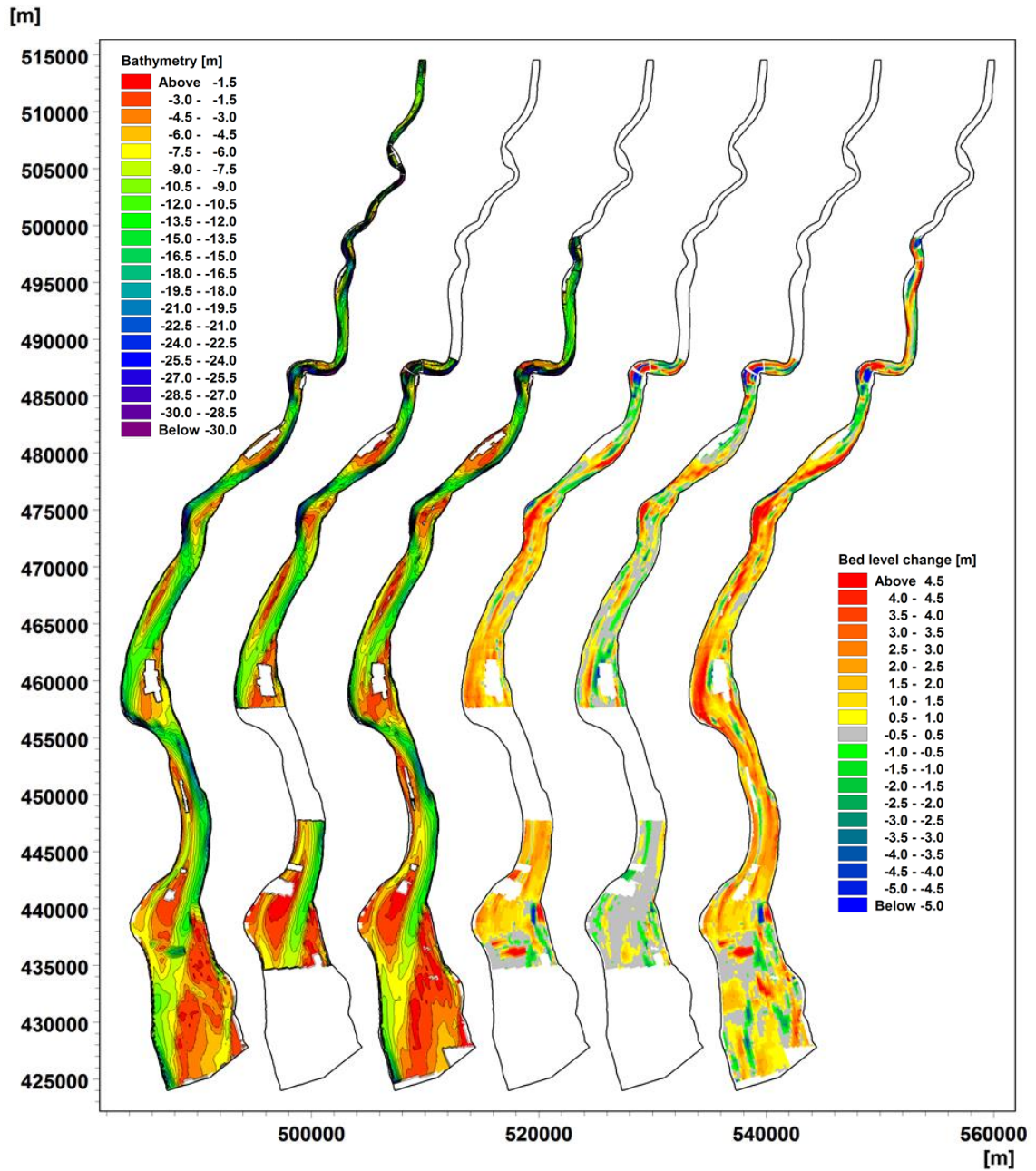


Figure 2-2 Observed bathymetries and bed level changes 2011-2015-2019. From left: 1) 2011 bathymetry, 2) 2015 bathymetry, 3) 2019 bathymetry, 4) bed level changes 2011-2015, 5) bed level changes 2015-2019, 6) bed level changes 2011-2019.

## 2.2 Hydrometric time-series

Hydrometric data includes water levels and discharges.

Observations of water levels are available at numerous stations in Bangladesh from two primary sources, viz. Bangladesh Water Development Boards (BWDB) and Bangladesh Inland Water Transportation Authority (BIWTA). In this study, water level data mainly collected by IWM was used

Joint Venture of



The expert in **WATER ENVIRONMENTS**

&



in association with



University of Colorado, Boulder, USA  
Columbia University, USA

in combination with simulated water levels from the South West Regional Model (SWRM) and some BDWB water level data.

Water level and discharges data collected as part of the project during 2019 were not used in the model development process, as the data were not available at the time when the model was developed.

Table 2-2 Measured water level data for Baleswar River.

Water level collection period	Station Name	Sources
2011	Chardoani	IWM (GRRP)
2011	Umedpur & Sarupkati	BWDB
2015	Tafalbari Launchghat & Telekhali Bazar	IWM (CEIP-1)
2019	Chardoani	Primary data (present project)

Table 2-3 Measured discharge data for Baleswar River.

Discharge collection year	Station Name	Sources
2011, 2012	Chardoani	IWM (GRRP)
2015	Charkhali	IWM (CEIP-1)
2016	Sarmasi (Rayenda)	IWM (CEIP-1)
2019	Chardoani	Primary data (present project)

Table 2-2 shows the available water level data, while discharge is tabulated in Table 2-3. The discharge data was collected by IWM, typically for one day using tide tables to plan for neap and spring data collection. Water levels were collected at the same time, and often IWM also collects suspended sediment concentration data with the ADCP data. Water level stations are often permanent and contain water levels collected every 30 min.

The Umedpur water level data was collected with too low frequency (6-hourly) to resolve the tidal variation. However, this data can still be used for model validation.

## 2.3 Sediment bed samples

In this section all readily available bed samples for Baleswar River are compiled. Many samples have been collected for various projects (2011, 2016, 2017 and 2019), but the data has not before been compiled to obtain a comprehensive picture of the sediment bed.

Table 2-4 Bed samples in Baleswar River compiled from various data sources. The Krumbein (1934) scale for size classes has been used, i.e. VFS = very fine sand, FS = fine sand, MS = medium sand. The three bed samples collected in 2016 were only available as  $d_{50}$ , while the particle size distribution curves were not known.

BTM X [m]	BTM Y [m]	Year	Name	Clay <0.005 mm [%]	Silt <0.063 mm [%]	VFS <0.125 mm [%]	FS <0.25 mm [%]	MS >0.5 mm [%]
484936	465534	2011	Shamkhola_RB	15.4	83.4	1.12	0	0
487164	464296	2011	Shamkhola_LB	11.2	88.1	0.72	0	0
490714	473165	2016	Sonnasi Left Bank					
489646	473427	2016	Sonnasi Centre					
488556	473652	2016	Sonnasi Right Bank					
499185	486870	2017	Baleswar_01	4.88	87.9	5.55	1.39	0.2
498794	486754	2017	Baleswar_02	6.24	87.4	4.7	1.11	0.5
498343	486597	2017	Baleswar_03	8.51	89.1	2.43	0	0
489825	474698	2017	Baleswar_04	5.94	79	9.1	4.46	1.5
490291	474537	2017	Baleswar_05	5.52	88.6	4.34	1.33	0.2
490759	474426	2017	Baleswar_06	5.52	92.3	2.22	0	0
483843	458345	2017	Baleswar_07	12.3	76	6.82	3.77	1.1
485418	458459	2017	Baleswar_08	11.7	79.1	4.68	3.31	1.2
487125	458624	2017	Baleswar_09	8.8	89.7	1.55	0	0
486410	438424	2017	Baleswar_10	15.3	82.5	2.22	0	0
488446	438583	2017	Baleswar_11	4.99	80.9	9.02	3.33	1.7
491860	430847	2017	Baleswar_13	0	3.92	54.3	41.1	0.7
499134	485341	2019	Baleswar_1B_LB	8.78	89.4	0.24	1.33	0.3
498006	485460	2019	Baleswar_1B_RB	7.62	79.3	7.41	4.66	1
486962	464017	2019	Baleswar_2B_LB	14.3	81.9	2.18	1.33	0.3
485041	464095	2019	Baleswar_2B_RB	5.73	66.6	16.2	10.8	0.7

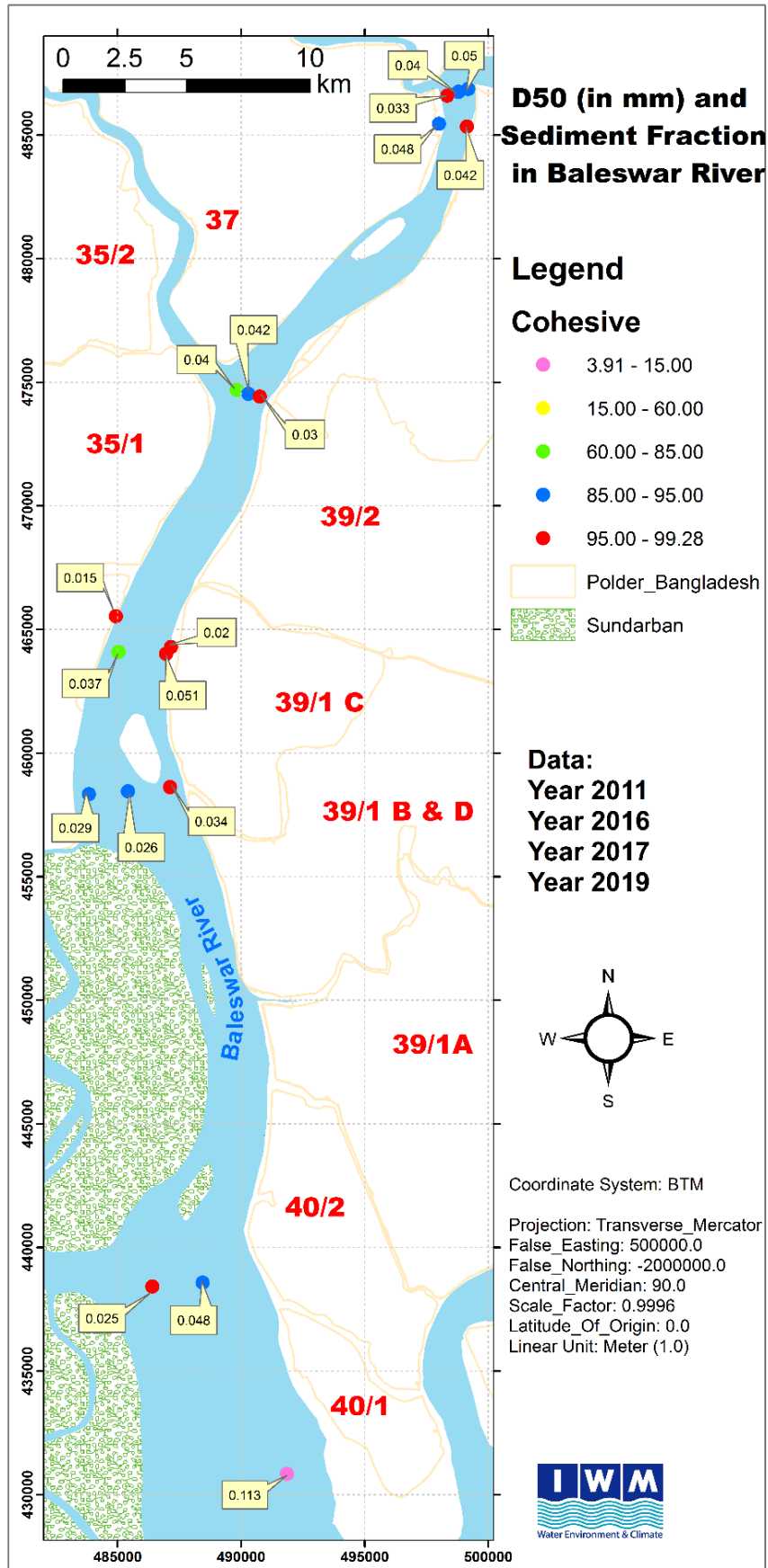


Figure 2-3 Measured sediment fractions in the Baleswar River.



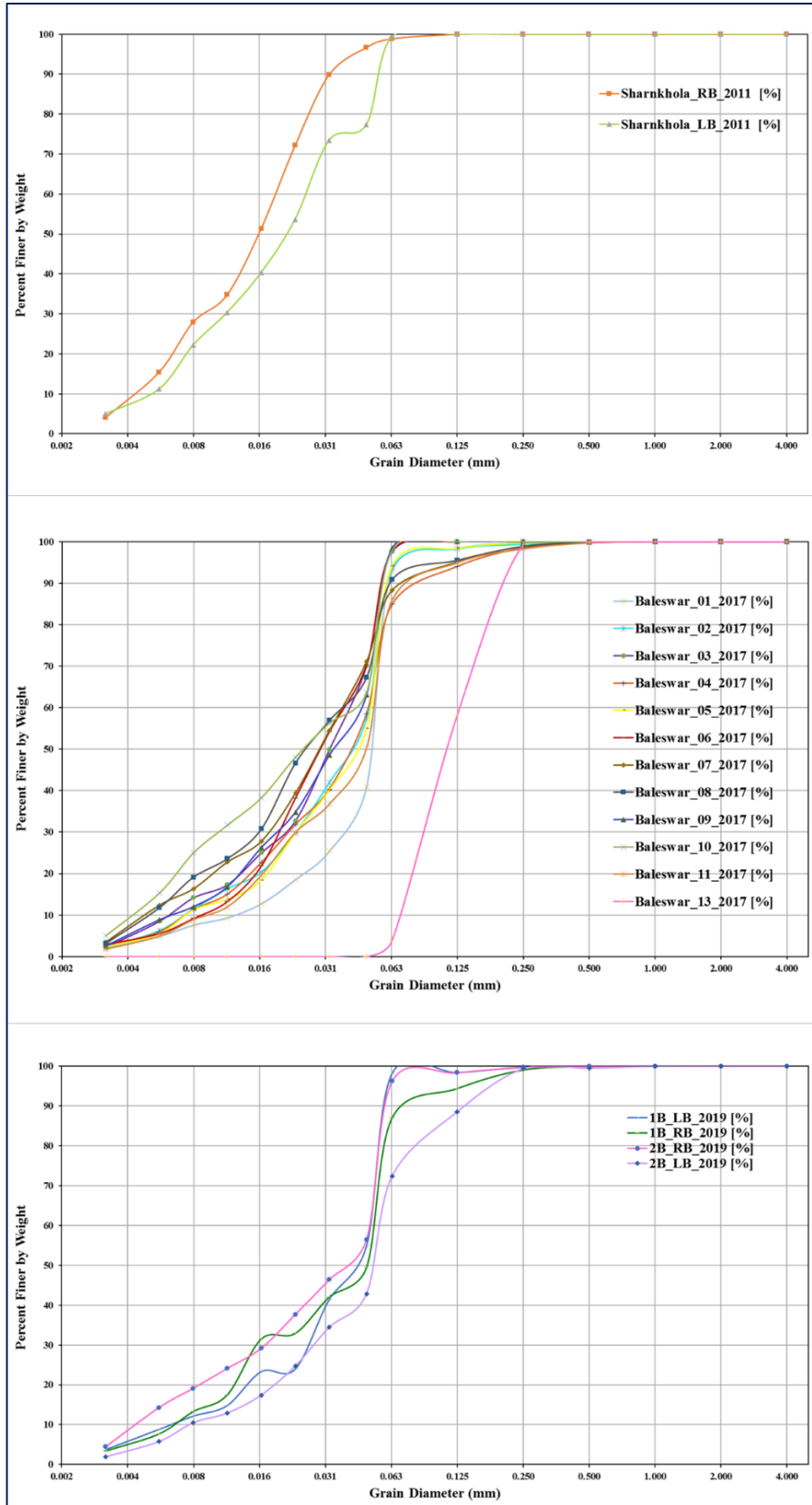


Figure 2-4 Particle size distribution of Baleswar River for 2011, 2017 and 2019.

Joint Venture of



The expert in **WATER ENVIRONMENTS**

&



in association with



University of Colorado, Boulder, USA  
Columbia University, USA

Table 2-4 shows the bed samples processed into the Krumbein (1934) scale for the sand partition and clay/silt for the cohesive partition. The locations of the samples are shown in Figure 2-3, while the corresponding particle size distribution curves are shown in Figure 2-4.

The compiled bed samples show a consistent picture:

- The sediment spectrum is dominated by silt
- There is little clay in the bed
- There is very little sand in the bed

Unfortunately, there are no sediment samples upstream of the very sharp bend. The bathymetries indicate that the river could be sandier upstream due to the stronger bar formation.

## 2.4 Suspended sediment data

Suspended sediment concentration (SSC) data was available for Chardoani (2011), Charkhali (2015), Sarmasi (2016) and Chardoani (2019). The observations were collected from various data sources, but the individual projects (conducted by IWM) were not recorded during the process.

It is noted that both 2011 and 2019 refer to the station Chardoani, but the coordinates are different. The stations are clearly different and were identified by coordinates rather than by name in the study.

Table 2-5 Suspended sediment measurement locations In Baleswar River compiled from available sources.

Station	Vertical	BTM X [m]	BTM Y [m]	Year
Chardoani	V-1	489239	446613	2011
Chardoani	V-2	490958	446638	2011
Charkhali		497992	484543	2015
Sarmasi		489306	473497	2016
Chardoani	V1	486880	460988	2019
Chardoani	V2	483709	461398	2019
Chardoani	LB	486880	460988	2019
Chardoani	RB	483709	461398	2019
Chardoani	V1LB	486261	460934	2019
Chardoani	V2RB	483674	461405	2019
Chardoani	V1CL	486795	460492	2019
Chardoani	V2LB	485156	460944	2019
Chardoani	V2RB	483844	460964	2019

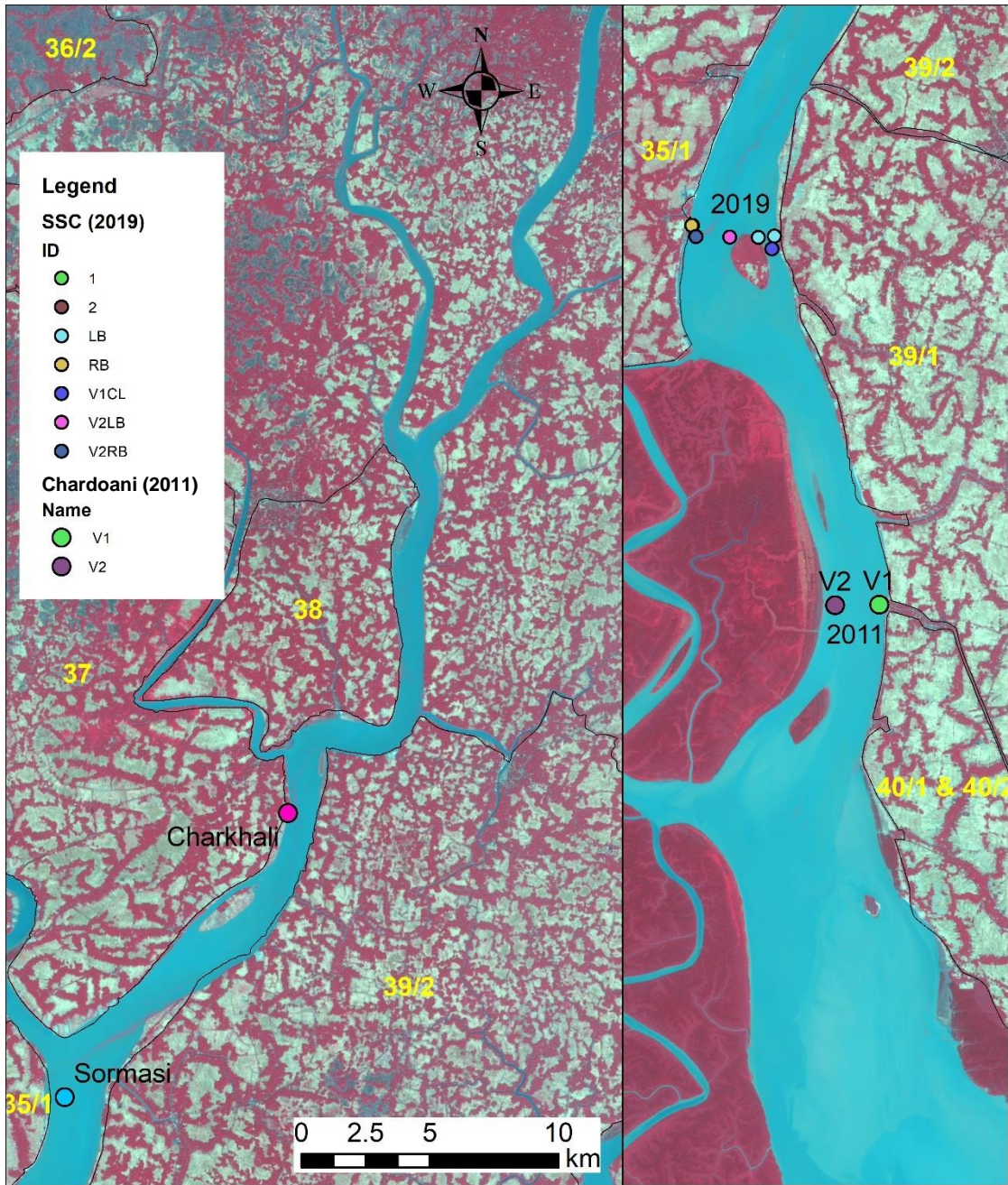


Figure 2-5 Suspended sediment concentration stations in Baleswar River.

The suspended sediment samples are summarised in Table 2-5, while the locations of the stations are shown in Figure 2-5. In the following, the C(Q) correlations (discharge versus sediment concentration) are processed for all the stations. This is a common approach in fluvial systems where it is used to establish a sediment transport rating curve. In fluvial systems flows and sediment transport will be slowly varying, and there will generally be a relation between discharge, water level and bed shear stress, so also a unique sediment rating curve. This is in contrast to a tidal system as the present, so a unique relation between discharge and sediment concentration cannot be expected. The plots, however, are useful for developing an understanding of the sediment dynamics and to generate continuous time-series to be used at the model boundaries.

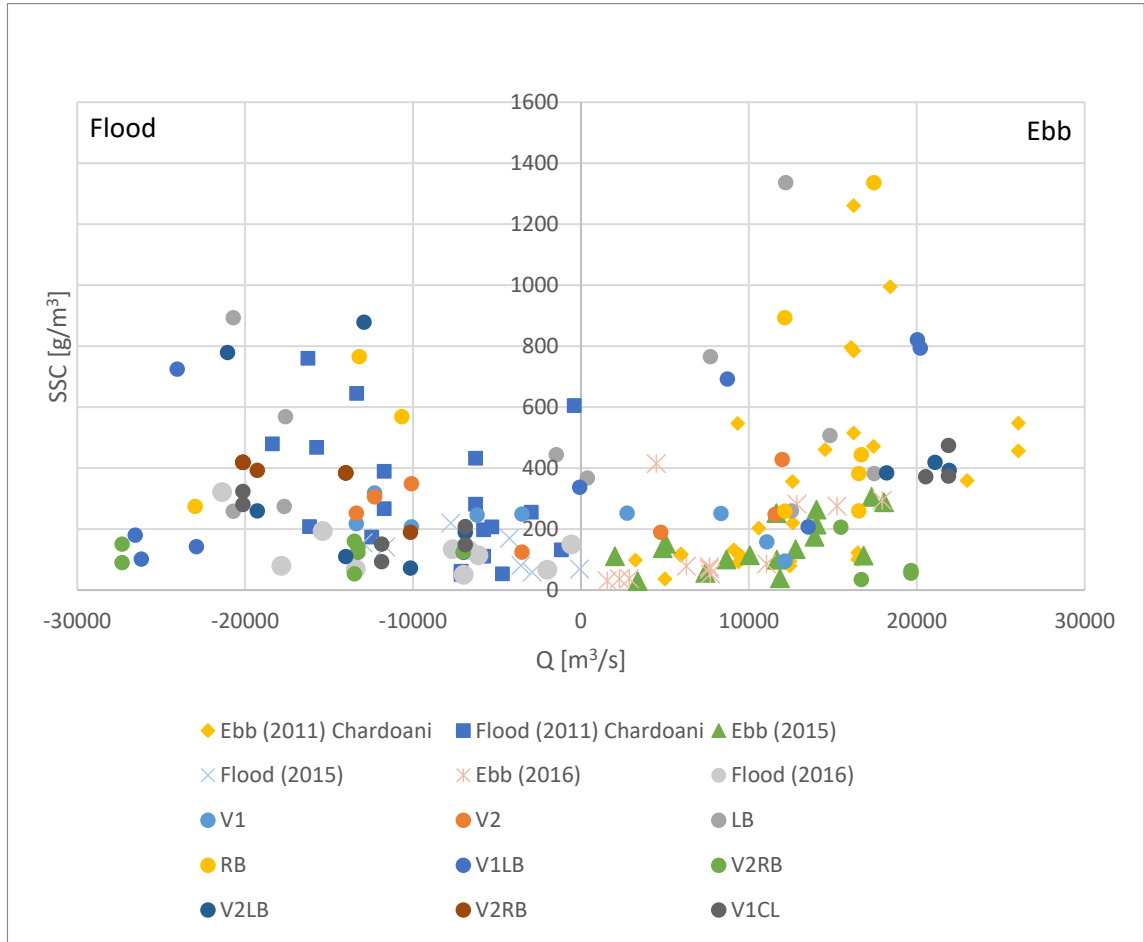


Figure 2-6 Correlation between discharge and sediment concentration for the all the stations in Baleswar River.

The observations were processed into one graph showing the concentrations as a function of the discharge, see Figure 2-6. This is not a particularly scientific way to show the data, as the data is from different stations, but the purpose is to illustrate that in general, the concentrations increase with the discharge.

## 2.5 Suspended sediment particle size distribution data

Particle size distribution data was collected by IWM in 2001.

The measured particle size distributions for the suspended sediment samples are shown in Figure 2-7. As expected, the suspended sediments are generally finer than the bed samples, with a median grain size around 0.005-0.02 mm, while the median grain size for the bed material is around 0.04 mm. The corresponding fall velocities are 0.03-0.4 mm/s for the suspended sediment and 1.7 mm/s for the bed sediment. Cohesive sediment with a fall velocity around 0.1 mm/s has a settling time through 20 m water longer than the tidal cycle and will therefore exhibit limited morphological activity. This is also reflected in the bed samples, which show very little of the finest material abundant in the suspended samples.

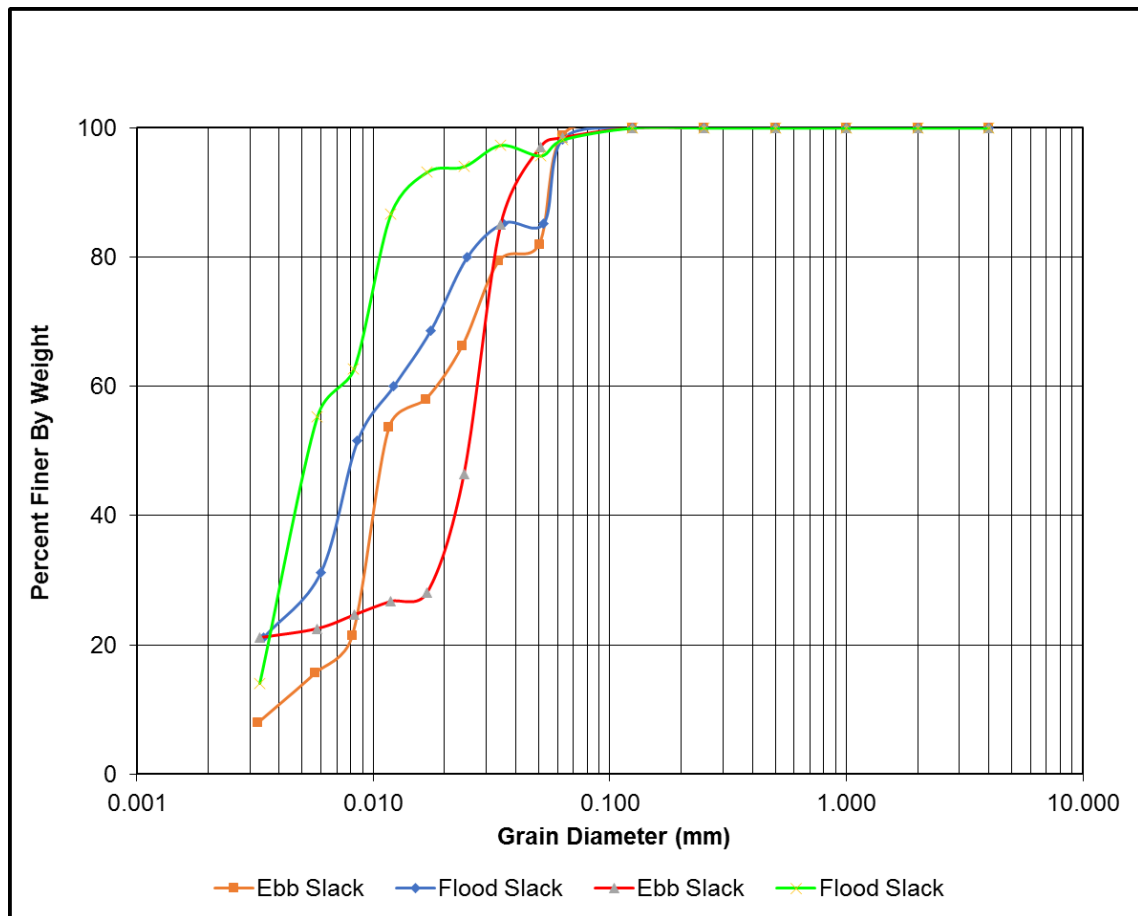


Figure 2-7 Particle size distribution of Bholgang River joining the Baleswar River at Shawrankhola (IWM, 2001)

## 2.6 Historical bank lines from satellite imagery

Historical bank lines were studied based on satellite images. To this end, nine cloud-free scenes of Landsat imagery were acquired for the period of 1988-2019 from the Earth Explorer database of the U.S. Geological Survey. The acquired images cover all the rivers in the coastal zone for which meso-scale modelling is carried out in this project, thus also the Baleswar River. All the images are from the dry season from November to February as there were no cloud free images during other seasons.

Bank lines were digitized from the images from 1988, 1995, 2001, 2011 and 2019 and are shown in Figure 2-8. In this figure, 17 locations with consistent and significantly eroding banks are indicated. It is observed that nearly all the locations with eroding banks are located along outer bends where the water depth adjacent to the bank is large (ebb channels). In addition, some eroding banks can be explained from smaller channels located between the bars and the inner bank (flood channels). For Baleswar River the bank erosion rates are generally very low for flood channels, but e.g. the bank east of the southern island (opposite of bank 3) has detectable erosion.

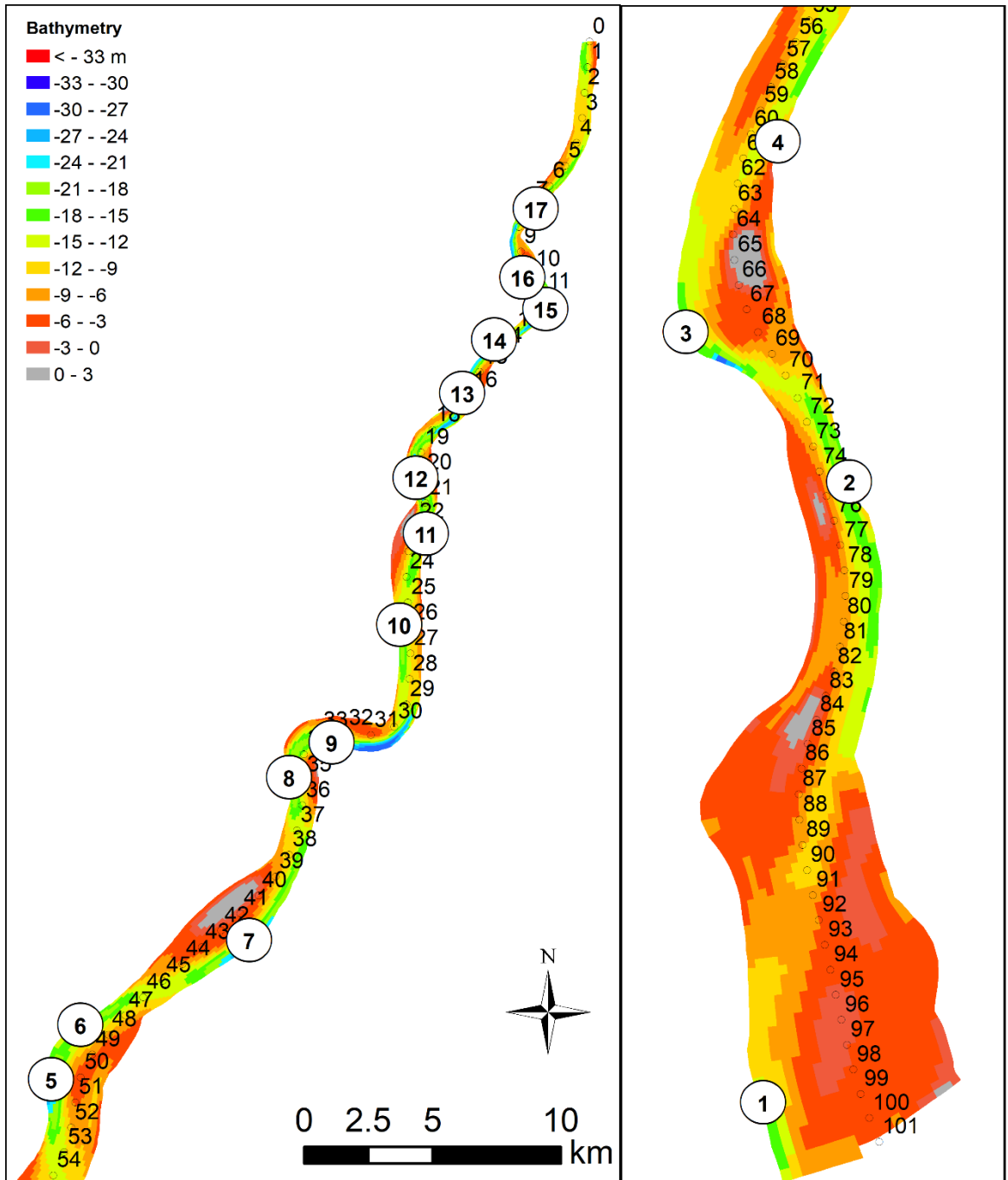


Figure 2-8 Locations of the 17 characteristic eroding banks along the Baleswar River based on digitized bank lines 1988, 1995, 2001, 2011, 2019. The bathymetry is based on the 2011 survey. The chainage coordinates (km) are shown along the river.

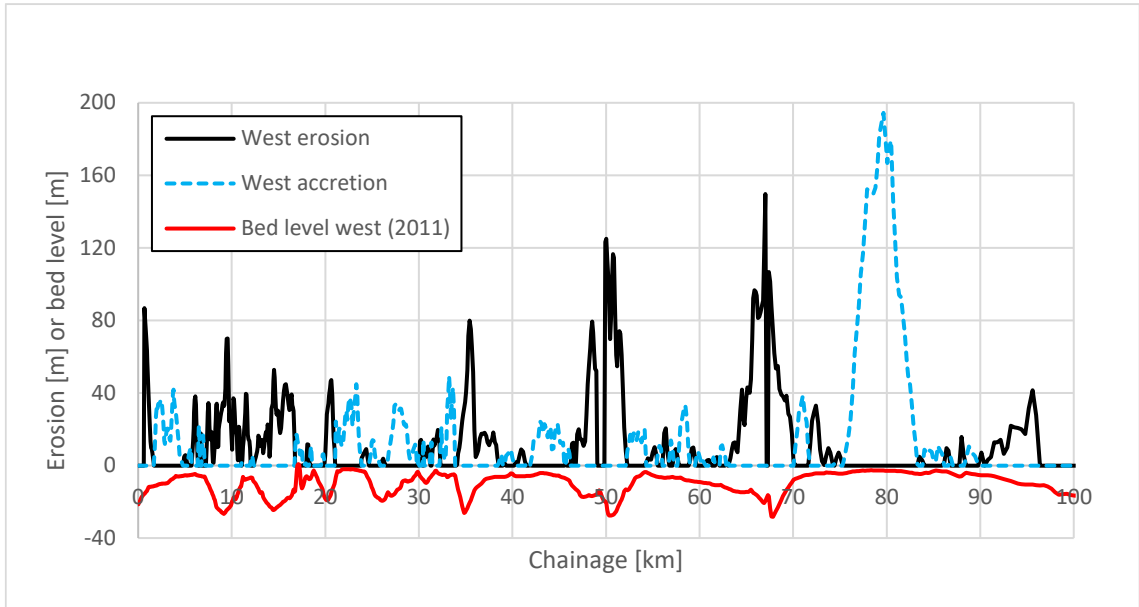


Figure 2-9 Observed west bank erosion 2011-2019 along Baleswar River as a function of chainage.

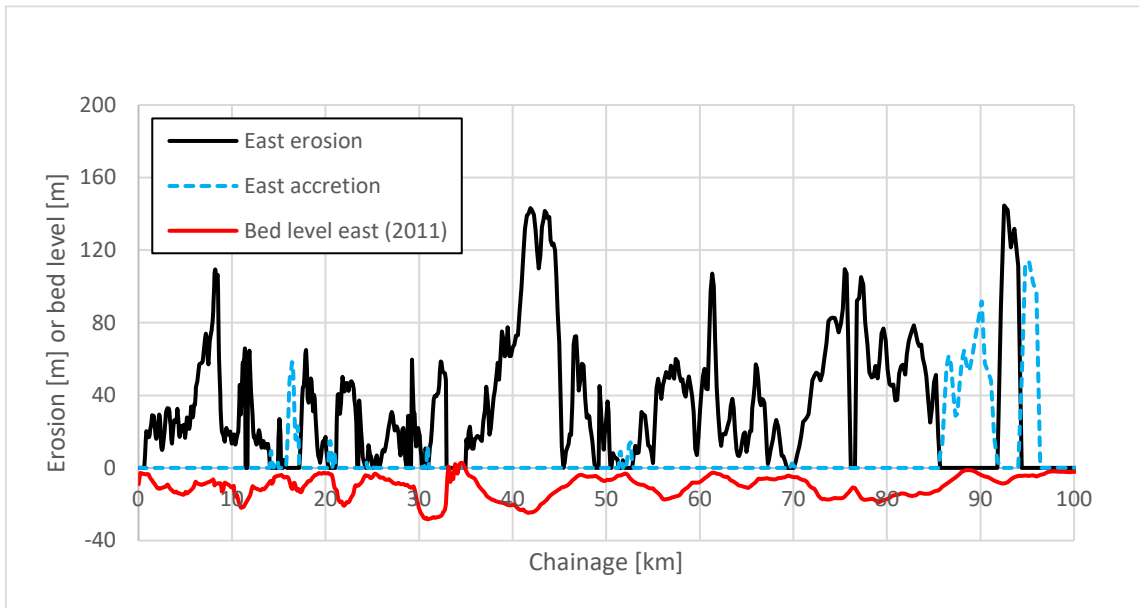


Figure 2-10 Observed east bank erosion 2011-2019 along Baleswar River as a function of chainage.

The bank erosion for the period 2011 to 2019 was processed from the digitised 2011 and 2019 bank lines by determining the distance from the 2011 to the 2019 bank line along normal vectors based on the 2011 bank lines. Bank erosion (and accretion) were calculated as a function of the chainage coordinates, which are also indicated in Figure 2-8. The results are shown in Figure 2-9 and Figure 2-10 where the 2011 bed levels adjacent to the eroding banks are also shown to illustrate the strong correlation between bed level and bank erosion. The figures also show the accretion rates calculated as positive, and it can be seen that accretion rates can be as high as bank erosion rates for some banks. Regarding accretion there are a few very strong signals, the most obvious being along the western bank downstream (chainage 80 km) where a large point bar has been accreting since 1988 as seen on the Landsat images.

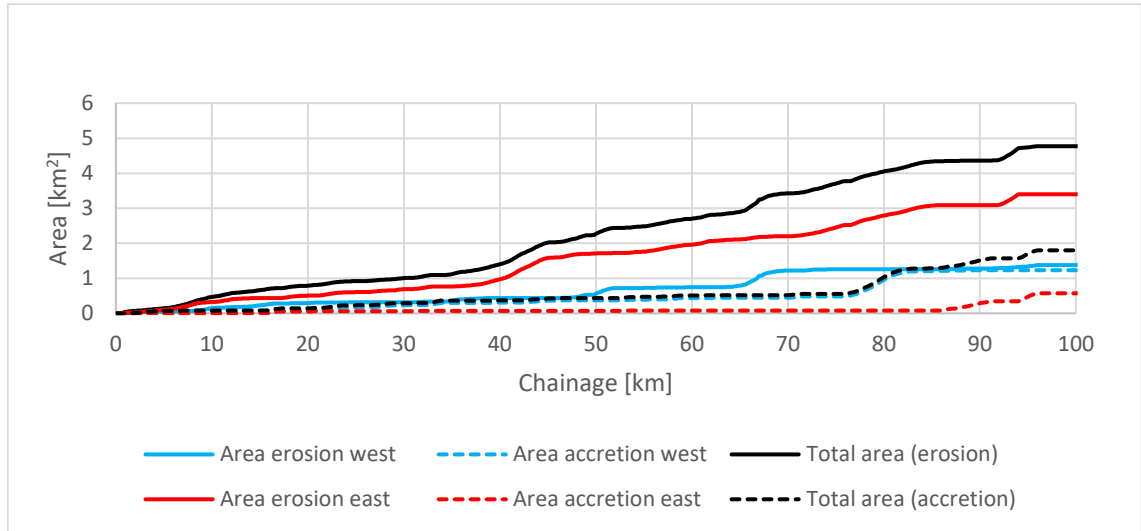


Figure 2-11 Accumulated area curves associated with bank erosion and accretion along each bank and total for the period 2011-2019.

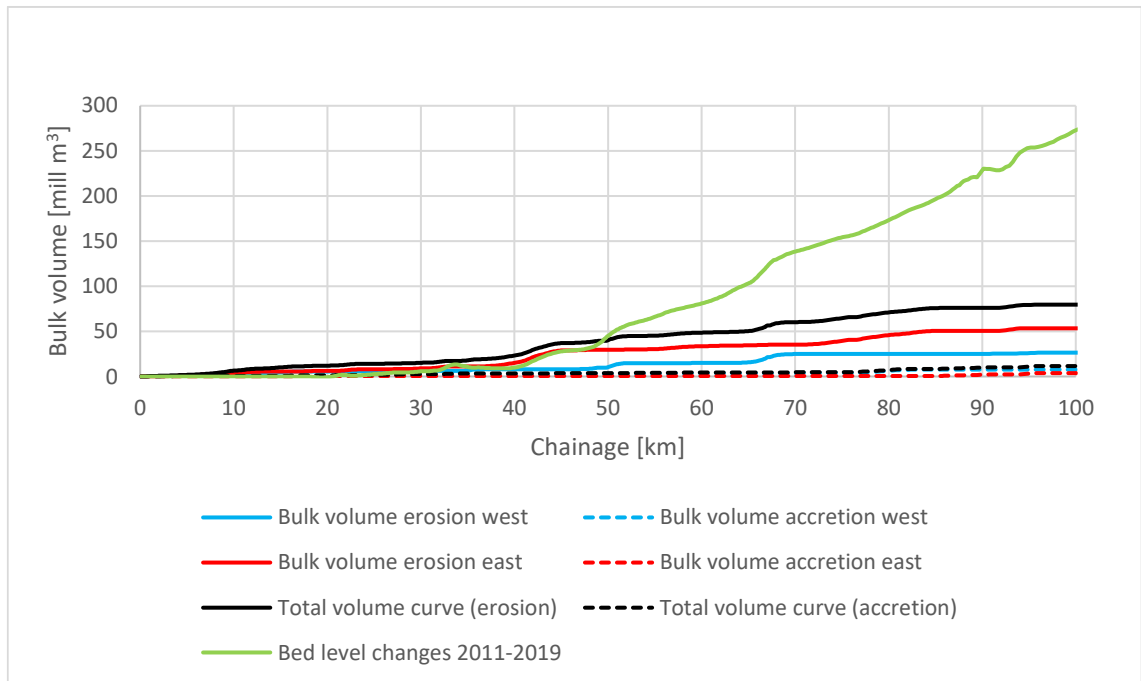


Figure 2-12 Estimated bank erosion accumulated bulk volume curves for Baleswar River 2011-2019 compared to the observed bathymetry changes bulk volume curve for the same period.

Figure 2-11 shows the integrated area curves associated with erosion and accretion along each bank. The figure shows that the west bank lost as much area as it gained, while the east bank clearly eroded much more area than it gained. Accretion amounts to 38% of the eroded area.

Erosion and accretion were also processed into accumulated bulk volume curves by using the bed levels along the banks to calculate the associated volumes, which were integrated as a function of chainage to give more meaningful curves for comparison with model results. The resulting bulk volume curves are shown in Figure 2-12 along with the bulk volume curve associated with the bed level changes for the same period. The bulk volume curves show that bank erosion is not insignificant compared to bed level changes, but the bed level changes clearly dominated the sediment budget. Some of the studied rivers show much bigger influence from bank erosion, but the Baleswar River is a very wide river, and although the eroding banks have very deep water, the volumes are still distinctly lower than those associated with bed level changes.



It was assumed in the calculations that the porosity is the same for the bank and the bed. It is likely that banks have lower porosity than the bed, but there is no data to quantify that.

It can also be seen from the figure that accretion amounts to a very small fraction of the bulk volumes, which are dominated by erosion. This is a common trend in the developed models. While the areas associated with accretion can be significant compared to eroded areas, the accreting banks have much higher bed levels, and therefore the bulk volume curves are much smaller for accretion. For the Baleswar River the total bulk volume associated with accretion is 14% of the bulk volume associated with erosion.

## 2.7 Subsidence

Subsidence was studied as part of the overall project and processed into a raster.

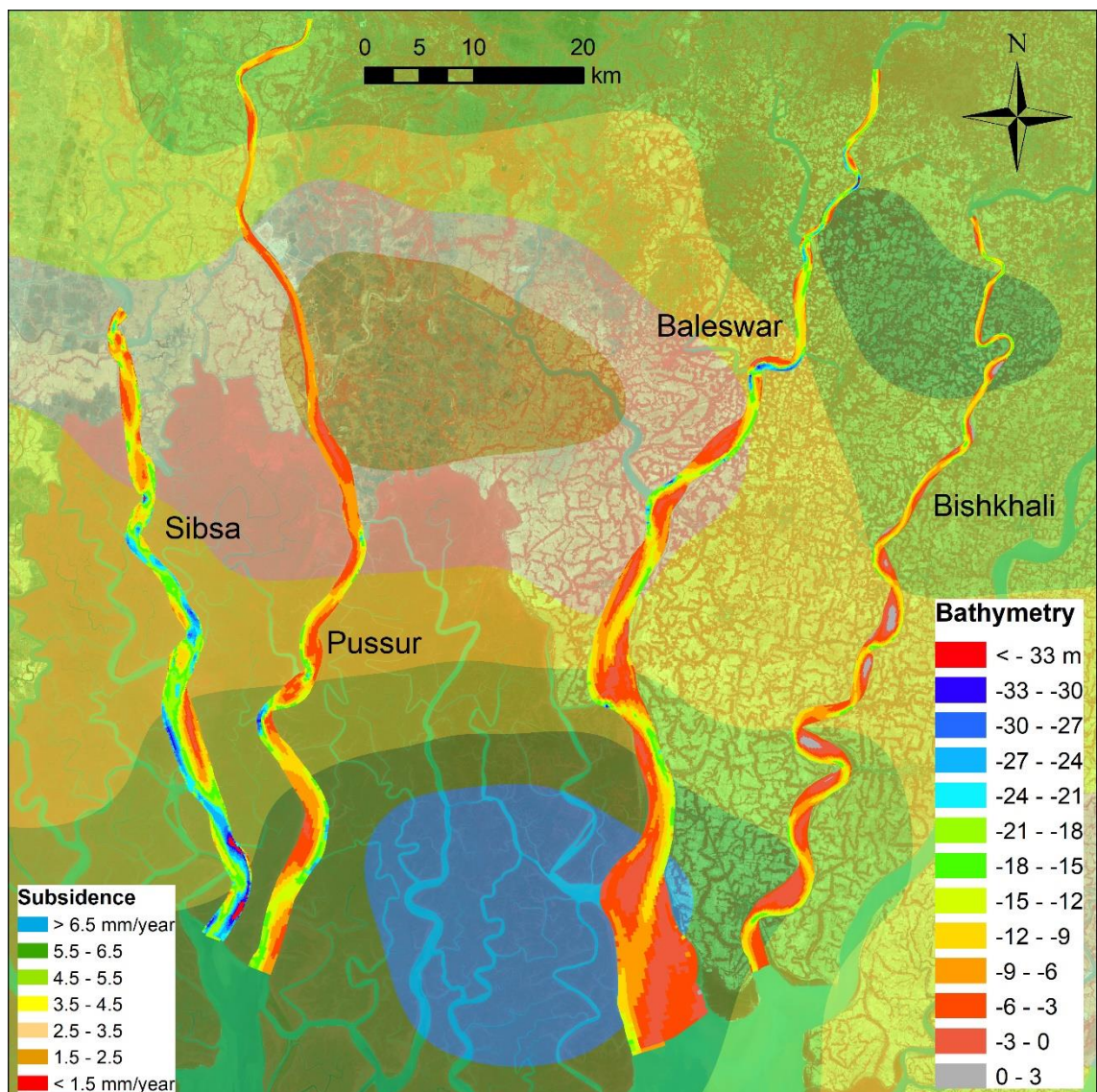


Figure 2-13 Subsidence spatial map in the area where the four models are located.

Figure 2-13 shows the subsidence based on the observations made for the project. The values were contoured to a 100 m raster for use with the MIKE 21C models, and the raster was converted to the individual curvilinear grids.

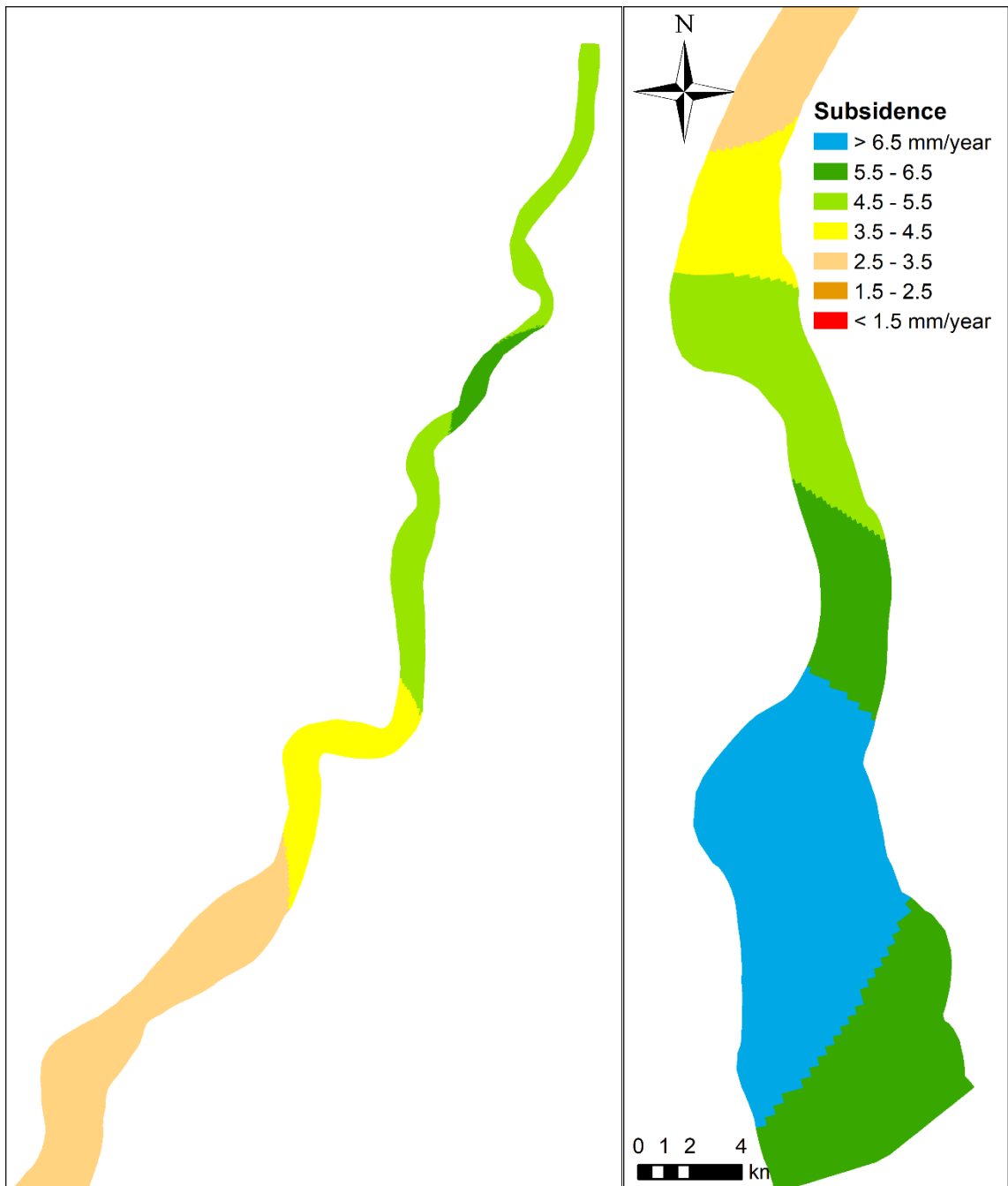


Figure 2-14 Subsidence interpolated to the Baleswar 2019 model grid.

Subsidence for the Baleswar is shown in Figure 2-14. The rates are generally around 5 mm/year, which means that over 30 years the riverbed will be lowered by 150 mm. The bed level changes associated with subsidence are hence small compared to morphological changes.

### 3 Model development

The model development process involves the following components:

- Curvilinear grid conforming to the bank lines
- Bathymetry contoured to the curvilinear grid
- Boundary conditions (upstream, downstream, side channels)
- Hydrodynamic calibration
- Sediment model formulation
- Sediment boundary conditions
- Sediment model calibration
- Bank erosion model calibration

The components are reported in this chapter.

#### 3.1 Grid and bathymetry

Baleswar River has very limited impact from floodplain due to the polders surrounding the river. Hence, the MIKE 21C model does not have to include a floodplain grid.

Initially, the MIKE 21C model was developed with a high resolution (1271x40). This model was used for initially exploring the hydrodynamics and sediment transport.

Originally it was not the intention to run models over several years. However, the available data (2011 and 2019 bathymetries with similar resolution suited for 2D contours) combined with the systematic and slow planform development made it ideal to run simulations hindcasting 8 years (2011-2019) for morphological calibration.

The grid resolution in the river channel was very high in the initial model. It is important to optimise the grid in the river channel to avoid excessive simulation times for the long-term morphological simulations. The model was subjected to stepwise coarsening until it was deemed that further coarsening would impact the result. In this way the coarsest grid that would ensure a grid-independent result was achieved.

The morphological model runs were conducted on a 792x20 curvilinear grid.

##### 3.1.1 2011 model grid and bathymetry

The 2011 model grid and bathymetry were used for morphological model calibration and validation. Figure 3-1 shows the 792x20 curvilinear grid conforming to the 2011 bank lines, while the 2011 curvilinear bathymetry is shown in Figure 3-2.

The longitudinal cell size ( $\Delta s$ ) varied in the range 26-640 m (average of 129 m), while the transverse cell size ( $\Delta n$ ) varied in the range 12-554 m (average 87 m). For the cell area the range was 303-403,000 m<sup>2</sup> (average 16,430 m<sup>2</sup>).

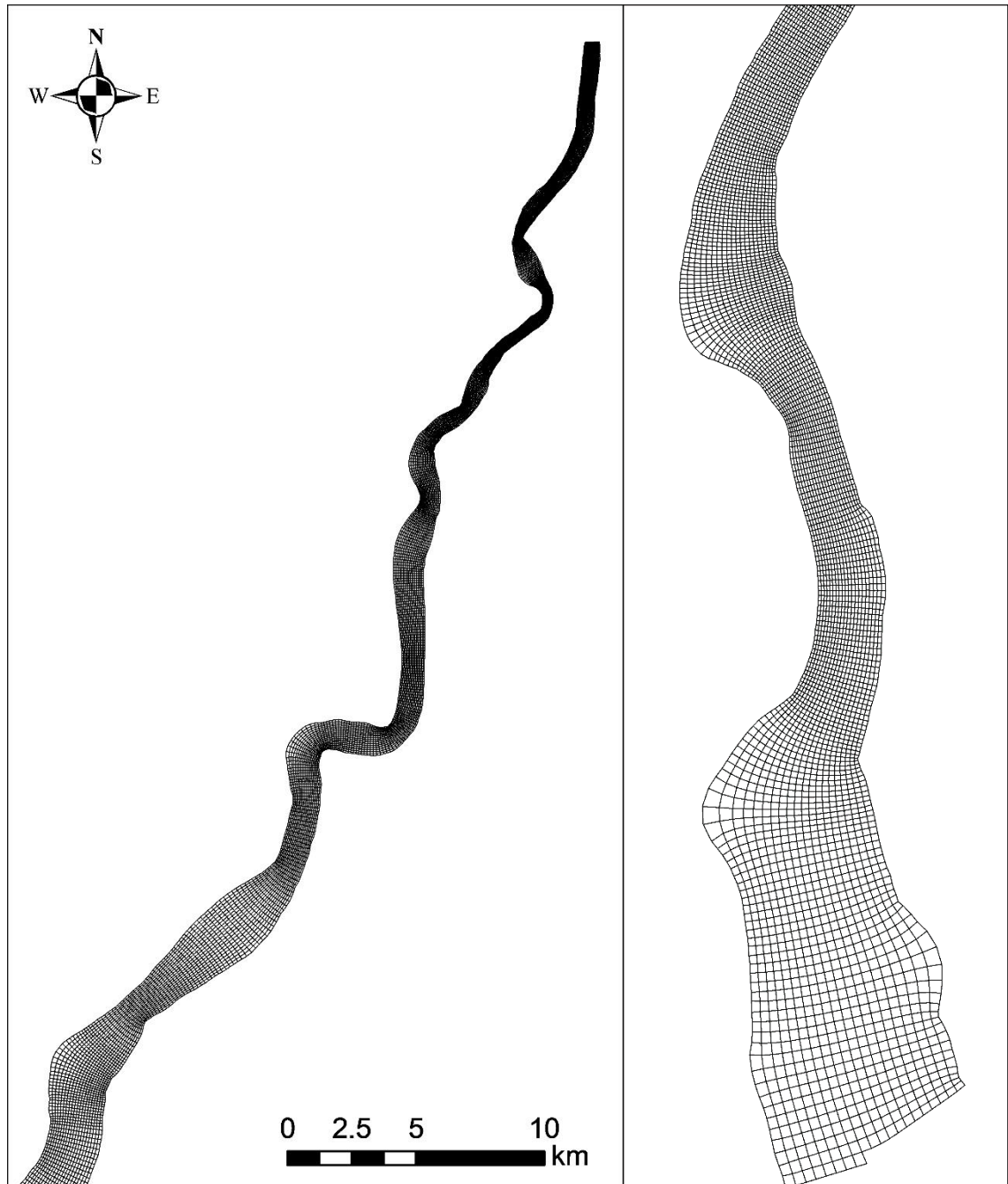


Figure 3-1 Baleswar River 792x20 curvilinear grid conforming to the 2011 bank lines.

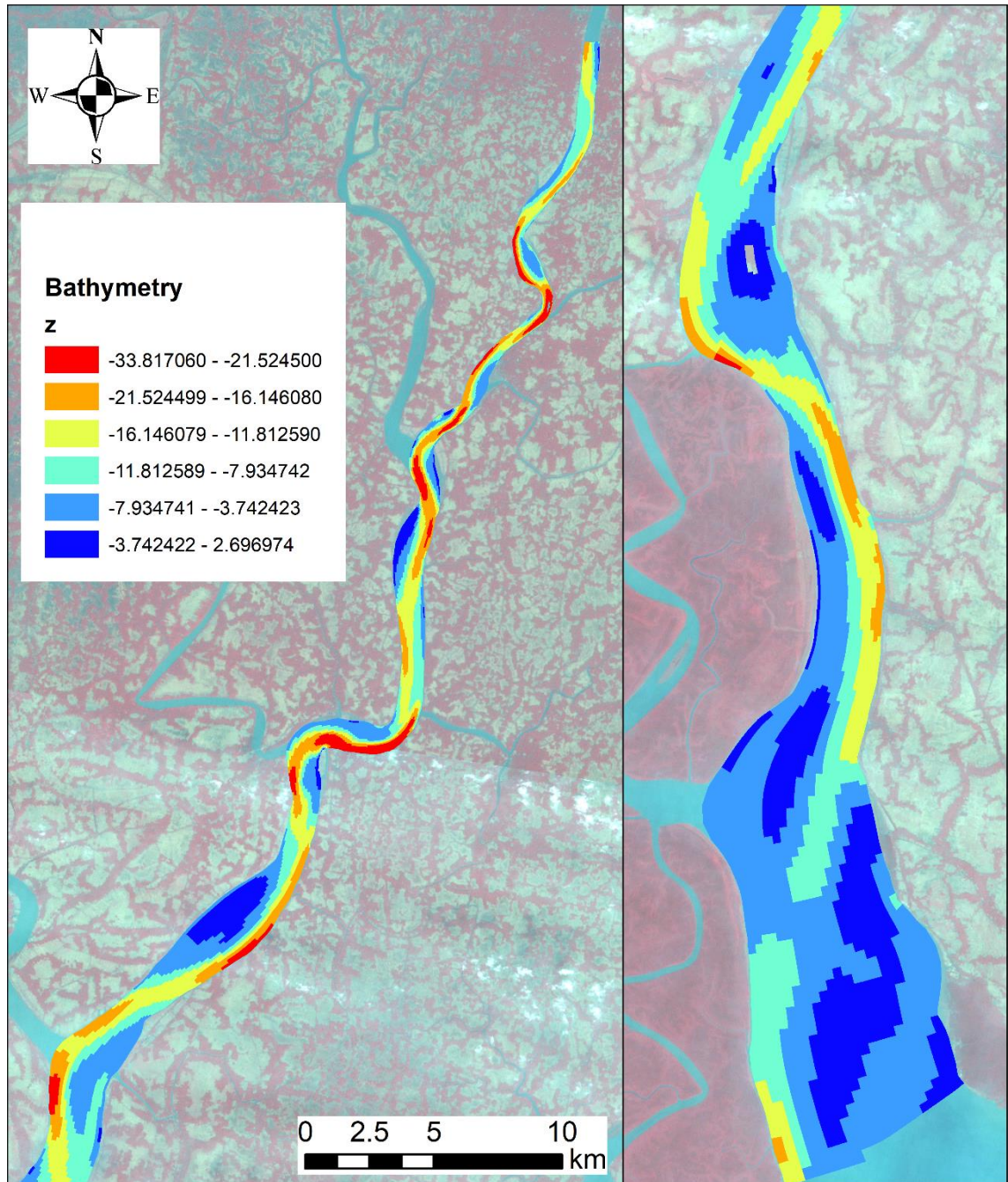


Figure 3-2 Baleswar River 2011 bathymetry contoured on the curvilinear grid with the 2011 Landsat image as background.

### 3.1.2 2019 model grid and bathymetry

The 2019 model was developed from the 2019 bathymetry collected for the project and the 2019 bank lines digitized from the 2019 Landsat image.

The 2019 model will be used for scenario simulations, e.g. bank erosion forecasting.

The 2019 bathymetry is shown in Figure 3-3.

It is not possible to tell the difference between the 2011 and 2019 grids without zooming in on local areas. Figure 3-4 shows a comparison of the 2011 and 2019 grids in a local area located at Polder 39/2 where the eastern bank exhibits high erosion rates.

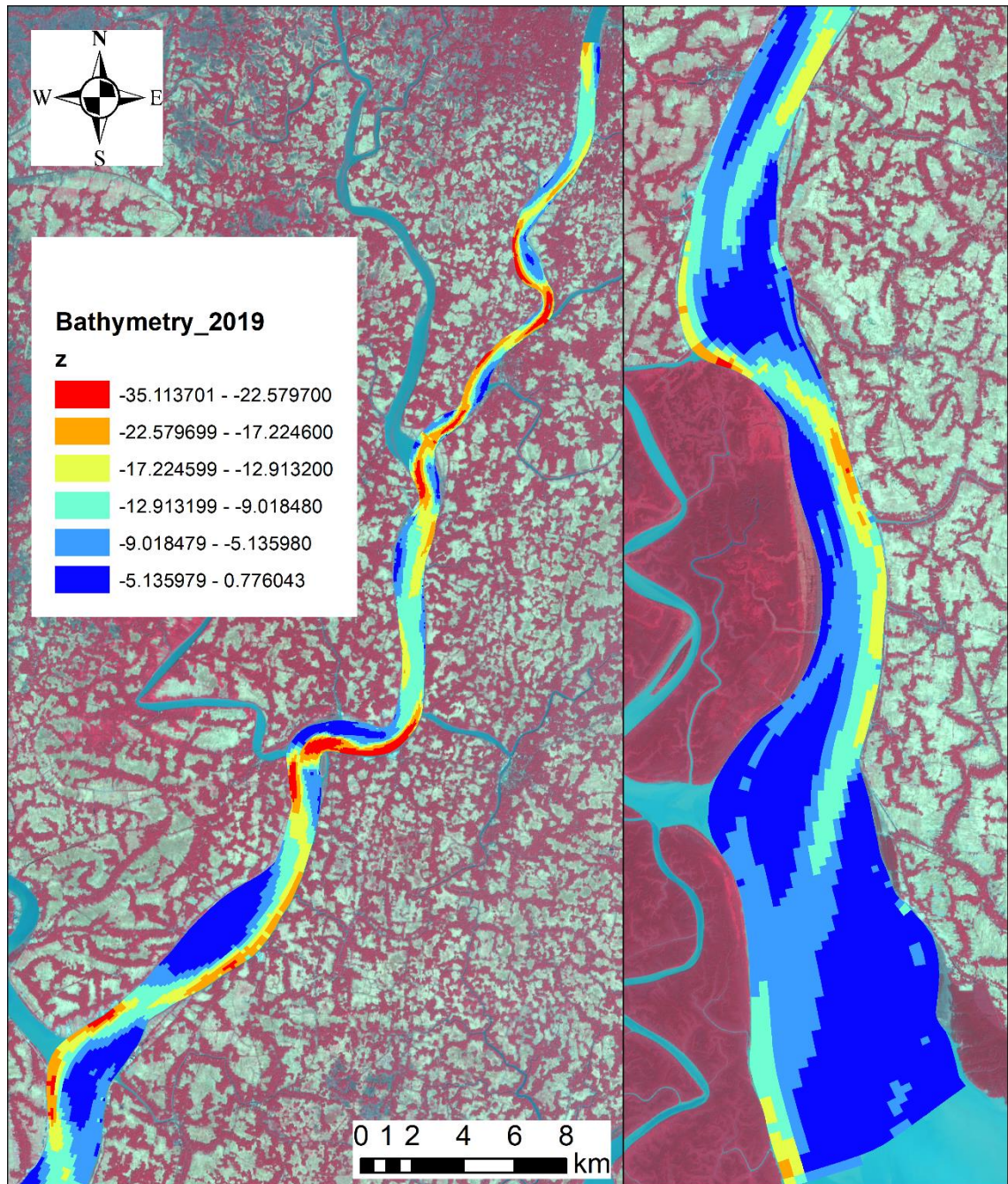


Figure 3-3 Baleswar River 2019 bathymetry on the 2019 grid with the 2019 Landsat image as background.

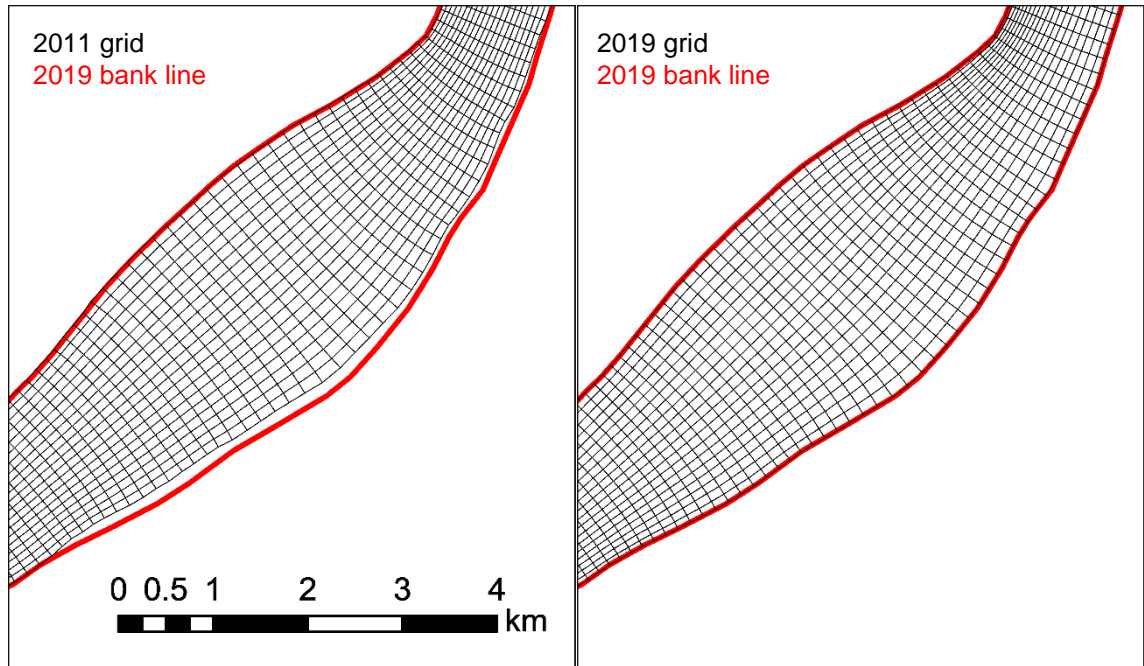


Figure 3-4 Illustration of the differences between the 2011 and 2019 grids, which cannot be identified without looking at the details. This is just upstream of the Gashiakali inflow where the eastern bank has been eroding consistently. The 2019 grid conforms to the 2019 bank line, as seen in the figure. The bank line moved roughly 100 m from 2011 to 2019.

### 3.2 Hydrodynamic boundary conditions

The Baleswar River model has one upstream boundary, one downstream boundary and several source/sink points representing flows from/to side channels. Upstream boundary and sources were collected from the calibrated and validated SWRM for 2011 and 2015. The water level of Haringhata was correlated from Hiron Point used as downstream boundary for the year 2011. Measured water level data at Fakirghat was used as downstream water level boundary for the year 2015.

The side channels locations are shown along with the model bathymetry and chainage system in Figure 3-5.

It is important to include the side channels in the hydrodynamic model, as the flow exchanges with these side channels are not insignificant. Without the side channels it is not possible to get the correct discharges in the Baleswar River model.

With the side channels added, the MIKE 21C model becomes very similar to the MIKE 11 SWRM model, with the exception that the MIKE 21C model does not include floodplain. The MIKE 11 model appears to include some floodplain, but today most of the floodplain around Baleswar River is polder, so one should not expect any floodplain influence, except in the downstream end (Sundarbans). This opens for the possibility that the MIKE 21C model will not calibrate using the same parameters as MIKE 11.

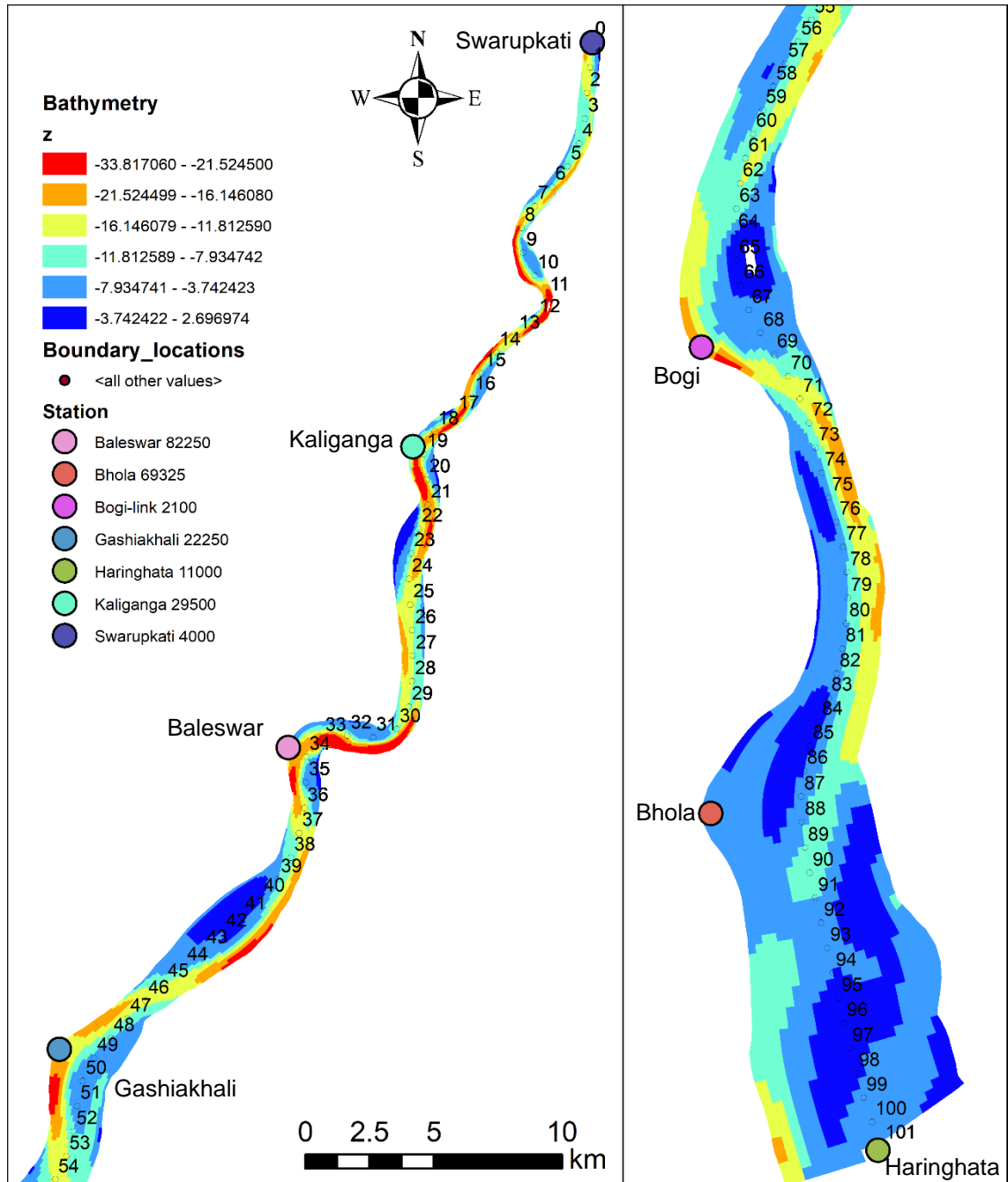


Figure 3-5 Baleswar River 2011 bathymetry, boundaries and chainages used for showing longitudinal variations.

The locations of the boundaries are shown in Figure 3-5 along with the chainages used for presentation of longitudinal variations. These are conveniently shown together to avoid too many figures.

The boundaries of the MIKE 21C models 2011 and 2015 are listed in Table 3-1.

At the time of model development, no continuous time-series of water level and flow boundary conditions were available for the period 2011-2019. Instead, the time-series from 2011 were repeated 8 times and used in the model to represent the 8 years in the period 2011-2019.



Table 3-1 MIKE 21C model boundaries for 2011 and 2015.

Boundary	2011	2015
Upstream flow	Sarupkati (SW-400)	Sarupkati (SW-400)
Source1: Flow	Kaliganga (SW-29500)	Kaliganga (SW-29500)
Source2: Flow	Baleswar (SW-82250)	Baleswar (SW-82250)
Source3: Flow	Gashiakhali (SW-22250)	Gashiakhali (SW-22250)
Source4: Flow	Bogi-Link (SW-2450)	Bogi-Link (SW-2450)
Source5: Flow	Bhola (SW-71575)	Bhola (SW-71575)
Downstream Water Level	Haringhata from Hiron point	Measured in Fakirghat

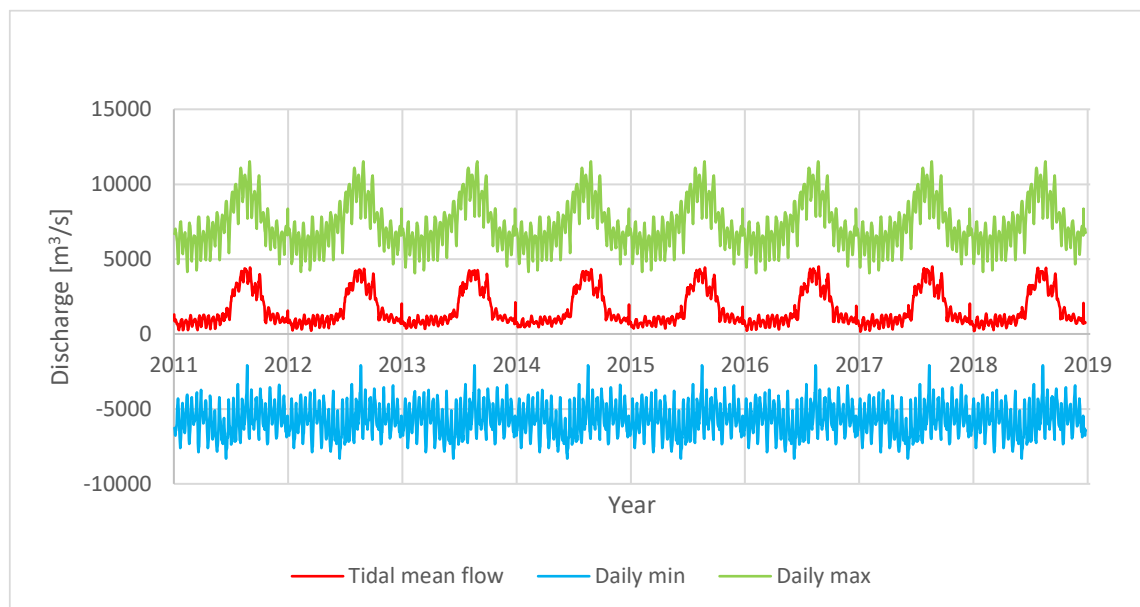


Figure 3-6 Daily minimum, maximum and mean flows 2011-2019 upstream boundary (Swarupkati) in the Baleswar River model. It is noted that the Baleswar River model repeated the 2011 SWRM results for the period 2011-2019.

Figure 3-6 shows the daily mean flow (flow averaged over two tidal cycles of 24 hour and 50 minutes) at Swarupkati along with the corresponding minimum and maximum values. The daily mean flow has a clear seasonal signal with a small mean flow in the dry season and a clear and sizeable mean flow during the monsoon. The annual signal is the same for the Baleswar River due to the repeating 2011 hydrograph.

The tidal discharges at the upstream end are up to about 11,000 m<sup>3</sup>/s, while the monsoon net flow is up to 4,000 m<sup>3</sup>/s.

### 3.3 Hydrodynamic boundary conditions for scenario simulations

The SWRM was used for generating boundary conditions for the MIKE 21C models with the inclusion of subsidence in the SWRM cross-sections and sea level rise in the Bay of Bengal tidal water level conditions, both calculated for the year 2050. A gradual calculation of annual variations from 2019 to 2050 is cumbersome because it would require preparation of new cross-sections every year due to subsidence, so instead only the years 2019 and 2050 were used in the MIKE 21C models. Both years simulations were made using the 2019 SWRM without (baseline) and with subsidence and climate change.

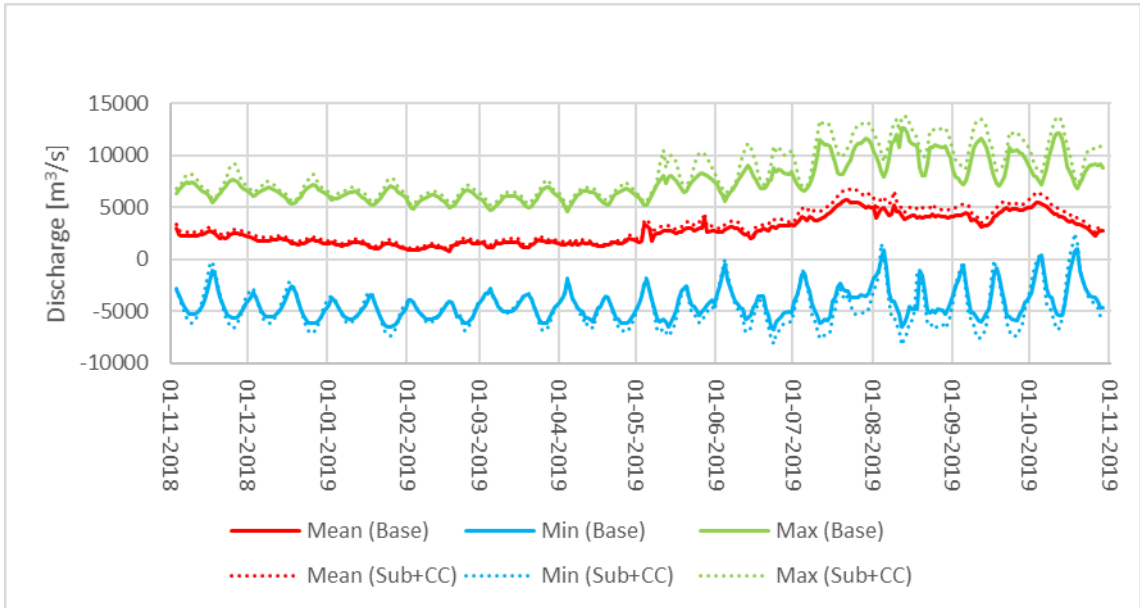


Figure 3-7 Daily minimum, maximum and mean flows 2018-2019 upstream boundary in the Baleswar River model for the two cases Base and Sub+CC.

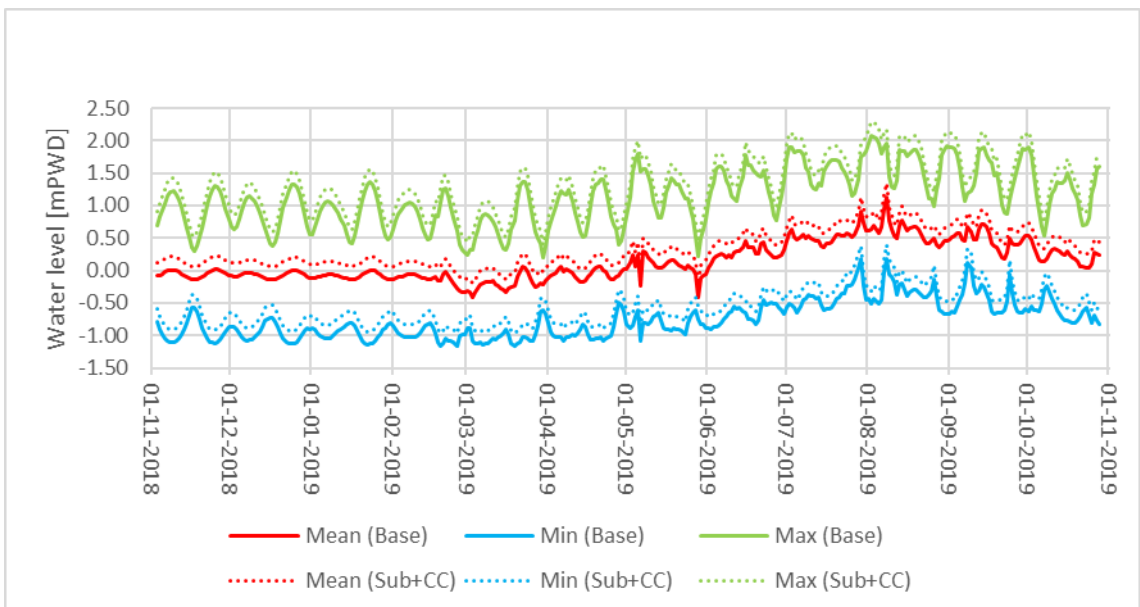


Figure 3-8 Daily minimum, maximum and mean water levels 2018-2019 downstream boundary in the Baleswar River model for the two cases Base and Sub+CC.

IWM ran the SWRM for the period:

- 2 November 2018 00:00
- 29 October 2019 16:30

Results were extracted for the Baleswar model for the two scenarios:

- Existing conditions (baseline)
- Climate Change and Subsidence (Sub+CC)

Baleswar has the following open boundaries:

- Upstream discharge
- Downstream water level

There are also several side channels in the Baleswar model for which the same procedure was followed. The boundary locations are shown in Figure 3-5.

It is not meaningful to show the full time-series due to the detail. Instead, the tidal time-series were post-processed to show the daily mean, minimum and maximum for the discharges upstream and for the water levels downstream.

Figure 3-7 shows the post-processed daily discharges. The results show that the 2019 SWRM has some dry season net flow, which was also the case with the SWRM model used for the model development. The monsoon net flows are smaller than the tidal discharges. Above all, the post-processed data suggests that in general the discharges increase with subsidence and climate change, which makes sense considering that all tide levels in the Bay of Bengal are increased and the bathymetry is lowered due to subsidence.

The water levels at the downstream boundary daily post-processed values are shown in Figure 3-8. This figure shows the expected rise in the water level due to climate change. The average tidal water level increase at the downstream boundary is 21 cm.

Future sediment concentration boundary conditions were not altered compared to existing concentrations. It should be kept in mind that the model uses sediment concentrations and not sediment fluxes, so while sediment concentrations are considered unchanged in the future, the sediment fluxes can change.

### 3.4 Hydrodynamic calibration and validation

The calibrated and validated hydrodynamic model is needed to develop a reliable MIKE 21C model capable of predicting sediment transport, bed levels and bank erosion.

The model was calibrated for 2011, while validation was carried out for 2015 and 2016. The 2011 grid and bathymetry were used in all calibration and validation simulations.

The resistance calibration was partly inherited from the MIKE 11 SWRM. The Manning number varies from 35 m<sup>1/3</sup>/s upstream to 50 m<sup>1/3</sup>/s downstream. Those Manning numbers also work in the MIKE 21C model.

The Manning number variation implies that the upstream end is sandy, while the downstream end is muddy. Sediment samples are available showing the latter, while the former is not documented by sediment samples (M=35 m<sup>1/3</sup>/s is typical for sand and difficult to believe for mud). The behaviour of the morphological model also implies that the upstream end should be sandy; the upstream bars are not always realistically simulated with a mud model.

### 3.4.1 Hydrodynamic model calibration for 2011

Figure 3-9 shows the location of the observation stations used for calibration of the 2011 model.

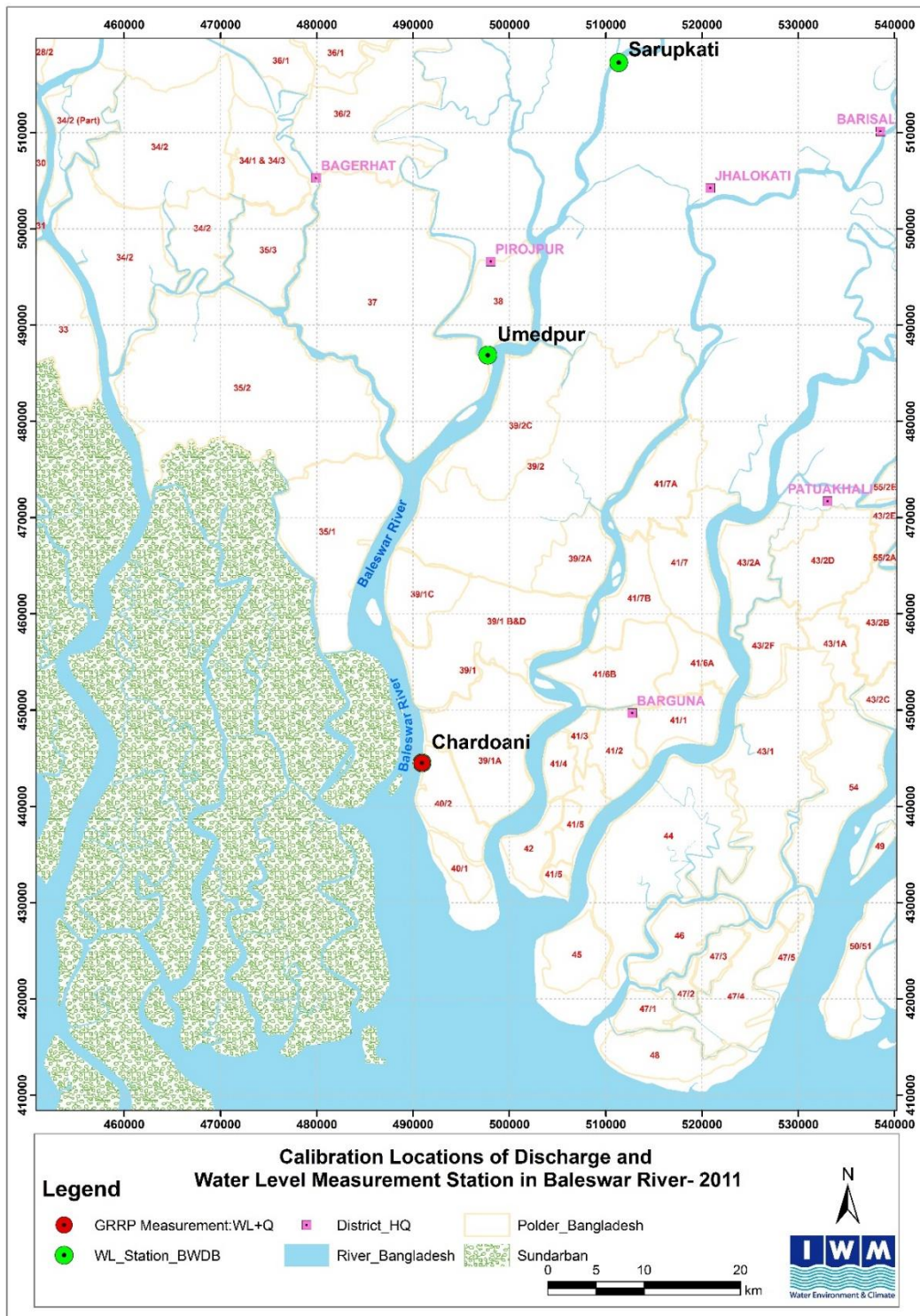


Figure 3-9 Discharge and water level calibration locations for 2011.

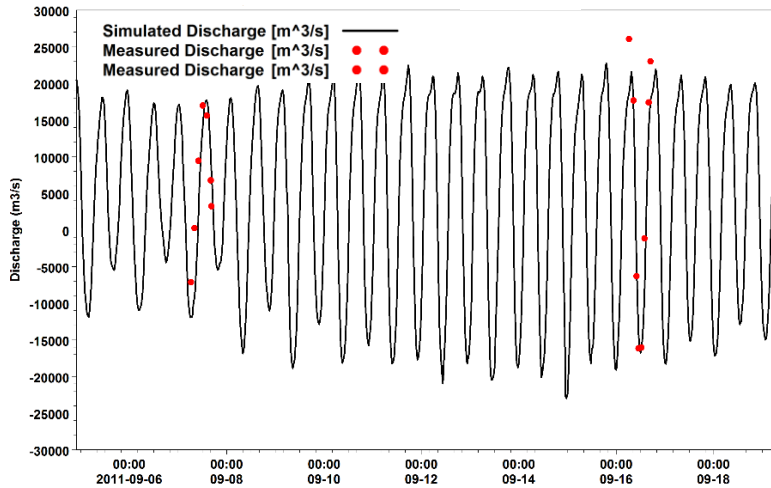


Figure 3-10 Discharge calibration at Chardoani during 2011 monsoon.

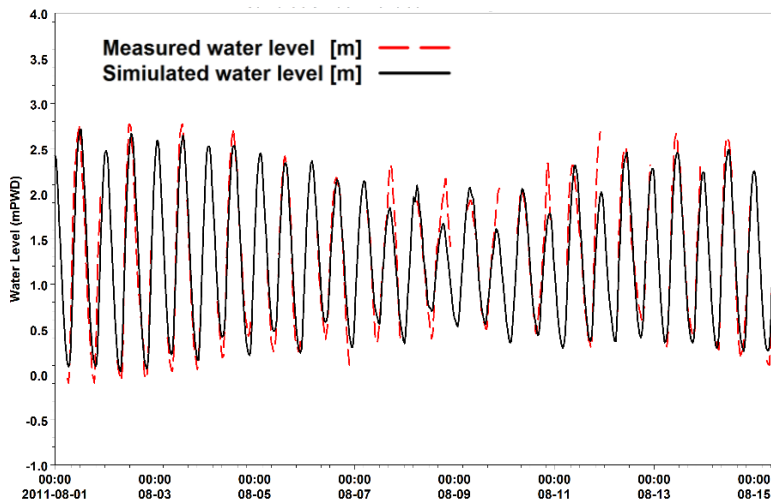


Figure 3-11 Water level calibration at Chardoani during 2011 monsoon.

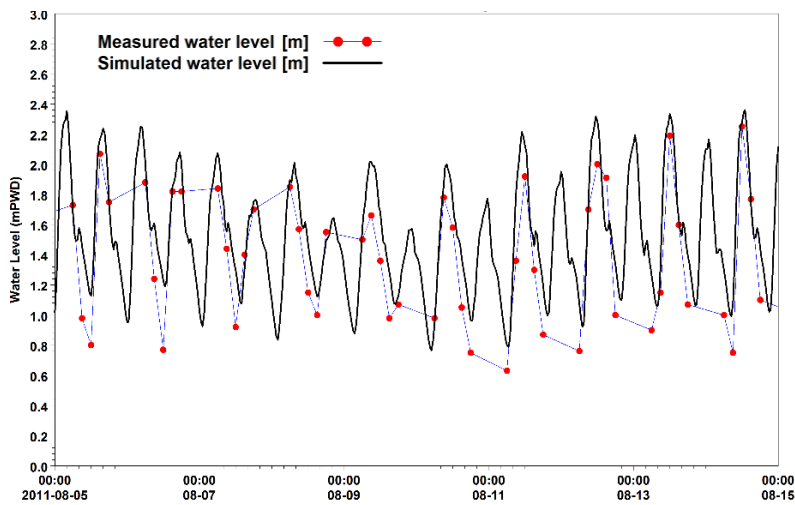


Figure 3-12 Water level calibration of BWDB station at Umedpur 2011 (6-hourly data).

Figure 3-10 shows the discharge calibration at Chardoani in Baleswar River during the 2011 monsoon. The computed discharge is underpredicted, especially in ebb flow. This may occur due to upstream boundary condition from South West Regional Model or be caused by the water level condition at the downstream boundary.

Figure 3-11 shows the calibration for 2011 at Chardoani. Chardoani is not very far from the downstream boundary and hence strongly influenced by the downstream water level boundary condition. The calibration suggests that the downstream boundary condition could be better.

Although there are shortcomings, the water level calibration is satisfactory.

Figure 3-12 shows the water level calibration at Umedpur in Baleswar River during 2011 monsoon. Although the Umedpur water level data is only 6-hourly, it is still useful for validating the water level calibration at this location. The phase is captured well by the model, but the water levels are a bit too low at Umedpur.

### 3.4.2 Hydrodynamic model validation for 2015

The 2015 validation is presented in this section.



Figure 3-13 Locations of discharge and water level stations used for 2015 validation.

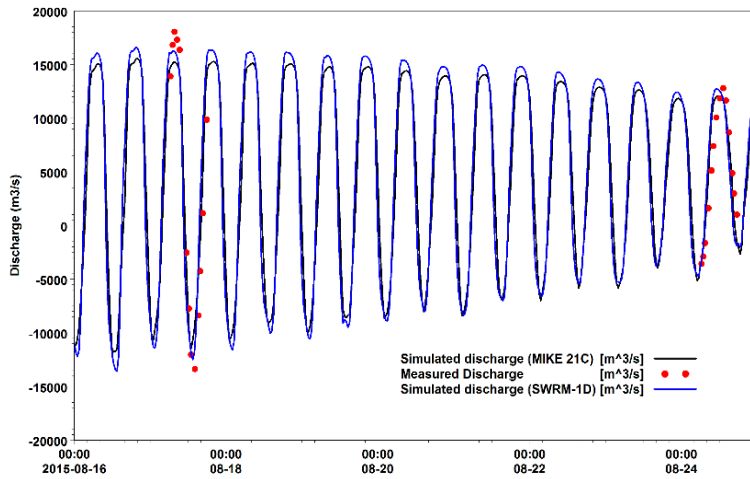


Figure 3-14 Discharge validation at Charkhali for 2015 (August), also showing the SWRM 2015 results.

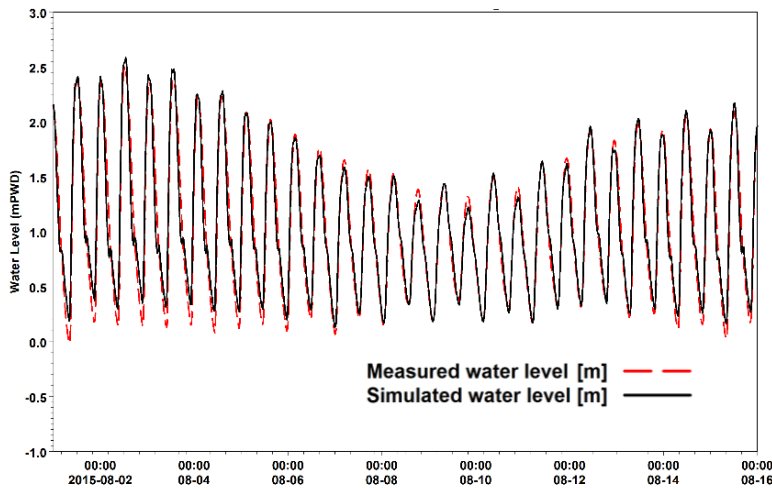


Figure 3-15 Water level calibration at Tele Khali Bazar for 2015 (August).

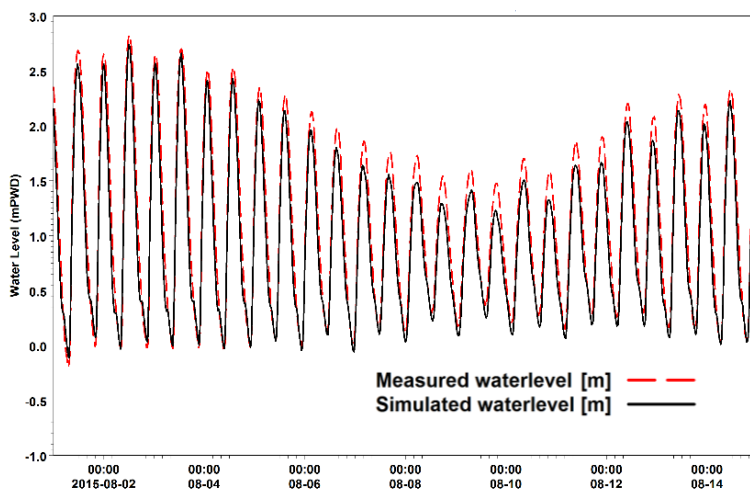


Figure 3-16 Water level validation at Tafalbari Lanchghat for 2015 (August).

The model was validated with the measured water level and discharge measurement for 2015. The locations of the measurement stations are shown in Figure 3-13. The validation plots for the year 2015 are shown in Figure 3-14, Figure 3-15 and Figure 3-16.

The validation for 2015 is very satisfactory.

### 3.4.3 Hydrodynamic model validation for 2016

The hydrodynamic model was also validated for 2016 at the Rayenda (Sarmasi) station located just downstream of the Gashiakhali confluence (location shown in Figure 3-5).

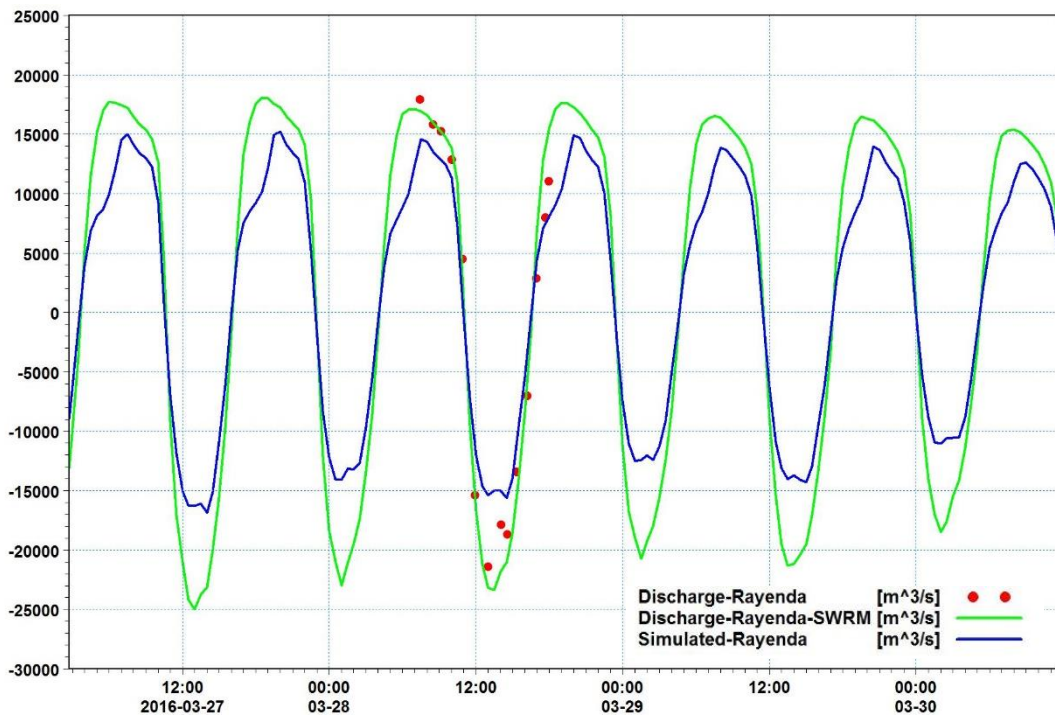


Figure 3-17 Discharge validation at Rayenda (Sarmasi) for 2016.

It was found from the 2D model validation (2016) at Rayenda that the discharges were too low, see Figure 3-17. The SWRM gives much better results, but when inspecting the 1D model for 2016, it uses 2009 cross-sections in the Baleswar River, which includes some floodplain. This explains why the 1D model captures the discharges correctly – which must be for the wrong reasons - while the 2D model does not. However, it is not defensible to use floodplain in the cross-sections for Baleswar River due to the polders. It is difficult to argue for the use of the (coarse) 2009 cross-sections in the 1D model, considering that the 2016 SWRM had more recent cross-sections available. However, it is possible that 2009 cross-sections were selected because they gave better results, but this does not help the 2D model. The 2D model uses boundaries from the 1D model, but without floodplain added, the tidal prism in the 2D model will be smaller than in the 1D model, and therefore the 2D model gives too low discharges.

It is not a satisfactory state of affairs that the 2016 SWRM uses cross-sections that contain obviously incorrect floodplain storage. However, little can be done to reproduce the SWRM discharges at Sarmasi without using the incorrect floodplain storage, unless the MIKE 21C calibration is modified.

The comparison suggests that the 2016 SWRM reproduced the correct discharges for the wrong reasons. Due to this, the importance of this validation was downplayed, while it is shown for the sake of completeness.



### 3.5 Sediment model

The bed samples from the Baleswar River show that the riverbed is dominated by cohesive sediment with very little sand. Hence, a 1-fraction mud model was adopted.

The cohesive sediment was modelled using the traditional cohesive sediment erosion (E) and deposition (D) functions, see Mehta et al. (1989).

The erosion rate [g/m<sup>2</sup>/s] was calculated from:

$$E = E_0 \left( \frac{\tau'}{\tau_{ce}} - 1 \right)^n, \tau' > \tau_{ce}$$

The deposition rate [g/m<sup>2</sup>/s] was calculated from:

$$D = w_s \gamma_0 C \left( 1 - \frac{\tau'}{\tau_{cd}} \right), \tau' < \tau_{cd}$$

Where:

E Erosion rate [g/m<sup>2</sup>/s]

D Deposition rate [g/m<sup>2</sup>/s]

E<sub>0</sub> Erosion coefficient [g/m<sup>2</sup>/s]

τ' Skin friction shear stress

τ<sub>ce</sub> Erosion shear stress threshold [N/m<sup>2</sup>]

τ<sub>cd</sub> Deposition shear stress threshold [N/m<sup>2</sup>]

C Simulated concentration [g/m<sup>3</sup>]

w<sub>s</sub> Fall velocity [m/s]

n Exponent (non-linearity)

γ<sub>0</sub> Ratio between near-bed and depth-integrated concentration (optional)

The calibrated parameters were:

$$\tau_{ce} = 0.2 \text{ N/m}^2$$

$$\tau_{cd} = 0.1 \text{ N/m}^2$$

$$E_0 = 0.02 \text{ g/m}^2/\text{s}$$

$$w_s = 1 \text{ mm/s}$$

$$n=1$$

$$\gamma_0 = 1$$

Porosity 0.6

It is noted that these parameters were only initially adjusted to match the observed concentrations, while more detailed adjustments were made by comparing to observed bed level changes in 2011-2015 and 2011-2019. Due to the large clay content in the suspended sediment, it is difficult to match the observed concentrations. If attempting to match observed sediment concentrations, the Baleswar River model will exhibit too much morphological activity, which makes perfect sense considering that a large portion of the suspended sediment is clay with very low morphological activity.

### 3.6 Sediment transport boundary conditions

There are three types of boundary conditions in the Baleswar River model:

- Upstream concentration 200 g/m<sup>3</sup>
- Bay of Bengal concentration 400 g/m<sup>3</sup>
- Side channels concentration 200 g/m<sup>3</sup>

The sediment boundary conditions were set to constant in the Baleswar River model because data were not available to allow a more sophisticated approach. This approach has implications only for the model results close to the model boundaries.

### 3.7 Calibration against observed bed level changes

The best way to calibrate a morphological model is always to hindcast the observed morphological development. In the present project, bathymetries for 2011, 2015 and 2019 are available. All three datasets have been collected by IWM using similar resolution and survey methodology. The time span between these two datasets and their quality offers an excellent basis for accurately determining the morphological changes and thereby the opportunity for calibrating the morphological model. The 2015 bathymetry has some significant gaps and was therefore never used as a model input bathymetry but was used for calibration running 2011-2015.

Figure 3-18 compares the model to observations for the period 2011-2015, while Figure 3-19 shows the same comparison 2011-2019. The latter was used for calibration, while the former was used for validation.

The bed level developments hindcasted by the model match the observations satisfactorily.

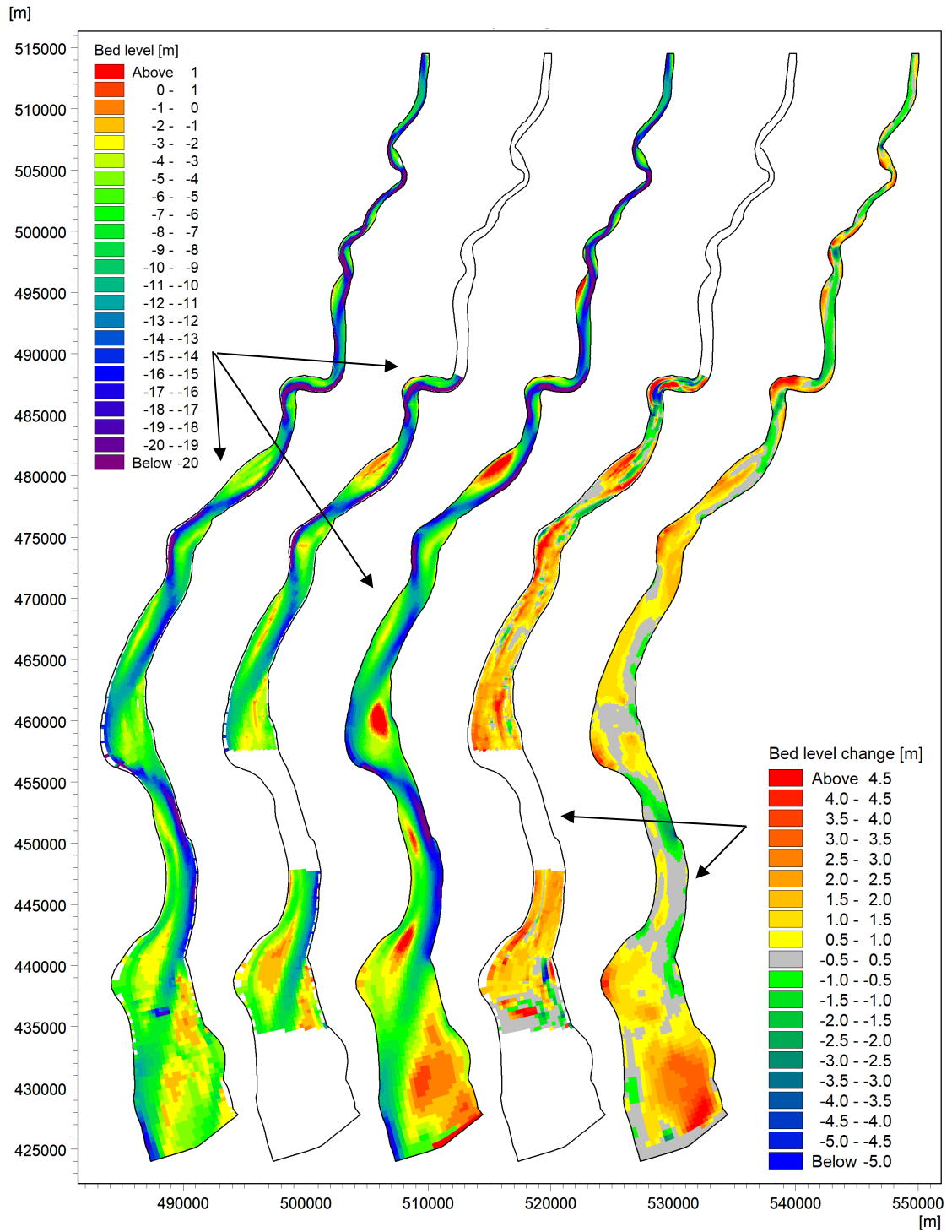


Figure 3-18 Comparison of observed and simulated bathymetry development 2011-2015. From left: Observed bathymetry 2011, Observed bathymetry 2015, Simulated bathymetry 2015, Observed bed level changes 2011-2015, Simulated bed level changes 2011-2015.

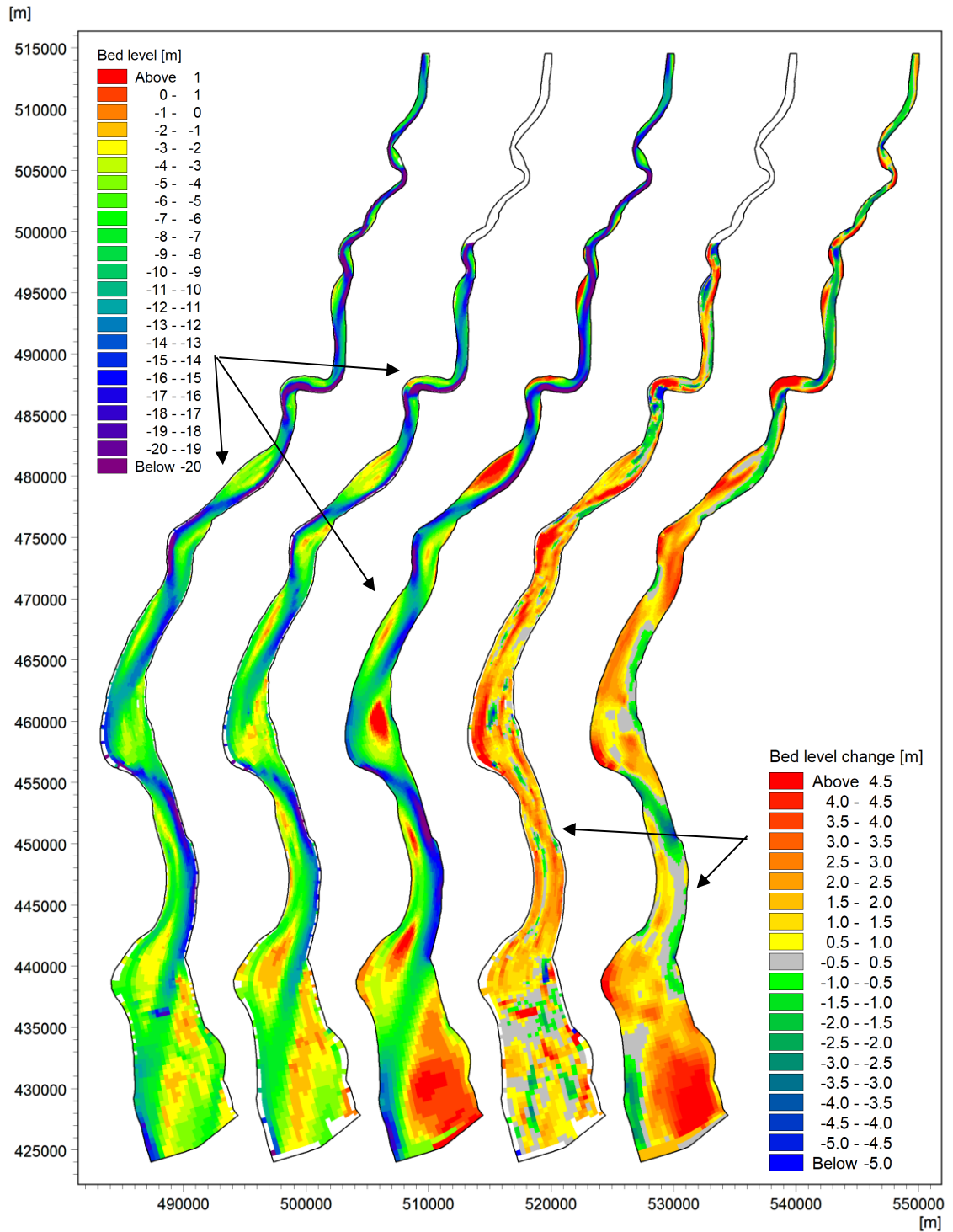


Figure 3-19 Comparison of observed and simulated bathymetry development 2011-2019. From left: Observed bathymetry 2011, Observed bathymetry 2019, Simulated bathymetry 2019, Observed bed level changes 2011-2019, Simulated bed level changes 2011-2019.

### 3.8 Longitudinal validations

The spatial bed levels and bed level changes are very useful for showing the model calibration. Another way to compare is to use volume curves, which are calculated by width-integrating the bed level changes to obtain:

- Width-integrated bed level change as a function of chainage
- Accumulated bulk volume curve showing the deposition upstream of the considered chainage

The volumes are calculated from bed level changes and are hence bulk volumes.

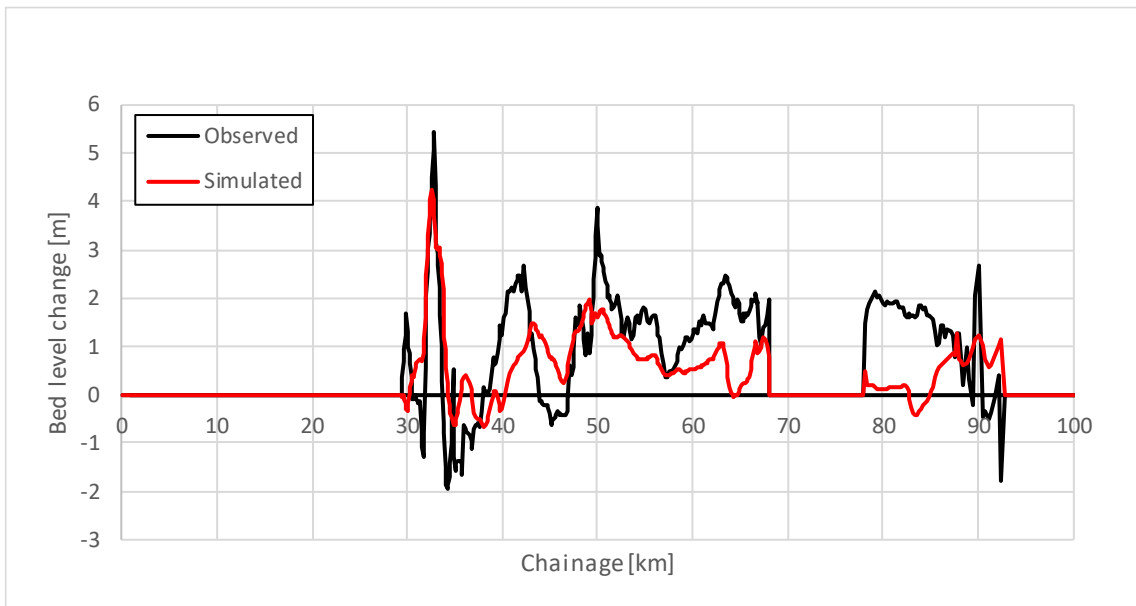


Figure 3-20 Comparison of observed and simulated width-integrated bed level changes 2011-2015.

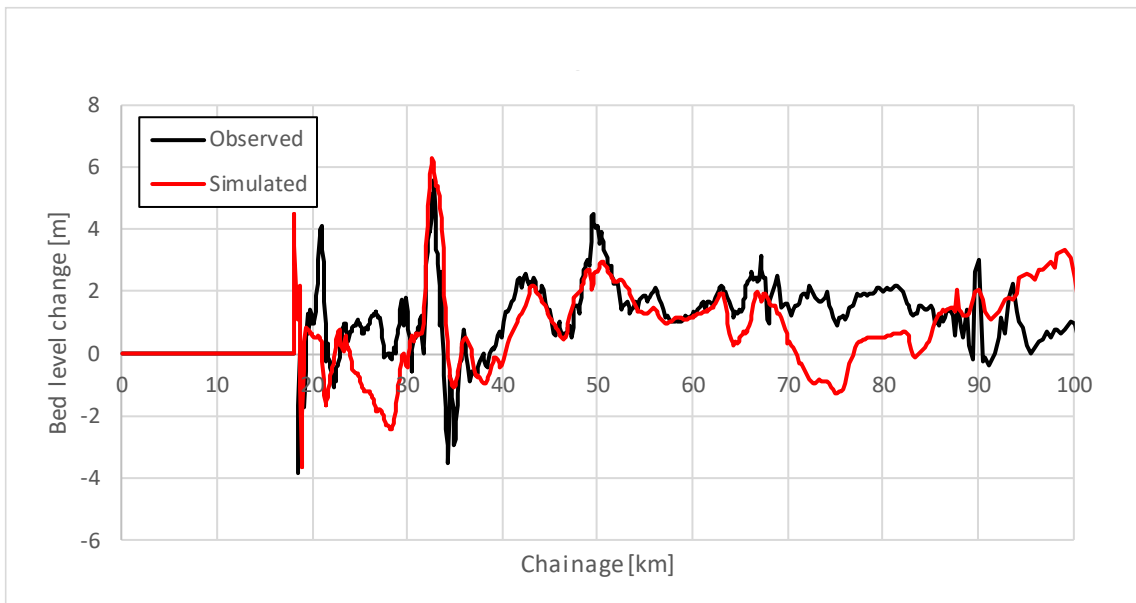


Figure 3-21 Comparison of observed and simulated width-integrated bed level changes 2011-2019.

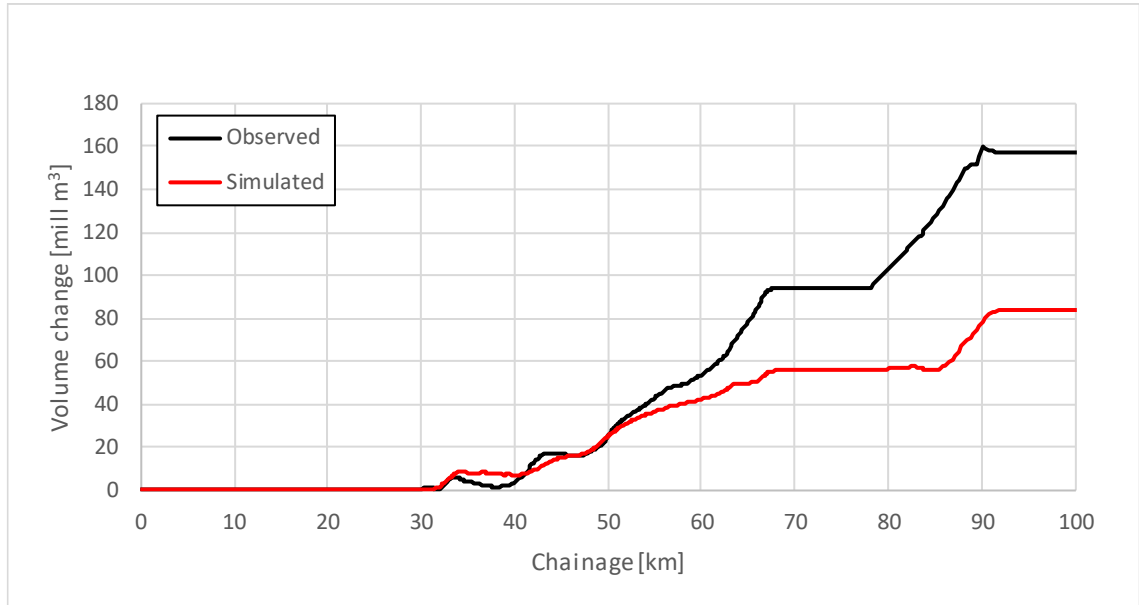


Figure 3-22 Comparison of observed and simulated bulk volume curves for 2011-2015. The bulk volume curve for 2011-2015 bank erosion was not calculated.

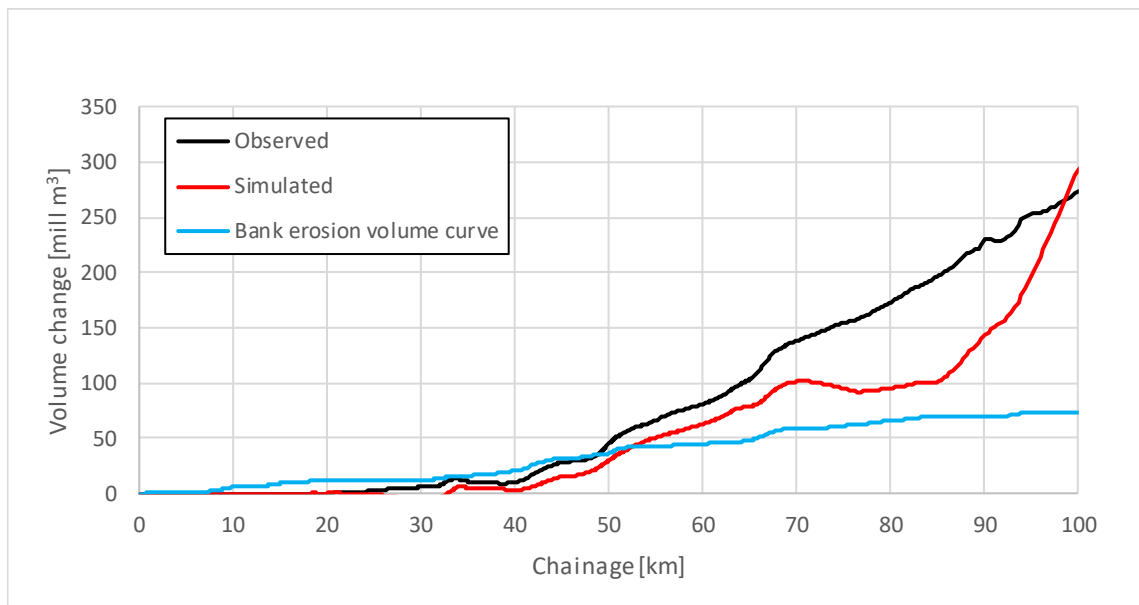


Figure 3-23 Comparison of observed and simulated bulk volume curves for 2011-2019.

The Baleswar River was depositional in 2011-2015 and 2011-2019. Therefore, the accumulated volume curve is good for showing that the model correctly distributes the sedimentation longitudinally.

Bank erosion has only a minor impact on the bulk volume curves.

### 3.9 Bank erosion model

Several bank erosion formulas were tested during the developments of the models. A formula based on Hasegawa (1989) was selected as the most optimal formula:

$$E = E_h |V| \left( 1 - \left( \frac{h_c}{h} \right)^{2/3} \right)$$

Where E is the erosion rate [m/s],  $E_h$  a non-dimensional calibration parameter, V is the near-bank flow velocity [m/s], h the near-bank water depth [m], and  $h_c$  the critical water depth [m] below which no erosion takes place. Calibration simulations resulted in the following parameters in the derived Hasegawa (1989) bank erosion formula:

$$E_h = 10^{-6}$$

$$h_c = 10 \text{ m}$$

The bank porosity was set to 0.4, while the bed porosity was 0.6.

The calibration results are presented and discussed in the following.

The observed bank erosion rates in 2011-2015 are less reliable than the 2011-2019 observations, and therefore the model was calibrated against the 2011-2019 bank erosion rates. Observed and simulated bank erosions are compared in Figure 3-24 and Figure 3-25. The model performance is generally convincing:

- The data analysis showed a strong correlation between bank erosion and bed levels. Practically all eroding banks in the Baleswar River are outer bends with deep water.
- Hence, the prediction of bank erosion is tied to the prediction of velocities along the banks, assuming that the bed levels do not change significantly.
- Over longer time, feedback mechanisms will probably deteriorate the predictions.

It is also worth noting that annual bank erosion rates in the Baleswar River are typically 10-20 m, which is less than 1% of the river width. This also suggests that bank erosion can be predicted over longer time compared to what one would anticipate. Larger planform changes add to the feedback mechanisms of the river by changing the all-important streamline curvature, which is the driver for bathymetry changes that will make it more difficult over time to forecast bank erosion in the Baleswar River.

As stated for other models, errors in the bank erosion prediction are not necessarily a problem with the bank erosion formula. Bank erosion is heavily influenced by the velocity distributions in the bends, which are problematic in all the developed models due to the lack of ADCP data for calibration, i.e. one should not go directly to altering the bank erosion formula. The Baleswar River model was developed early in the study, and later models showed that the flow resistance model is very important for the flow distribution in the bends.

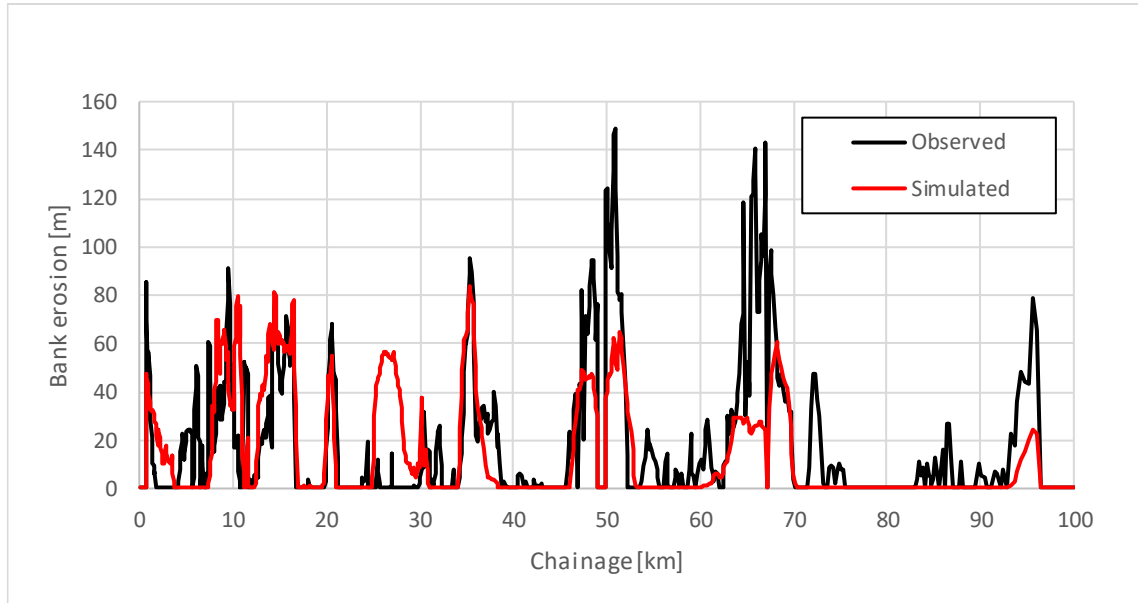


Figure 3-24 Observed and simulated west bank erosion for the Baleswar River model 2011-2019.

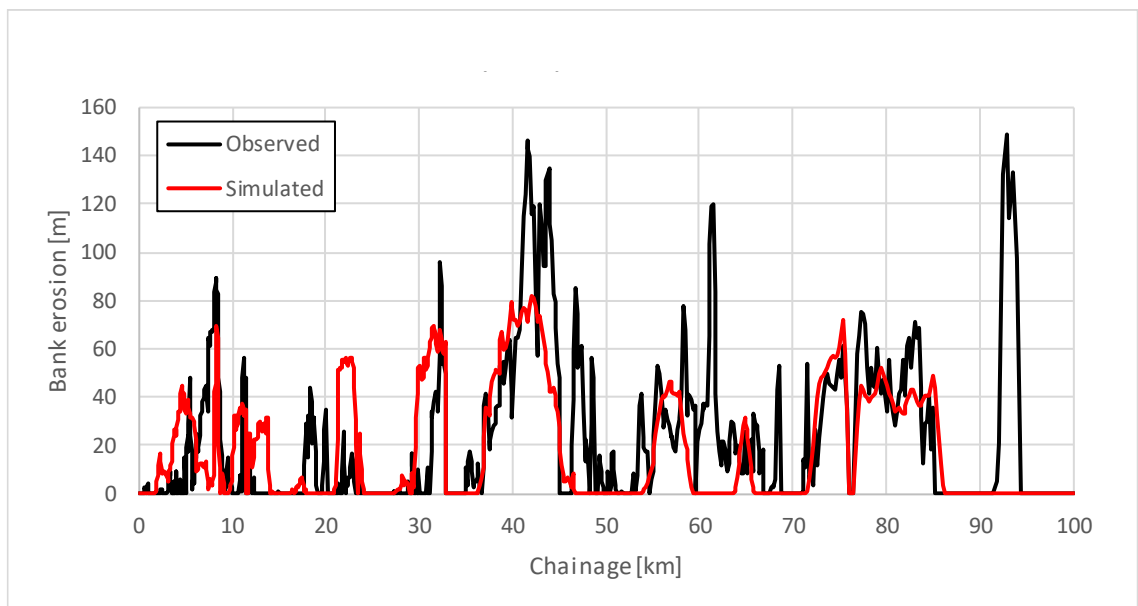


Figure 3-25 Observed and simulated east bank erosion for the Baleswar River model 2011-2019.

### 3.10 Comparison of observed and simulated bank lines 2011-2019

The bank erosion hindcast simulation was conducted without updating the bank lines. This is easier for calibration purposes because updating of the bank lines will change the grid, leading to many complications when post-processing the results. The error associated with not updating the bank lines is small for cases where the bank erosion is much smaller than the width, which is the case for 2011-2019. However, for longer model runs, the feedback between planform and bathymetry must be accounted for. Considering that the application model should run much longer timescales compared to 2011-2019, the application model was prepared for using dynamic grid updating.



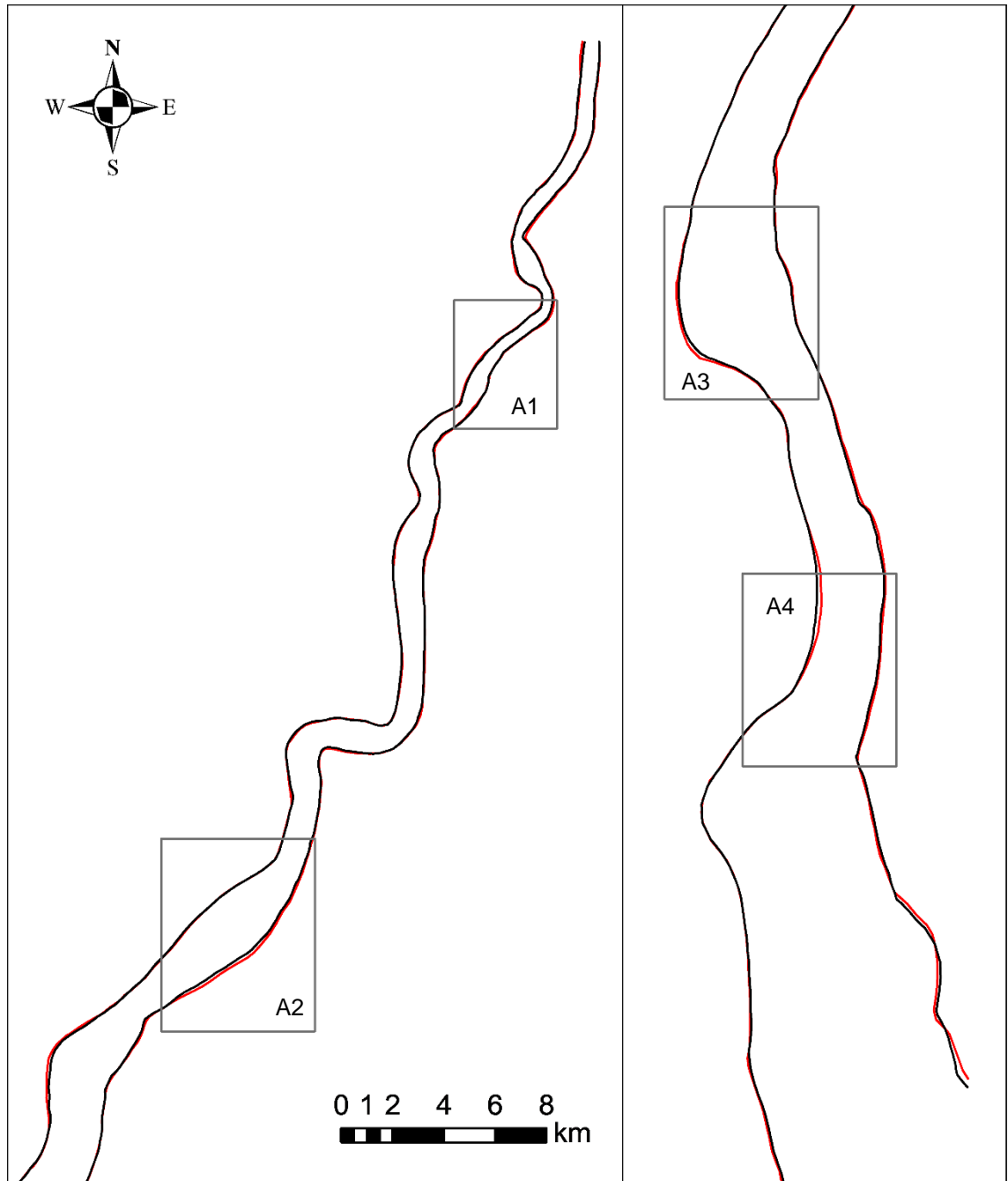


Figure 3-26 Observed bank lines 2011 and 2019 with four local areas shown, which are zoomed in the following.

Bank lines are compared in Figure 3-27 showing the four zoom areas indicated in Figure 3-26:

A1: This is the first area from upstream, and it shows underpredicted bank erosion along the east bank and overpredicted bank erosion along the west bank.

A2: This is one of the characteristic east banks with significant erosion since 1988. The model captures the eroding reach accurately but predicts too low erosion in the downstream end of the outer bank, while the upstream end is correctly predicted.

A3: This is a very important outer bend where the model has had problems capturing erosion correctly from the beginning of the model development. The erosion along the east bank (associated with scouring in the flood channel) is qualitatively correct in the model, but the magnitude is underpredicted.

A4: The eroding east bank is correctly captured, and it is seen that the west bank is accreting, which is not included in the model.

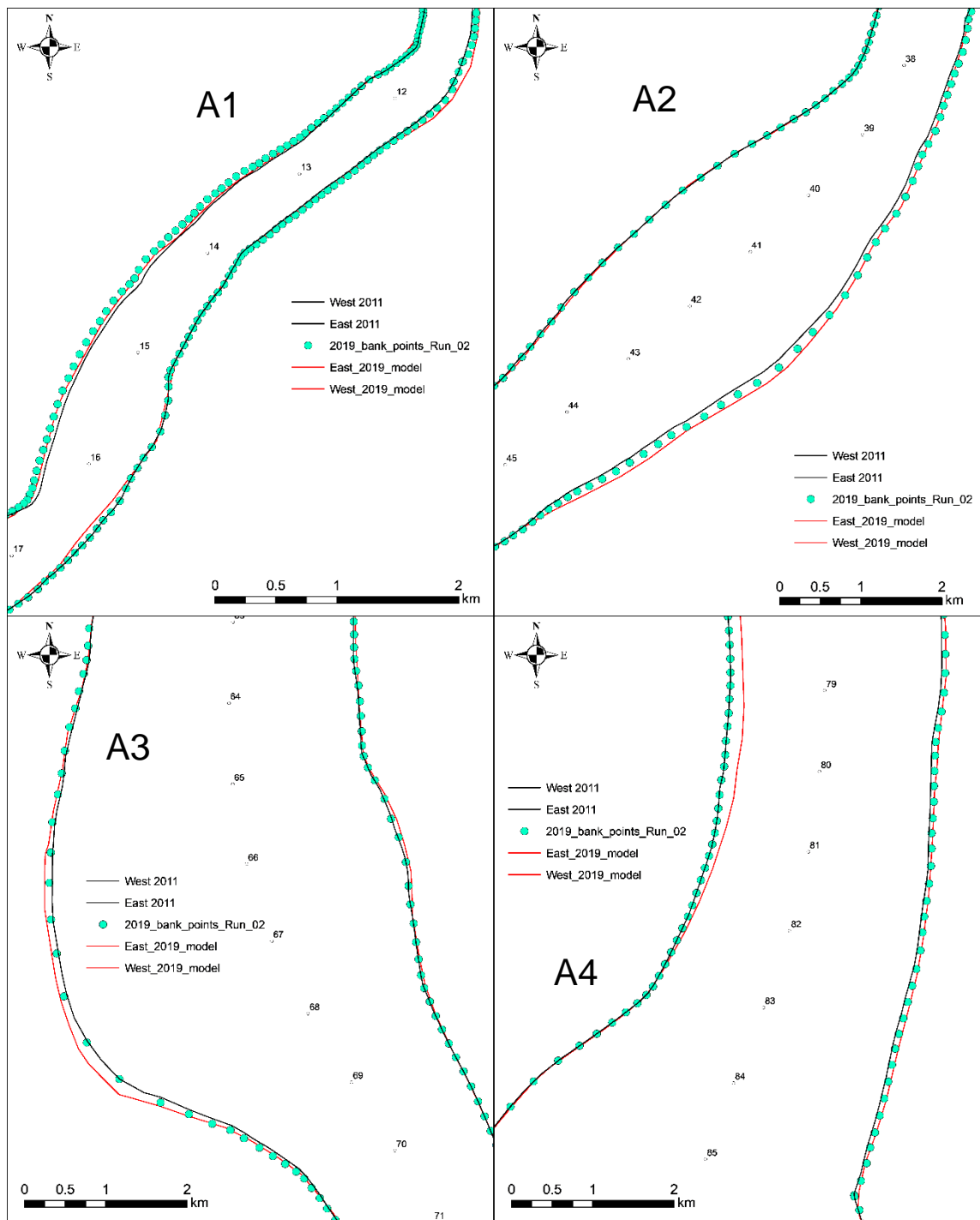


Figure 3-27 Bank lines 2011 (observed) and 2019 (observed and simulated) for the Baleswar River model in the four sub-areas.

## 4 Model applications

The model applications are reported in this section.

### 4.1 Dredging the shoal opposite of the eroding bank at the downstream tip of Polder 35/1

This application was conducted before the final model was ready. It is reported for the sake of completeness.

The (east) flood channel in the figure below has been cutting down since 2009. Sedimentation occurred in the ebb channel (west). The bend could already now be switching the main flow channel to the east; the east channel is deeper than the west channel in the 2019 survey.

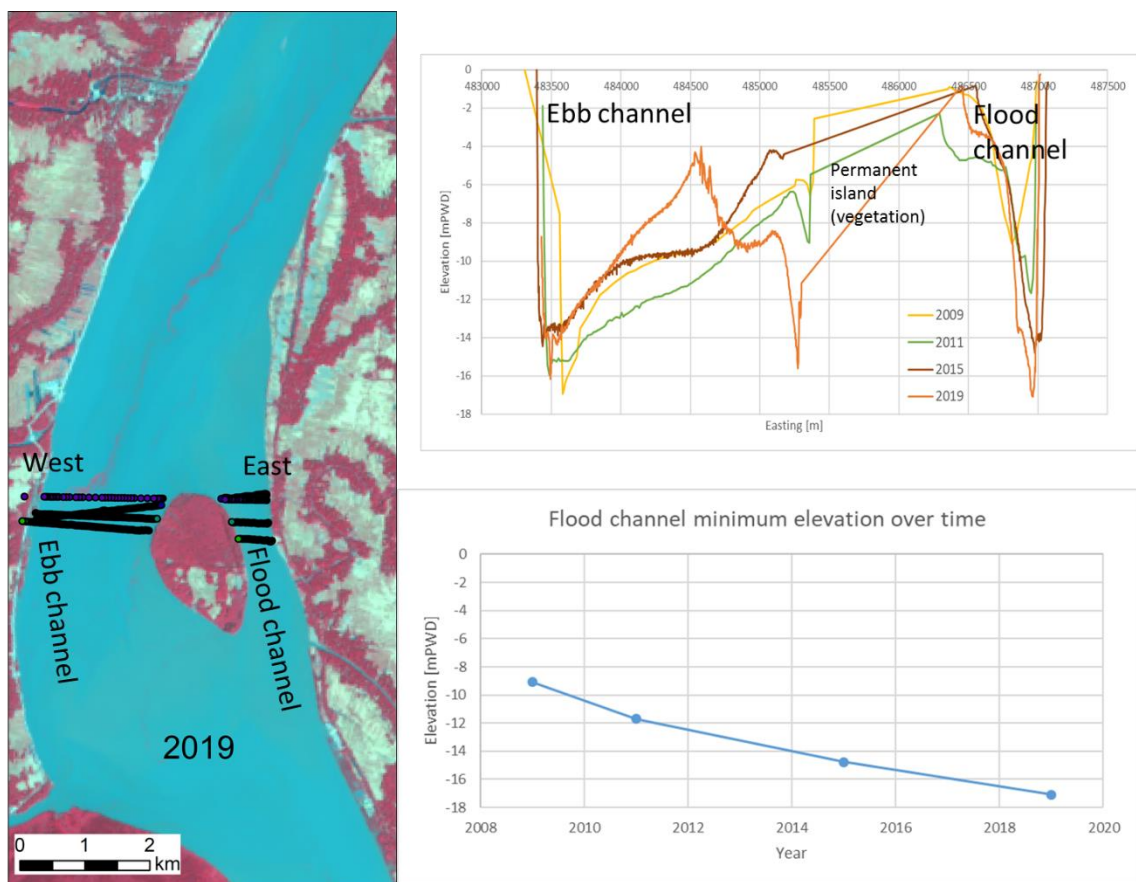


Figure 4-1 Historical bathymetry around the ebb channel (west) and flood channel (east).

The key morphological features and developments can be summarized as follows:

- The island has been there since at least 1988
- 250 m erosion along west bank 1988-2010
- 100 m erosion 2010-2019
- Average 10 m/year
- Erosion along east bank barely detectable from Landsat

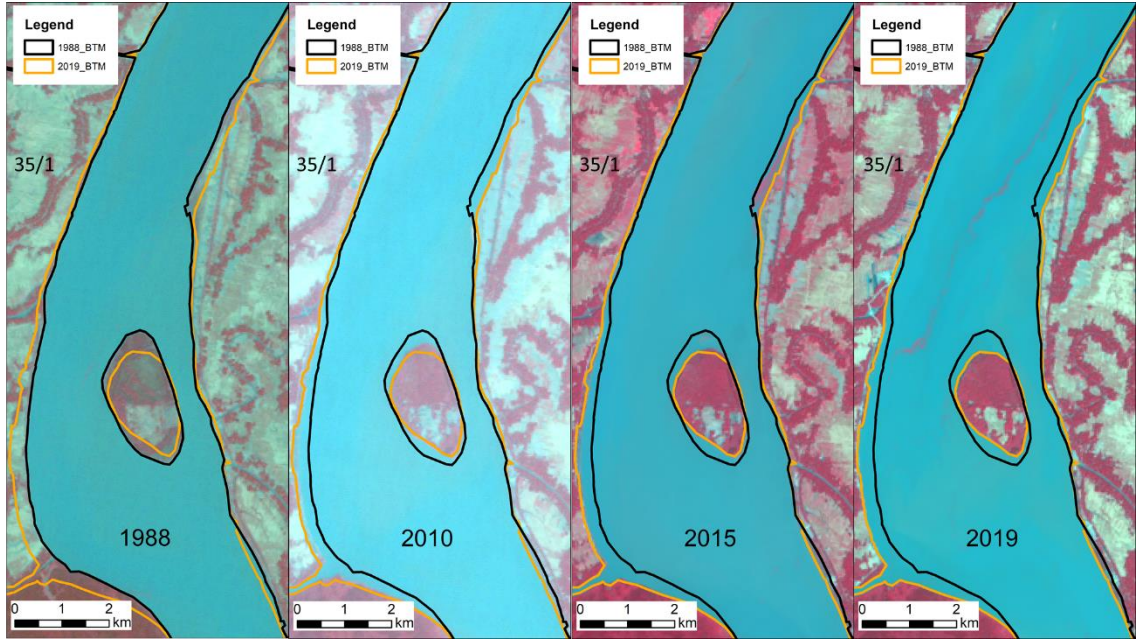


Figure 4-2 Historical bank line and planform changes around Polder 35/1.

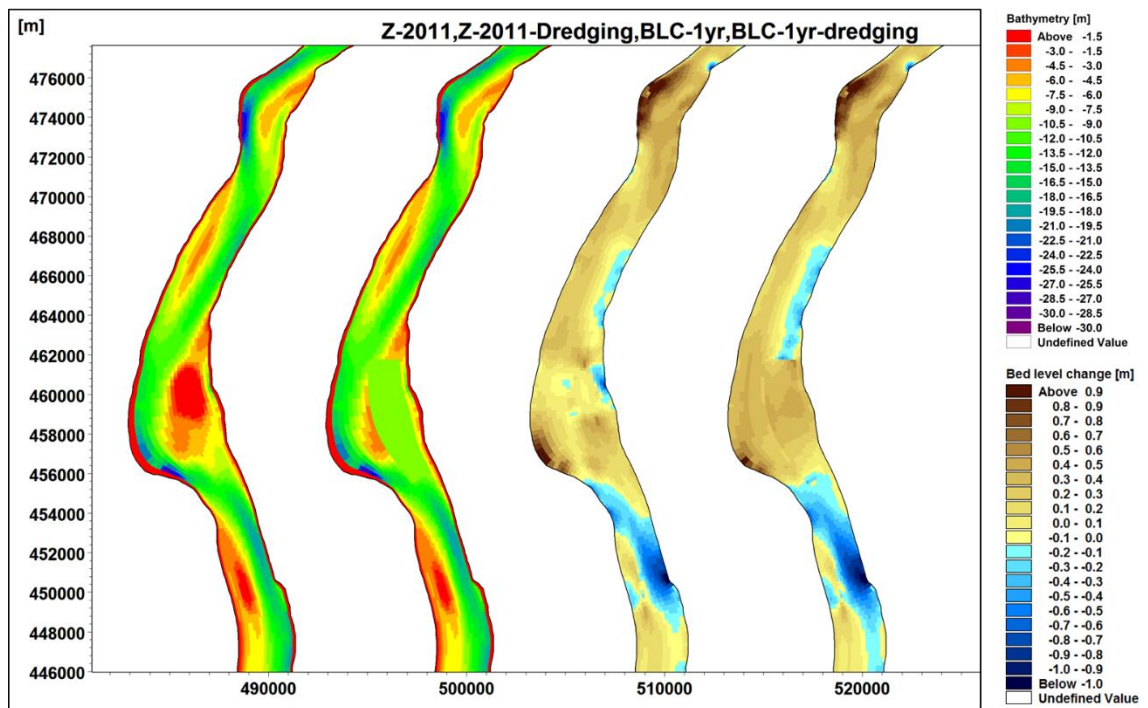


Figure 4-3 Bed level and bed level changes for base and shoal dredging option around Polder 35/1

We have used the model to study possible mitigation of the erosion at Polder 35/1 through dredging of the bar/shoal adjacent to the eroding bank. The results from the scenario simulation are:

- Velocities significantly reduced
- The backfilling rate is 0.4 m/year
- Bank erosion has been significantly reduced

The maximum current speed near the eroding bank has been found to be 0.90-1.40 m/s for existing conditions. However, with the shoal dredging scenario, the maximum current speed reduced to 0.60-1.00 m/s around the eroding bank of Polder 35/1 (Figure 4-4).

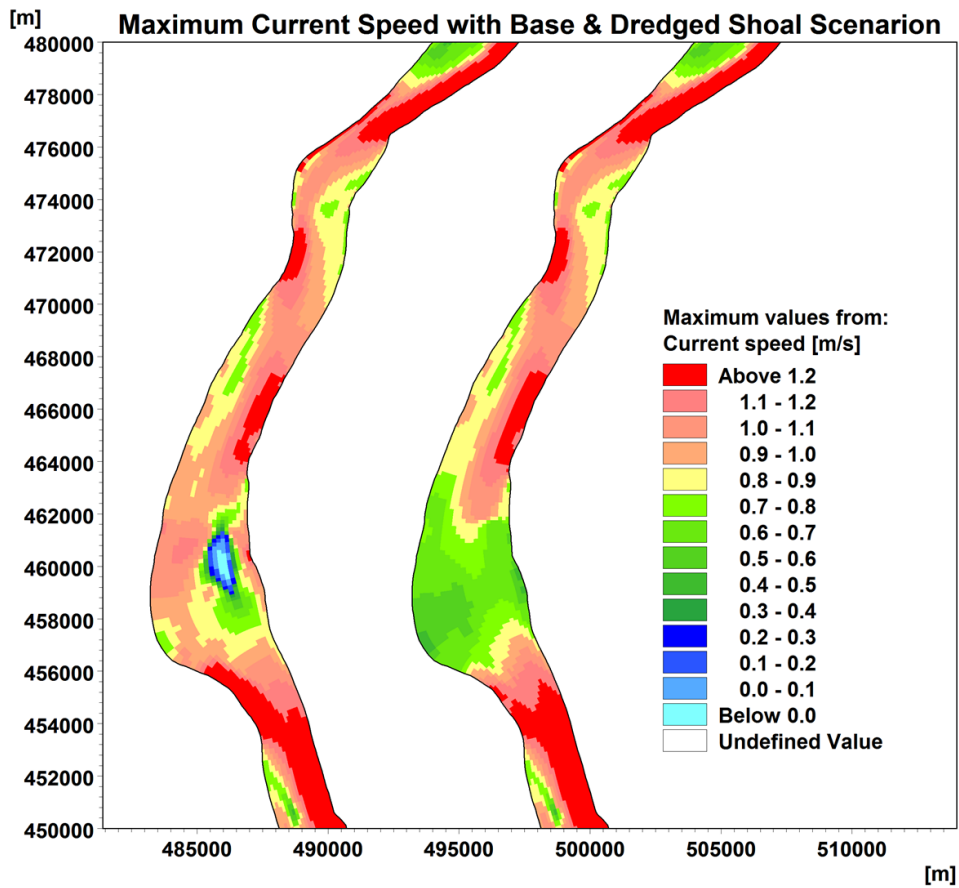


Figure 4-4 Maximum current speed for base and shoal dredging option around Polder 35/1

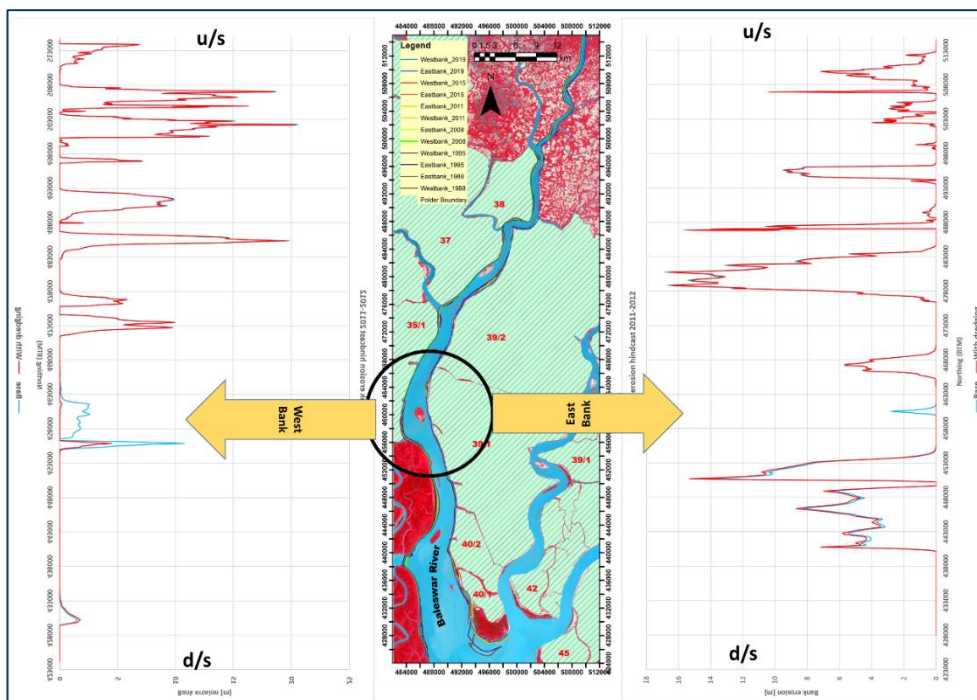


Figure 4-5 Erosion of both banks from 2011 to 2012 in the Baleswar River (baseline and option).

The calibrated and validated bank erosion model has been simulated for the shoal dredging option. The simulated bank erosion with base and option is shown in Figure 4-3. The bed level of the shoal has been assumed to 2.8 mPWD. Shoal has been dredged to -10 mPWD.

From the observed bank line of the Baleswar River (Figure 4-5), around 250 m of erosion along west bank of Polder 35/1 was observed for the period 1988-2010. An average of 100 m erosion has been found since 2010-2019. Around 10.8 m erosion was found from model simulation near the southern tip of Polder 35/1 since 2011-2012. However, bank erosion has reduced significantly after shoal dredging. Around 4.50 m of west bank erosion has been found from option simulation at the same location since 2011-2012.

## 4.2 Bank erosion forecast 30 years into the future

The existing and 30 years into the future boundary conditions were applied in conjunction to represent a reasonable time-series representing the next 30 years. Ideally, a continuous time-series should be available for the whole period to reflect the gradual increase in sea level and gradual lowering of the bathymetry due to subsidence. However, this is very cumbersome to do in the SWRM that provides boundary conditions for the Baleswar model. Instead, the 30 years are covered by two simulations. The first simulation covers 15 years starting from the 2019 conditions (grid and bathymetry) using the existing 2019 boundary conditions generated by the SWRM. When this simulation is done, the results are processed into conditions representing 15 years into the future with subsidence representing 30 years into the future subtracted from the bathymetry. The second simulation uses that bathymetry and the associated grid as initial condition and runs 15 years using the future boundary conditions from the SWRM.

This is hence a stepwise approach in which the first 15 years represent existing conditions and the next 15 years represent conditions 30 years into the future.

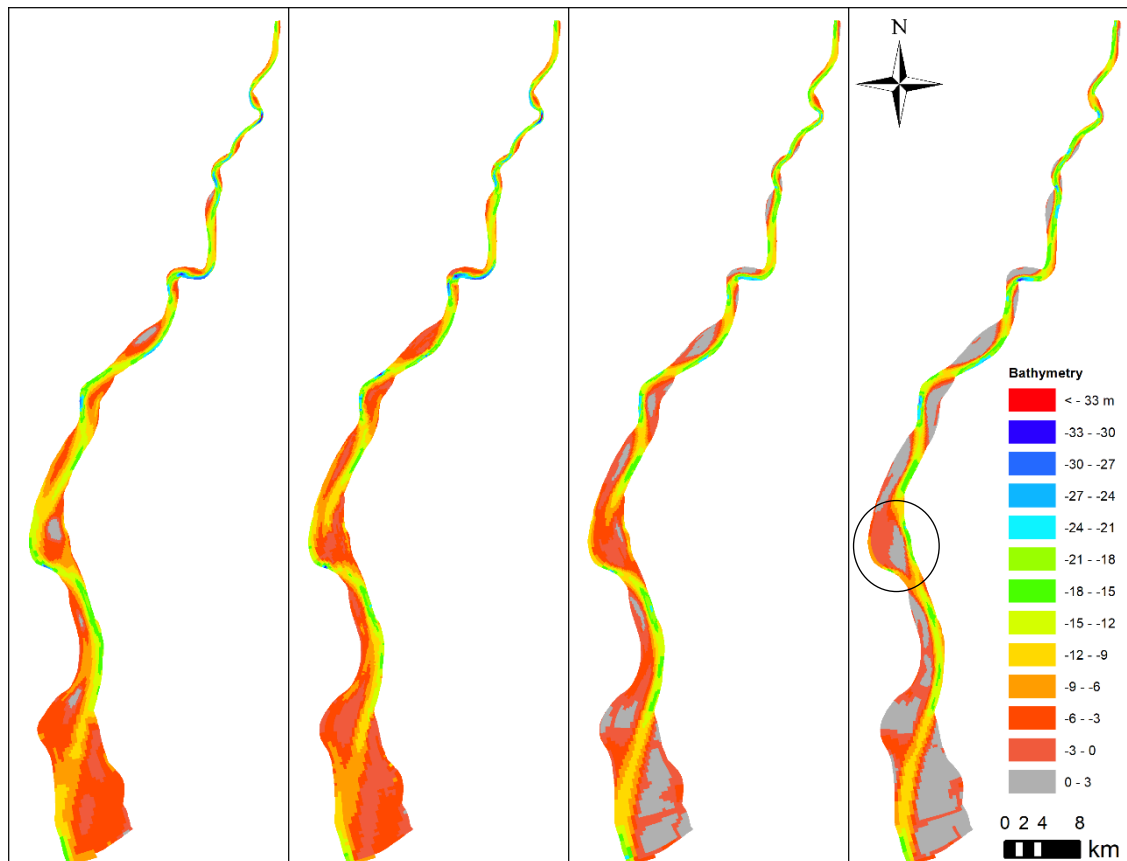


Figure 4-6 Bathymetries from various years, from left: 2011 (observed), 2019 (observed), 2034 (simulated), 2049 (simulated).

Figure 4-6 shows observed bathymetries from 2011 and 2019 along with simulated future bathymetries from 2034 and 2049.

The bathymetries are qualitatively similar, i.e. the locations of bars and channels are similar, which implies that the bank erosion pattern will not change over the considered timescale of 30 years.

The results also show what is apparently a general weakness in these models: The bars grow well above elevation 0 mPWD, which is not the case in observations. This can be partly explained by the lack of bathymetry observations on high bar elevations, but the model probably tends to grow the bars to higher elevations than reality. In the model, the bars continue growing due to silt deposition for the highest tide levels, and the growth does not stop until the bar reaches the highest tide level. The tidal flows over bars are unlikely to generate enough shear stress to entrain mud. However, a process like mud sliding is not included in the simulation, and this process could be important in stabilizing the bar crest level at a value below the highest local tide.

The Baleswar sediment model is a single fraction silt model, and the flow resistance is a longitudinally but not transversely varying Manning  $M$  varying from  $M=50 \text{ m}^{1/3}/\text{s}$  downstream to  $M=35 \text{ m}^{1/3}/\text{s}$  upstream. In other rivers this sediment and flow description can cause problems with bar stability, but in the Baleswar it is observed that the bars in 2049 are generally similar to the bars in 2019. It is known from local hydrodynamic models tested during the project that the upstream Manning  $M=35 \text{ m}^{1/3}/\text{s}$  causes much stronger flow deflection from bars, while the typical silt Manning  $M=60 \text{ m}^{1/3}/\text{s}$  causes very weak deflection. Only the Baleswar model has such low Manning  $M$  (suggesting sand in the upstream end), and that could explain why the model sustains the bars at the same locations as in the 2019 bathymetry data.

When inspecting the results in detail, it becomes apparent that, although the future bathymetries are generally similar to existing bathymetries, there is one major deviation, which is shown with a circle in the figure. At this location, the model suggests that the current flood channel east of the island will over time take over the flows, while the existing channel running past bank protection at Polder 35/1 will silt up. The Bogi channel located just south of the bank protection works will continue exchanging flows with the Baleswar. This area was visited by the project in February 2019 and has been the subject of discussions with the CEIP DTL. The 2019 bathymetry data already showed that the bed levels in the eastern channels were below the bed levels in the main flow channel to the west, which suggests that the eastern channel could become dominating.

The CEIP DTL also informed the project team that bank erosion takes place along the eastern bank. The project team showed to the DTL that the eastern channel in the model simulation indeed grows and generates a small bank erosion signal along the eastern bank.

Finally, it is also pointed out that it is difficult in the model to reproduce erosion along the western bank because the flow path along the channel has simply become too long, which is why the eastern channel in the model also grows.

In the model the capture of the main flow by the eastern channel takes a long time. Some tendency can be seen in the 2034 bathymetry, while it is fully captured in the 2049 bathymetry.

The forecasted capture of the main flow by the eastern channel should, as all other forecasts, not be interpreted as a fact but as a possible future development suggested by the model. The suggested development coincides with the current tendency in the data, although the model suggests that the process will take a very long time. It might be possible to play into this suggested development in the management of Baleswar.

The capture of the flow by the eastern channel does not seem to cause disturbances in other bends, which would be a concern in a sand river. In other words, it appears that the eastern channel can capture the flow with relatively local impacts.

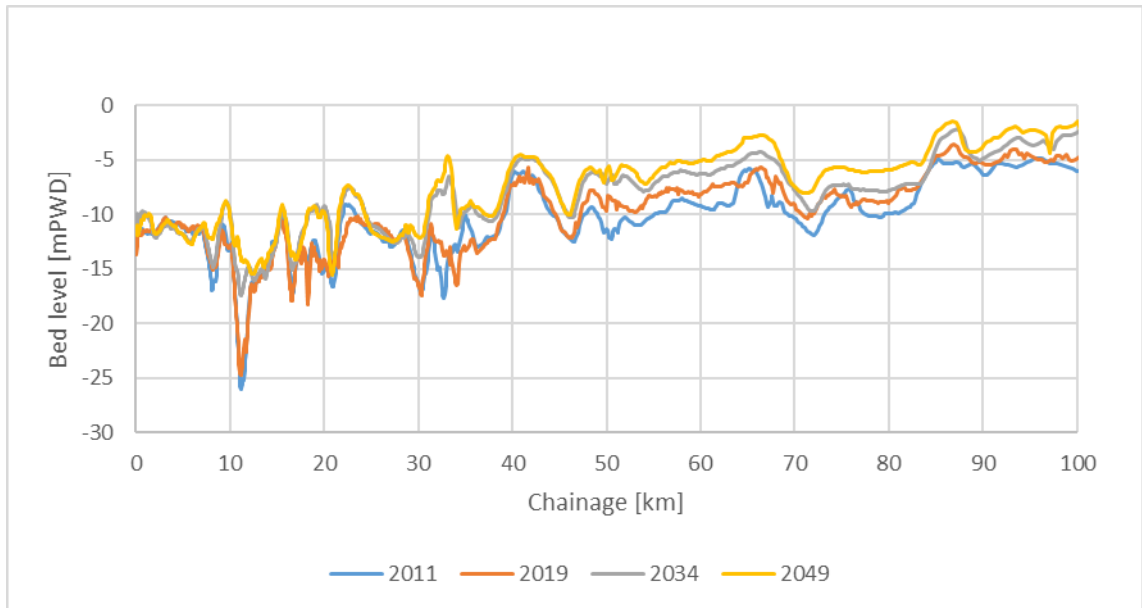


Figure 4-7 Width-integrated bed levels as a function of chainage in the Baleswar River for 2011 (observed), 2019 (observed), 2034 (simulated) and 2049 (simulated).

The width-integrated bed levels are shown in Figure 4-7. The width-integrated bed levels show that in the simulations the Baleswar is generally depositional over time, but part of the reason lies in the potentially unrealistic bar growth leading to bar elevations close to the local maximum tide level.

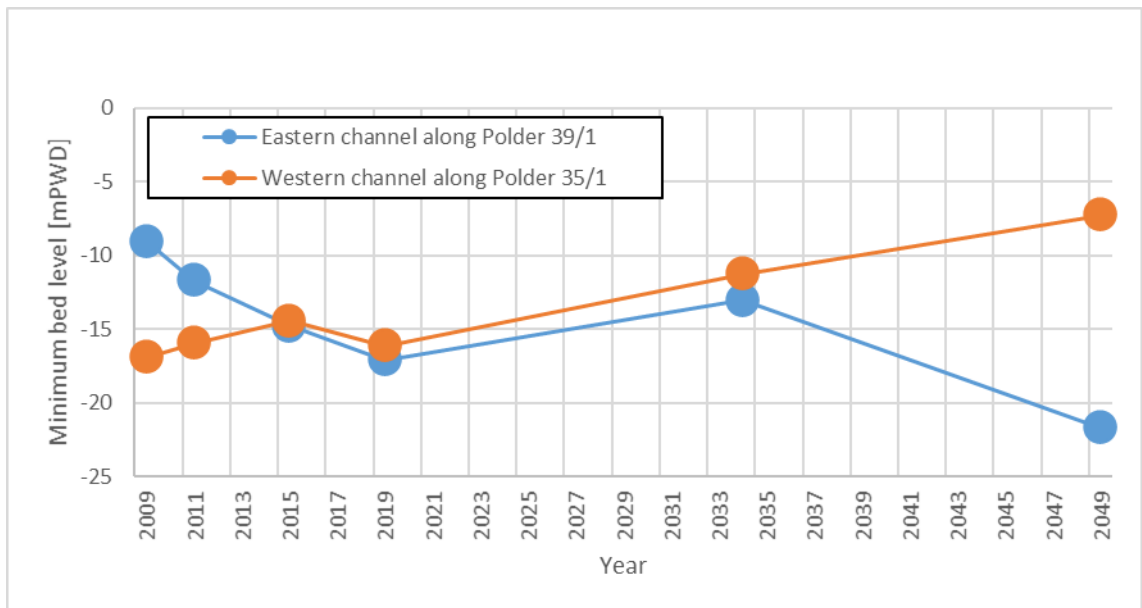


Figure 4-8 Minimum bed levels in the area between Polder 35/1 and 39/1. The observed bed levels were extracted from cross-sections, while the simulated bed levels were extracted from model results. Hence the comparison is not completely valid.

Figure 4-8 illustrates the capture of the main flow by the eastern channel at the Bogi location. The comparison was based on a single transect with the same x-sections collected in 2009-2011-2015-2019 and simulated bed levels from the model for 2034 and 2049. Hence it is not a fully valid representation of minimum bed levels because those were unlikely to have been consistently captured in the bathymetry surveys. However, if disregarding that, the figure shows clearly how the eastern and western channels in the period 2009-2019 developed from a dominating western channel to similar minimum elevations, and over time in the simulation, the eastern channel becomes dominant.



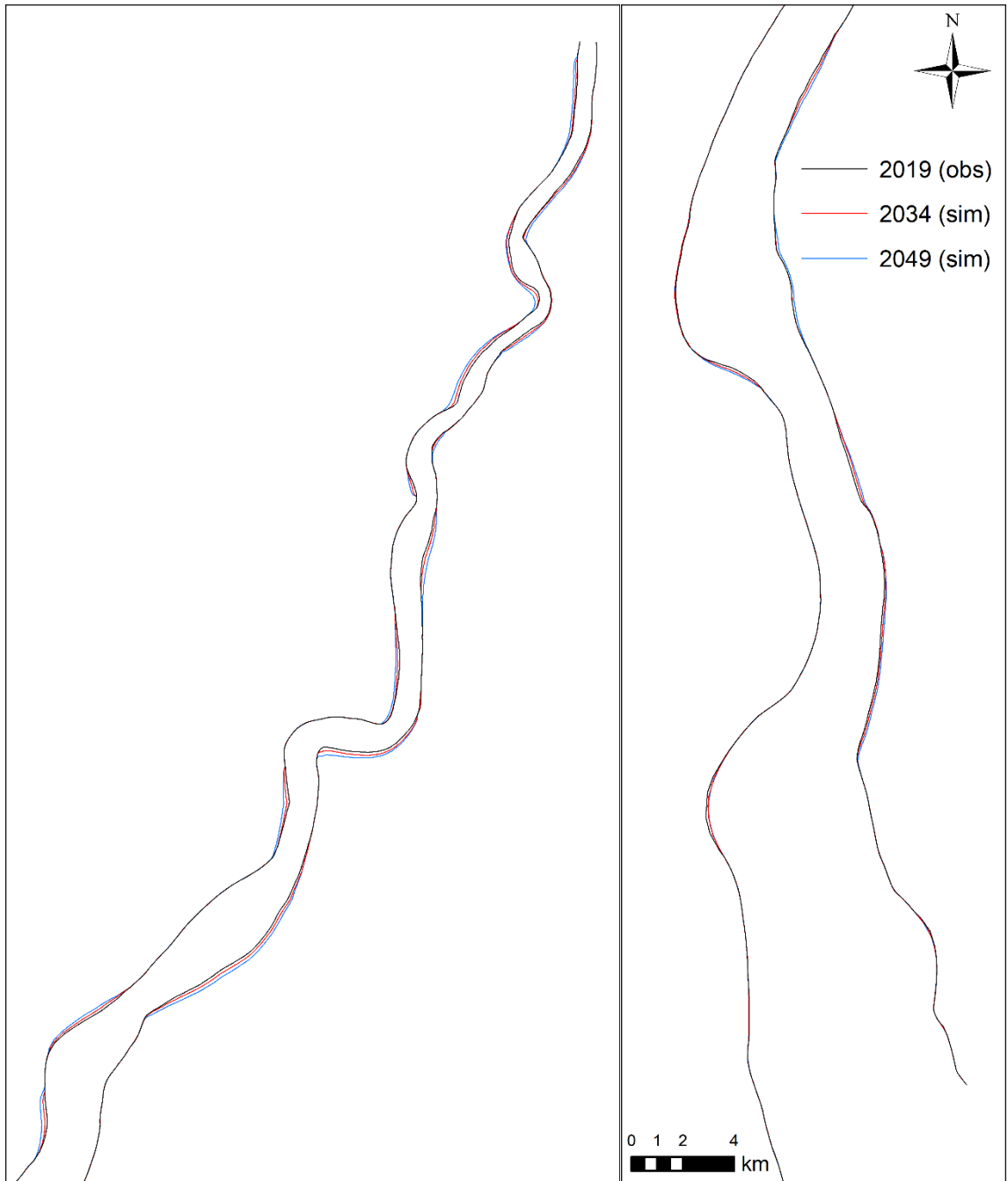


Figure 4-9 Bank lines 2019 (observed), 2034 (simulated), 2049 (simulated).

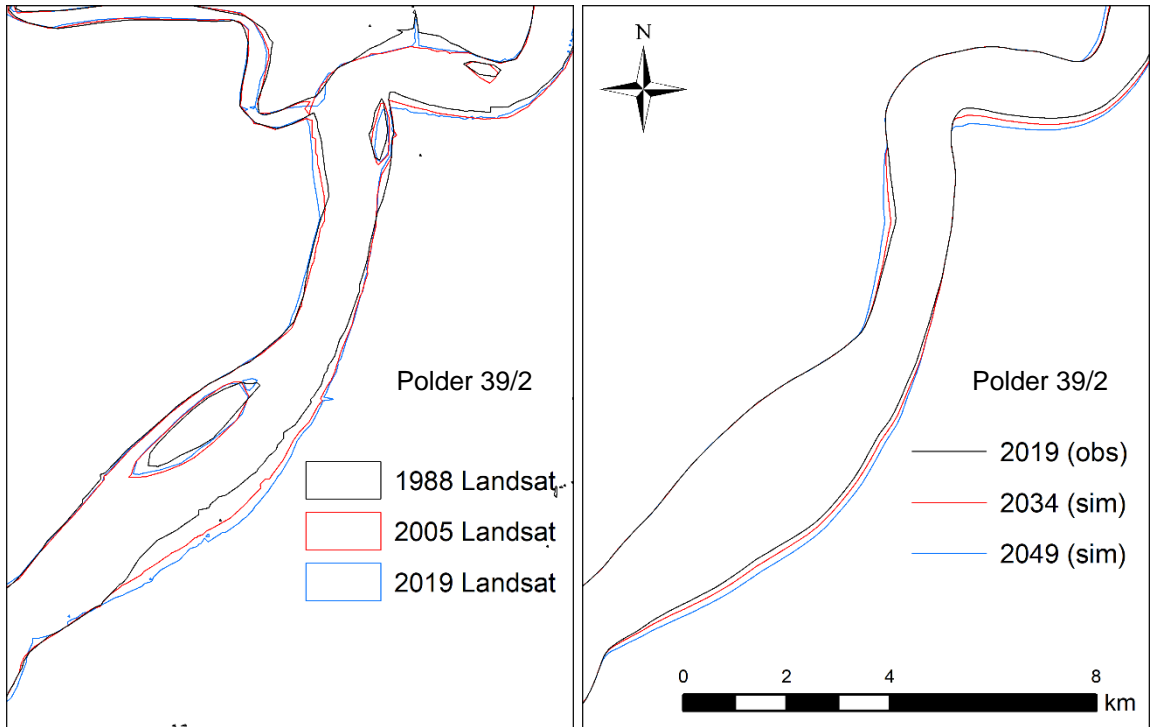


Figure 4-10 Comparison of bank lines digitized from Landsat 1988-2005-2019 and model results 2019-2034-2049. The bank lines hence cover comparable timescales and are shown in the very sharp bend in the middle of the Baleswar model.

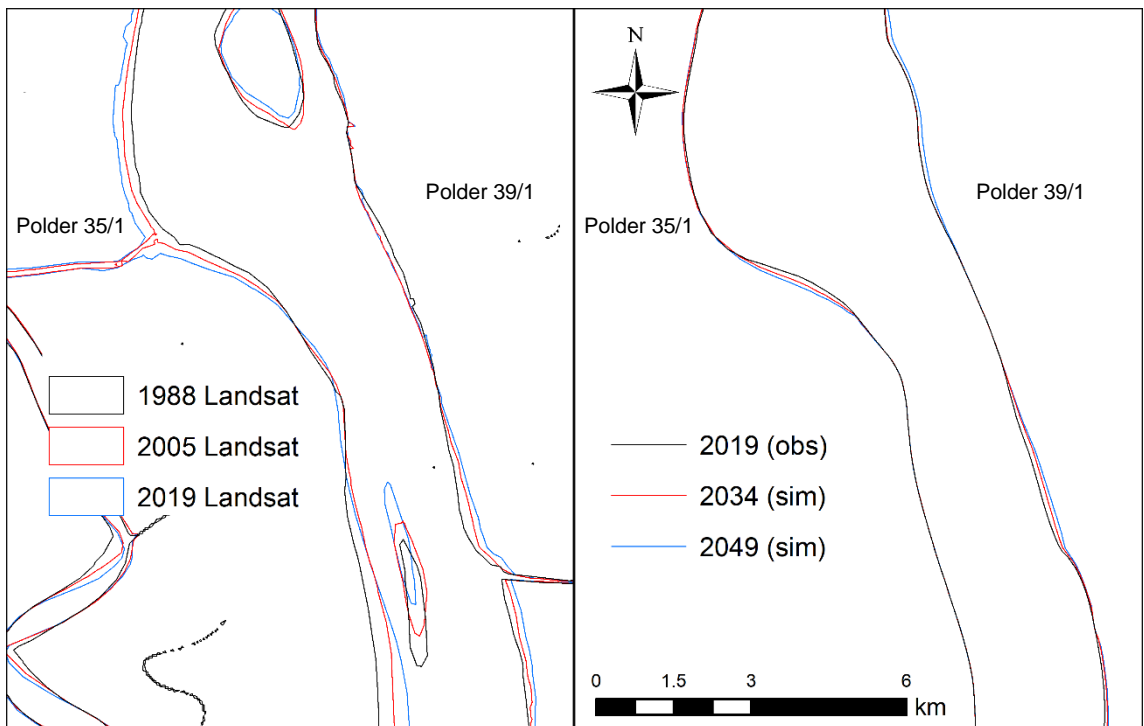


Figure 4-11 Comparison of bank lines digitized from Landsat 1988-2005-2019 and model results 2019-2034-2049. The bank lines hence cover comparable timescales and are shown in the downstream end close to the Bogi channel.

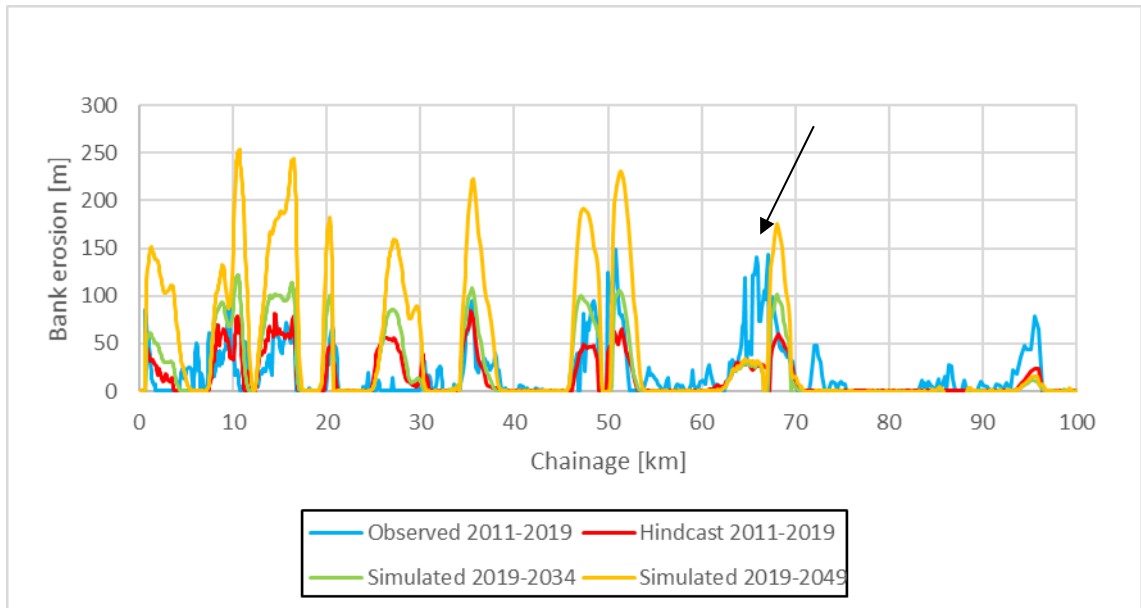


Figure 4-12 Bank erosion along the Baleswar River west bank for 2011-2019, 2019-2034 and 2019-2049. The arrow shows the location where the embanked west bank is projected to cease eroding due to the bend cut activating the eastern channel (currently a flood channel, then becoming an ebb channel).

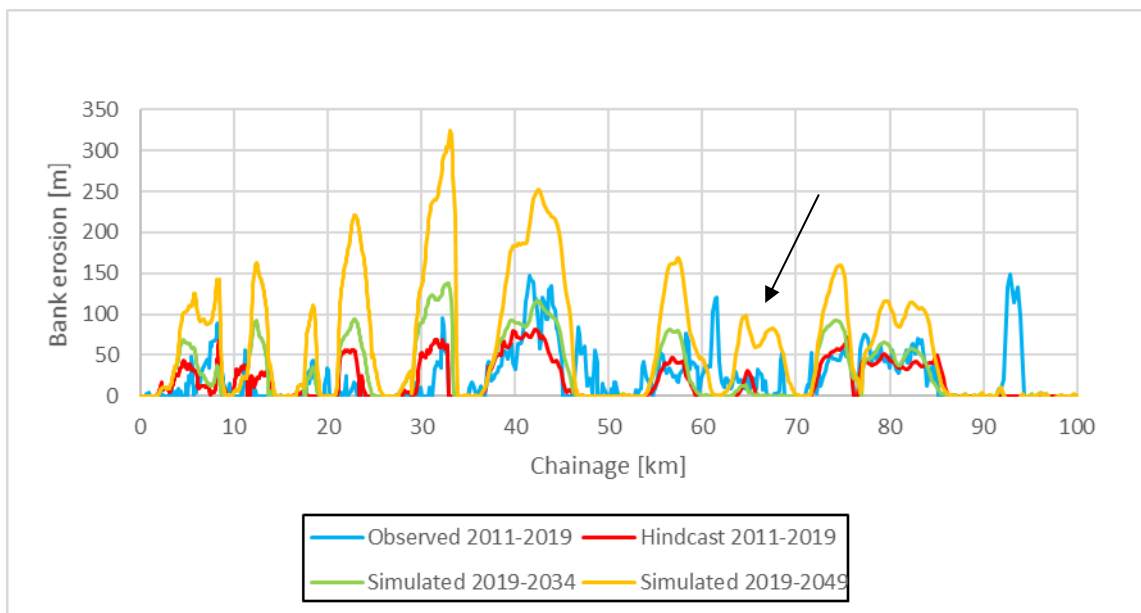


Figure 4-13 Bank erosion along the Baleswar River east bank for 2011-2019, 2019-2034 and 2019-2049. The arrow shows the eastern bank projected to erode up to 100 m during the next 30 years, and it can also be seen that the erosion starts after 2034.

Figure 4-10 shows a comparison of Landsat bank lines and model results for comparable timescales, namely Landsat 1988-2005-2019 and model results 2019-2034-2049. To the east of this area lies Polder 39/2, while Polder 37 is to the west. The two eroding banks along Polder 39/2 are seen to continue eroding, although the bank furthest to the south has reduced erosion rates over the future period compared to 1988-2019.

Figure 4-11 shows a comparison of Landsat bank lines and model results for comparable timescales, namely Landsat 1988-2005-2019 and model results 2019-2034-2049. This is in the downstream area where the Bogi channel is connected to the Baleswar western bank. The comparison of historical and future bank lines shows significant differences at this location. The western bank has been eroding consistently during 1988-2019, while in the future forecast only the bank south of the Bogi will continue eroding at low rates. Opposite of this bank the eastern bank is projected to erode, although the rates are only around 5 m/year and only in the period 2034-2049. Again, it must be kept in mind that these are not categorical predictions, but more suggested developments from the model, and this eastern bank is a plausible candidate for future erosion associated with cessation of erosion along the western bank (which currently has a sizeable embankment).

Figure 4-12 and Figure 4-13 show the simulated bank erosion as a function of the chainage coordinate for reference compared to the 2011-2019 simulations and observations. It is seen that the same banks will erode in the future, but there are also some quantitative changes. Overall, it is safe to say that the model does not project significant changes to the erosion rates, and the curves should be inspected with the fact in mind that bank erosion is essentially shown over 8 years, 15 years and 30 years.

### 4.3 Impact of climate change on future bank erosion

The impact of climate change was quantified by running a 2034-2049 simulation starting from the same condition in 2034 with subsidence included but running 2034-2049 without climate change included in the boundary conditions.

Such a comparison is tricky due to the different grids, i.e. one cannot just take the difference between the bathymetries, which is a traditional approach when looking for differences between scenarios.

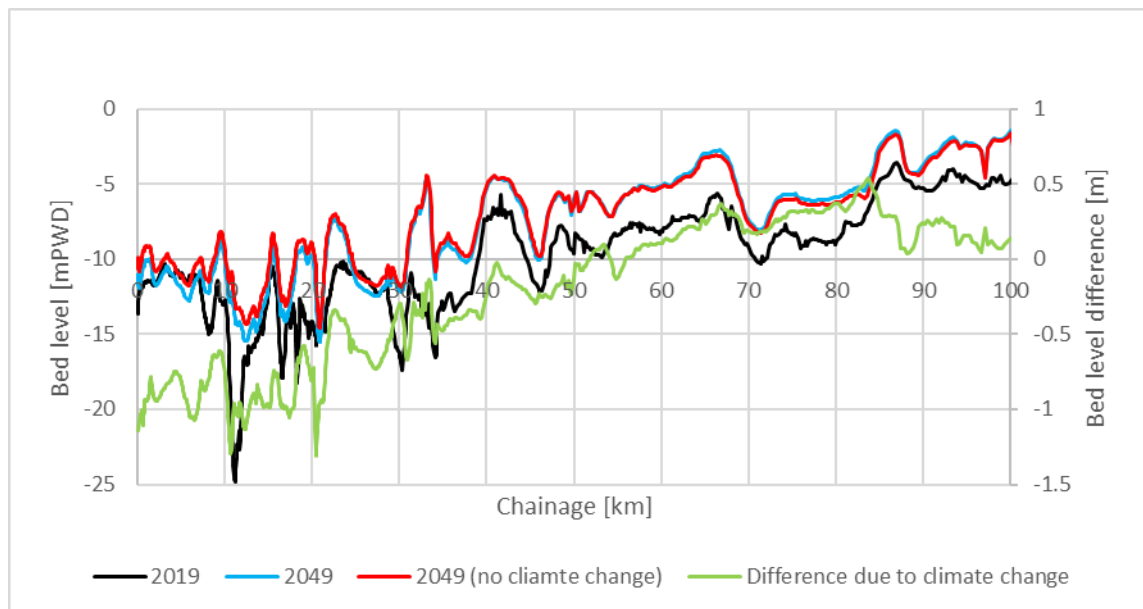


Figure 4-14 Width-integrated bed levels as a function of chainage in the Baleswar River for 2049 with and without climate change (subsidence included in both simulations).

The width-integrated bed levels are shown in Figure 4-14. The differences between existing conditions and future conditions with climate change are small (subsidence is included in both 2049 results), but it can be observed that upstream bed levels are lowered 1 m in 2049 due to climate change, while in the downstream end the bed levels increase up to 0.5 m.

The explanation for this is to be found in the boundary conditions. It is known that climate change increases the water levels in the downstream area and increases both ebb and flood tidal discharges. Hence the observed impact makes sense, as it shows sediment being moved downstream due to climate change.

Induced changes need to be interpreted with caution. The induced changes are differences between scenarios, but the figure shows that the changes over time are much bigger. Hence, it cannot be concluded that climate change leads to erosion upstream over time, but it can be concluded that climate change will reduce upstream bed levels in 2049 compared to what they would be without any change.

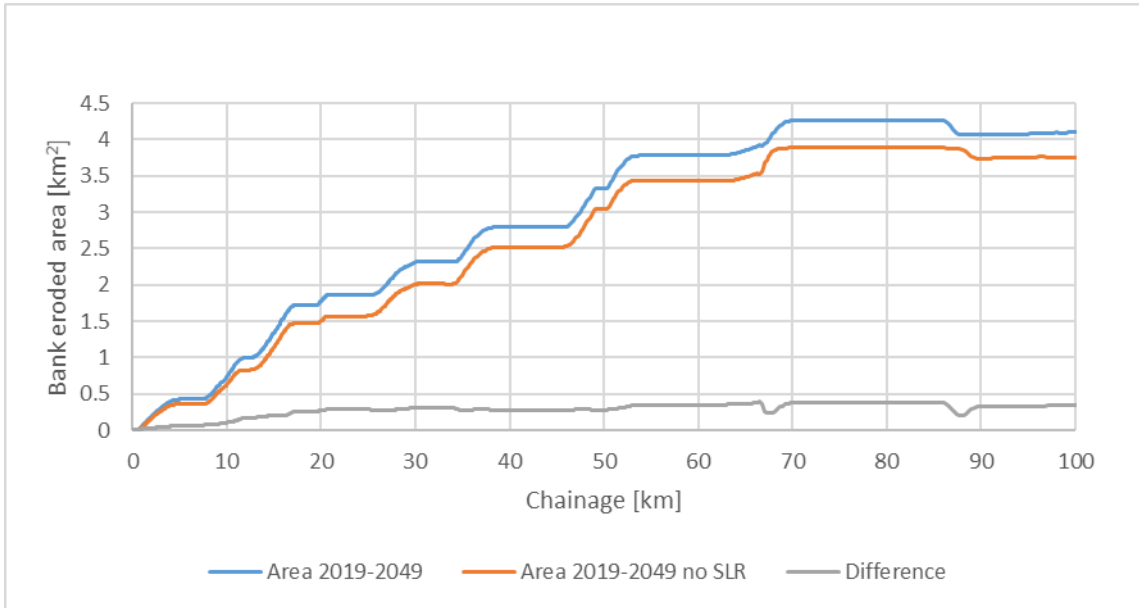


Figure 4-15 West bank eroded areas integrated along the river for the period 2019-2049 with and without climate change.

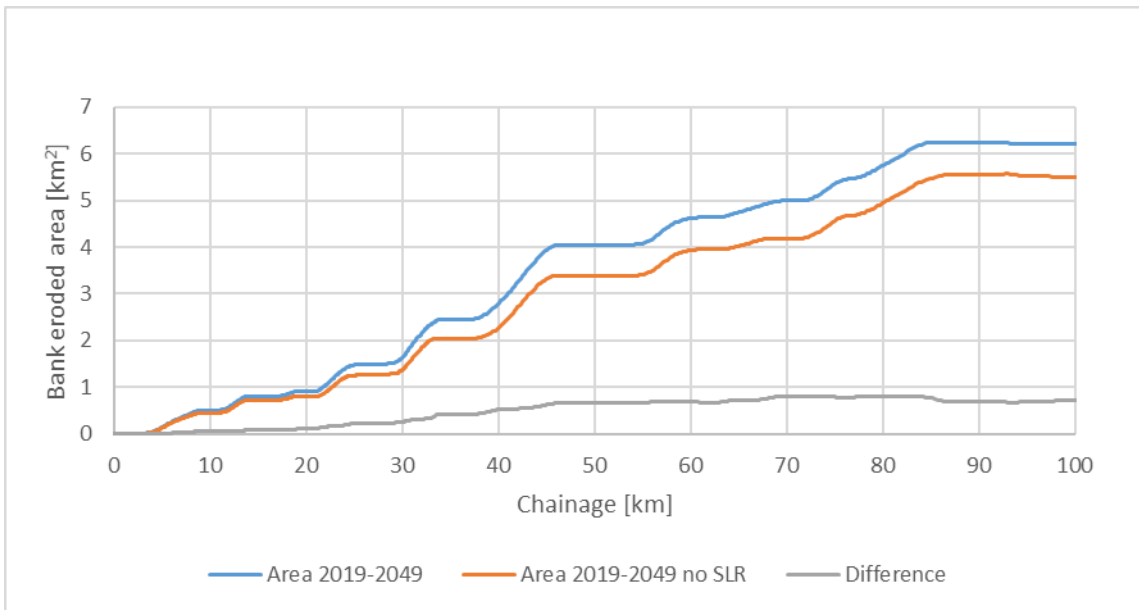


Figure 4-16 East bank eroded areas integrated along the river for the period 2019-2049 with and without climate change.

The climate change impact on bank erosion is quantified by integrating the eroded areas along each bank, see Figure 4-15 and Figure 4-16. These show that climate change causes an increase in bank erosion, mainly in the upstream end, and there is even a small decrease in the eroded area difference in the downstream end.

Climate change clearly causes increased bank erosion, and the reason is that the tidal discharges increase along the river. The integrated areas show that climate change causes the eroded area to increase by 9% along the western bank and 13% along the eastern bank.

## 4.4 Impact of bank protection

Bank protection was tested for the eroding bank located at Polder 39/2.

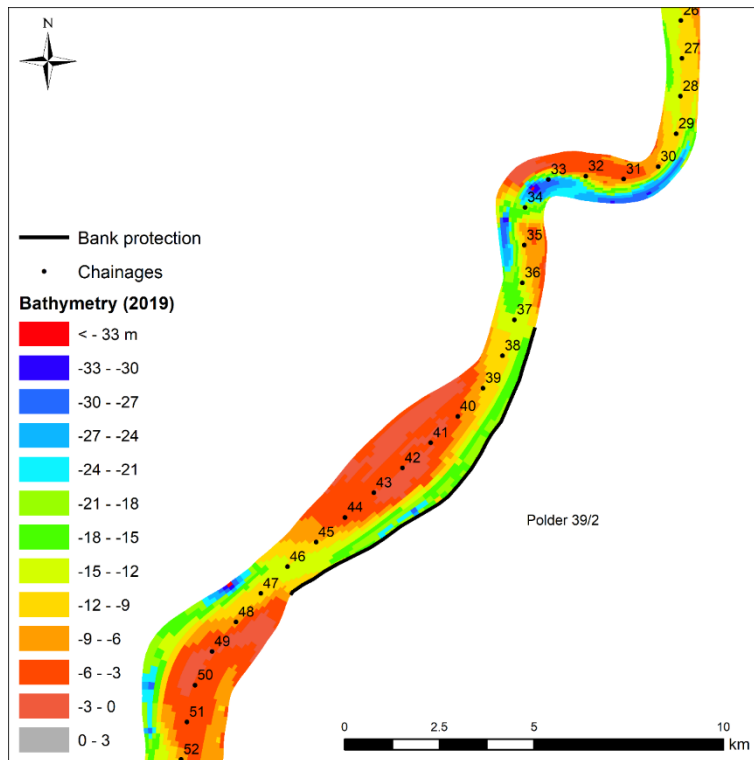


Figure 4-17 Bank protection added along the Polder 39/2 east bank.

The scenario is illustrated in Figure 4-17 showing the bank protection covering the eroding bank along Polder 39/2. This bank is protected in the scenario, while all other banks are allowed to erode.

Two simulations were conducted:

- Existing conditions 2019-2034
- Protected bank 2019-2034

The simulations were conducted without updating the curvilinear grid due to bank erosion, while the bank erosion material was still included in the sediment budget by adding it to the near-bank concentration during the simulation. This was done to make it easy to compare the simulated bathymetries, which is otherwise difficult to do with moving grids.

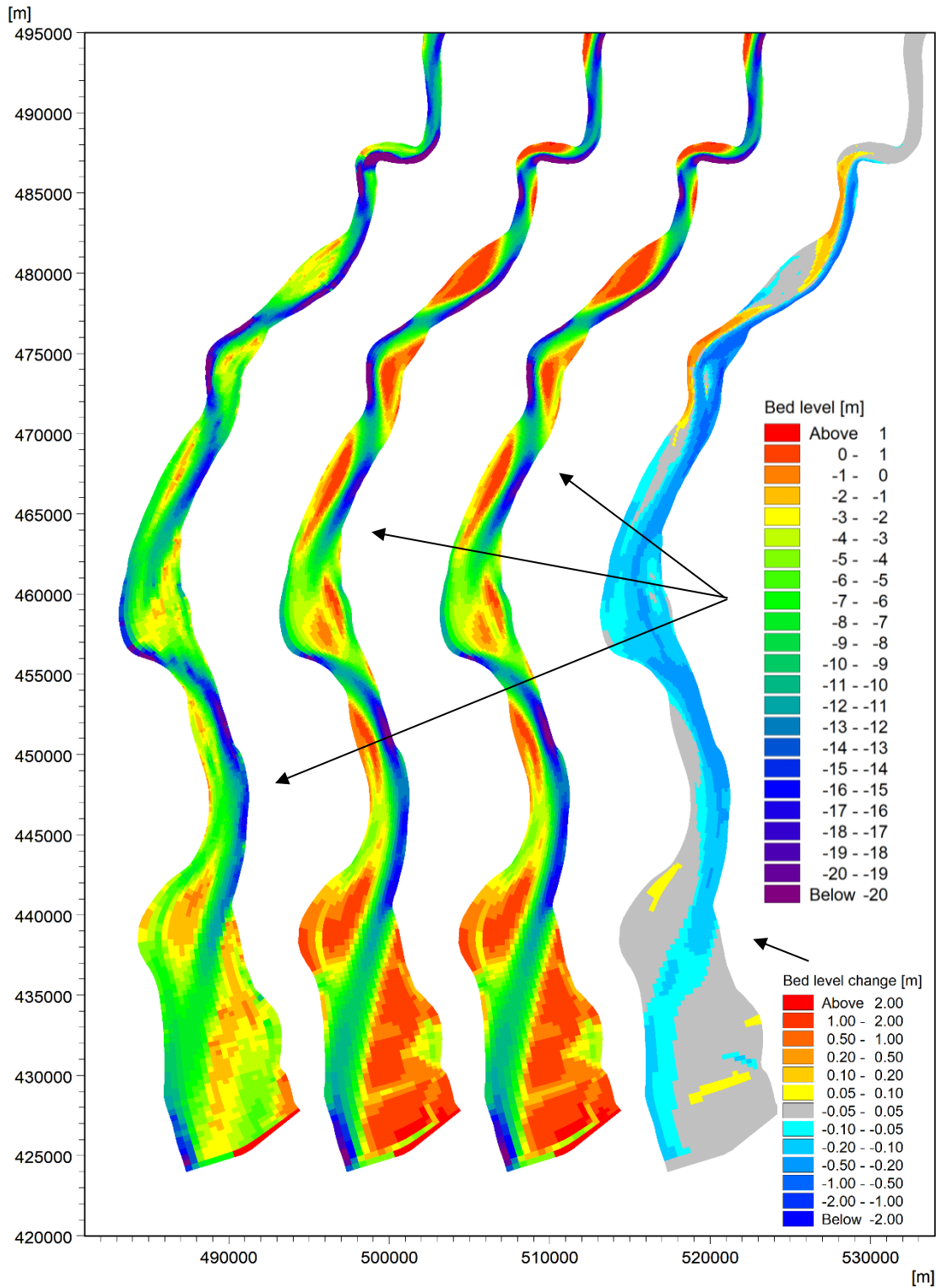


Figure 4-18 Bathymetries and induced bed level changes. From left: 1) observed 2019 bathymetry (initial condition), 2) simulated 2034 bathymetry, 3) simulated 2034 bathymetry with protected bank, 4) induced bed level changes in 2034 caused by bank protection.

The simulated bathymetries and induced bed level changes are shown in Figure 4-18.

Induced bed level changes mean the bathymetry difference caused by the bank protection works, which is calculated as the difference between the 2034 bathymetry with bank protection and the 2034 bathymetry without bank protection.

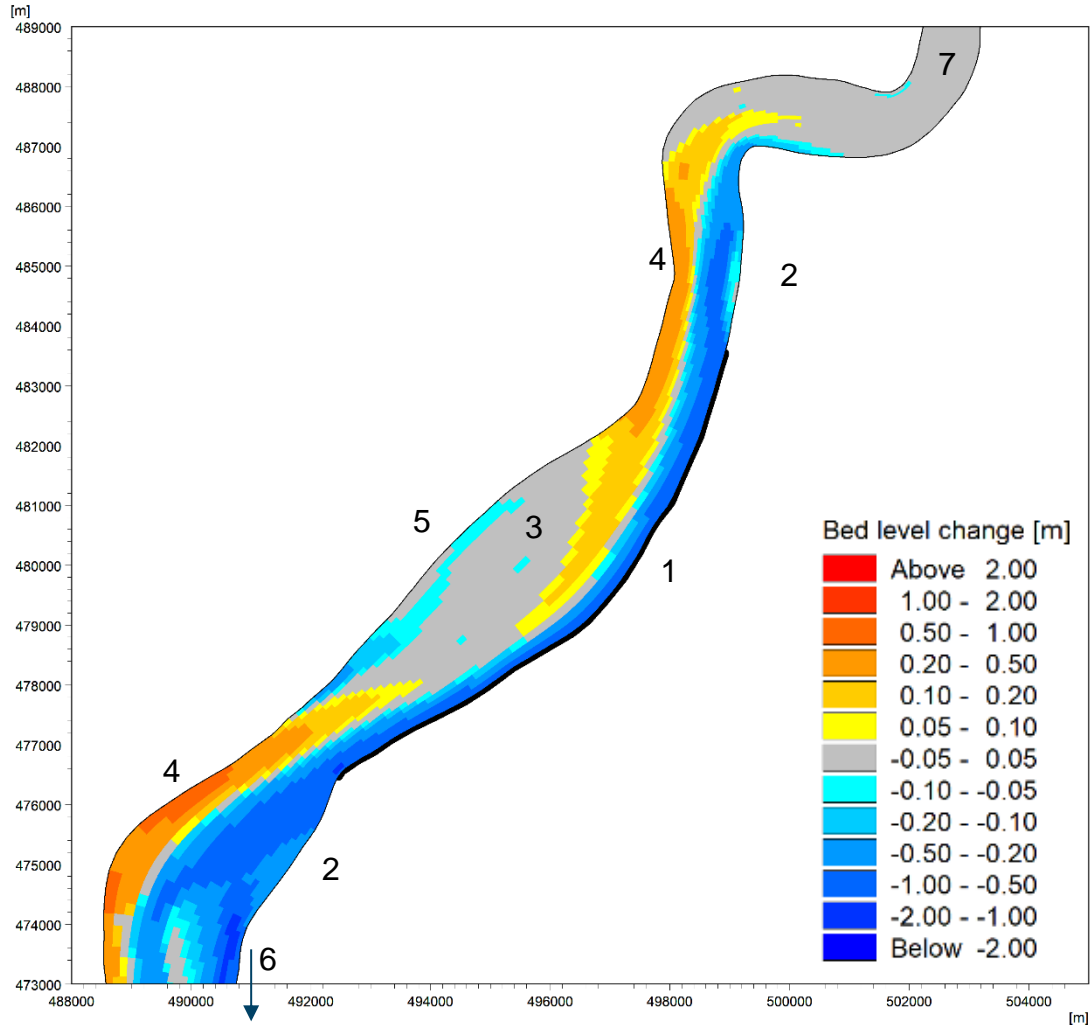


Figure 4-19 Simulated induced bed level changes 2019-2034 caused by bank protection shown in the black line along the bank. This zoom is used for discussing the impacts.

There are several important observations to be made from the bathymetries and especially the induced bed level changes, refer to Figure 4-19 for the numbers in the list:

1. Bank protection causes a reduction in the bed level along the bank.
2. Bank protection causes scouring of the two bars located along the same bank upstream and downstream of the protected bank.
3. Bank protection causes sedimentation on the shoal located opposite of the bank.
4. Bank protection causes sedimentation in the two outer bends located upstream and downstream of the protected bank.
5. Bank protection causes the flood channel opposite of the protected bank to scour.
6. Bank protection causes scouring in the river main channel all the way down to the Bay of Bengal.
7. The impact of bank protection has very short upstream impact, ending before the very sharp bend.



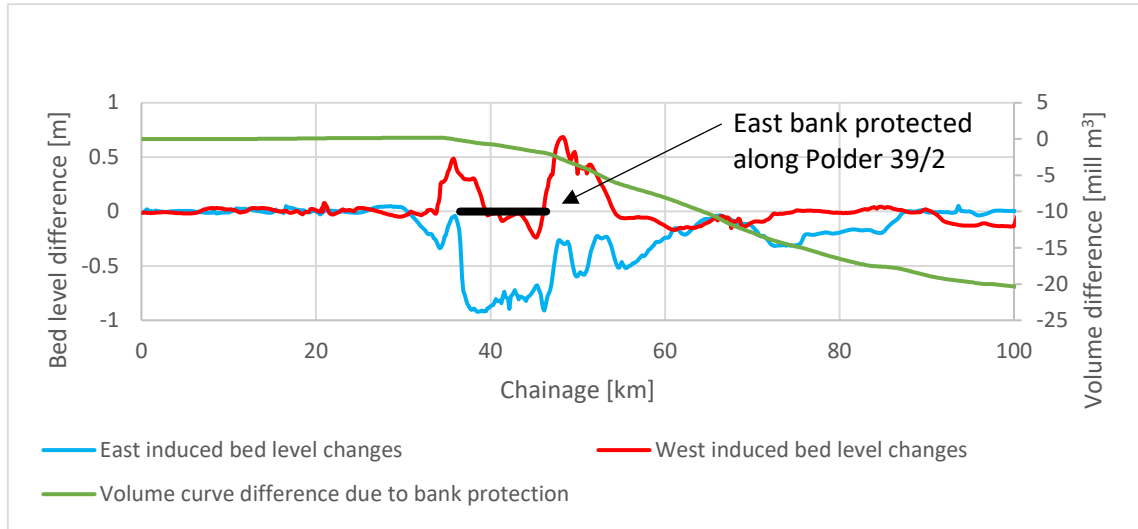


Figure 4-20 Induced bed level changes along the east and west banks.

Figure 4-20 shows the induced bed level changes extracted along the two banks. The complex pattern can also be seen from this figure. It is seen that bank protection causes about 1 m reduction in the bed level along the bank, while the increase in bed levels in the two opposite outer bends upstream and downstream is around half the reduction in bed levels.

The 1 m reduction in bed level is not insignificant, and it should be kept in mind that this is only for protecting this specific bank from erosion. If more banks are protected, the impacts accumulate in the downstream direction, although not with 100% carried over to the next bank.

The volume difference between the two scenarios was also calculated and shown in this figure. The volume deficit extends all the way to the Bay of Bengal, and the volume difference at the downstream boundary is around 20 mill m<sup>3</sup>, which is what can be estimated as the bank volume that would not be eroded due to bank protection.

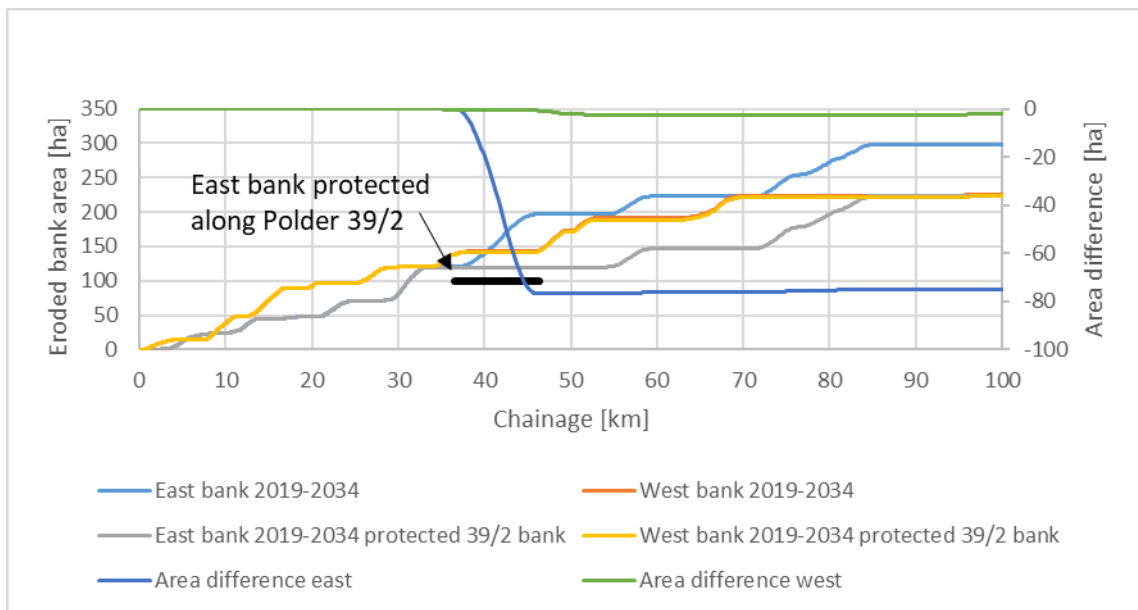


Figure 4-21 Bank erosion integrated in eroded areas along the east and west bank as well as differences between the scenarios.

The bank erosion impacts are illustrated in Figure 4-21. Since the changes to the bank erosion magnitude are very small, the impacts are better illustrated by integrating the eroded areas. The area not eroded in the period 2019-2034 is around 77 ha, while all other changes to eroded areas are very small.

It is worth noting that a 20 cm bed level difference does not have much impact on bank erosion.

In summary, bank protection causes 1 m reduction in the bed level along the bank. There are several complex local induced bathymetry changes associated with protecting one bank, in particular the upstream and downstream eroding banks appear to benefit from bank protection, but it is likely that this behaviour varies with the width of the river. Since Baleswar is very wide, bank protection will cause scouring of the bars upstream and downstream of the eroding bank, which appears to be the key to the observed pattern.

The upstream impact of bank protection extends only by a short distance, while protecting just one bank can be felt all the way down to the Bay of Bengal.

The results suggest that protecting one bank is beneficial to some nearby banks, while further downstream the impact is always negative. However, the impact on bed levels is clearly larger than the impact on bank erosion.

## 4.5 Impact of protecting all banks

In this section, the extreme case when all banks are protected from erosion is tested. The purpose is to determine the potential for reducing bed levels. Although the test case is extreme, the results underline the importance of taking the cascading induced scour effect into account when protecting banks from erosion. Protecting one bank from erosion will reduce local bed levels as well as downstream bed levels.

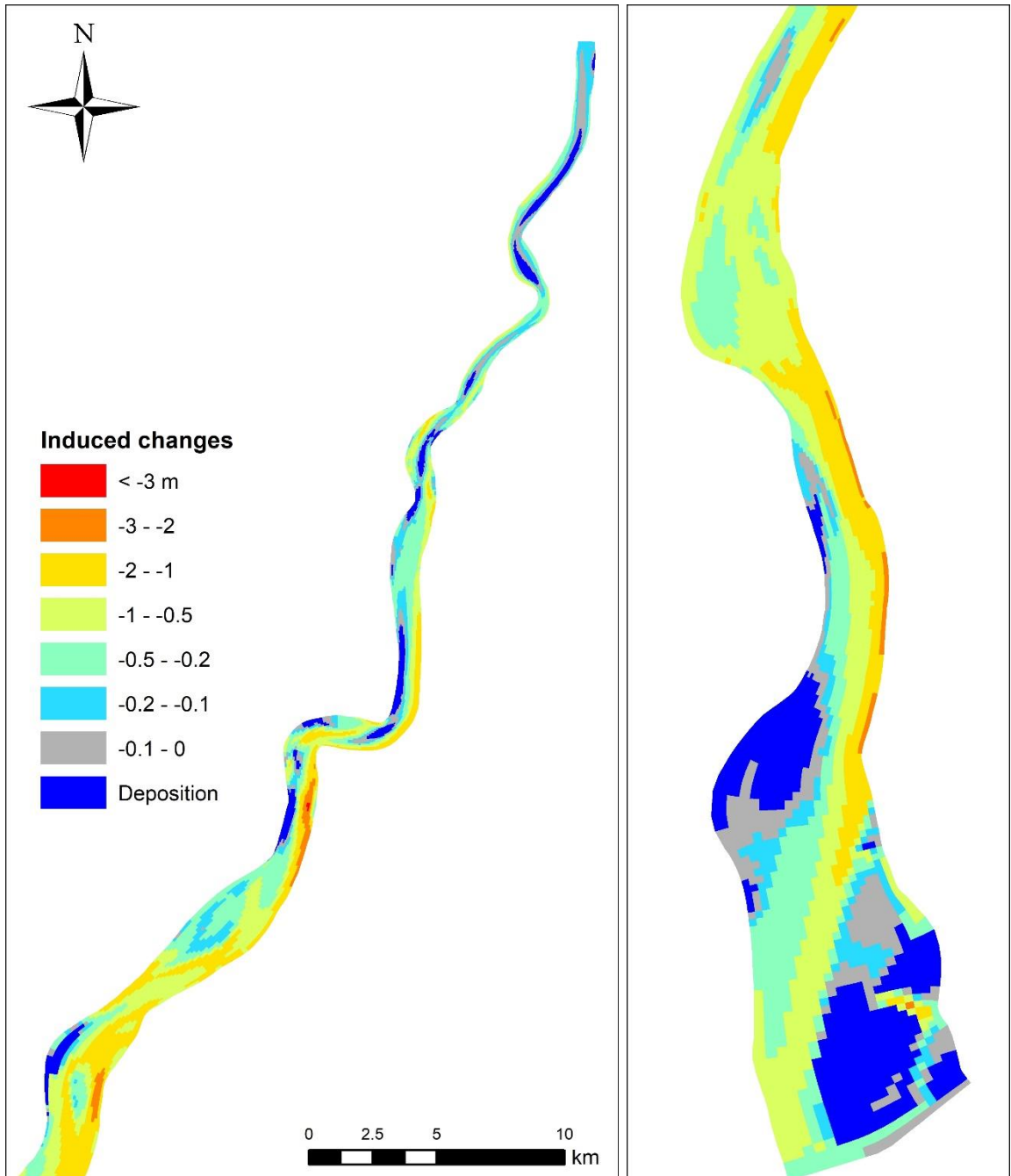


Figure 4-22 Induced bed level changes 2019-2034 caused by protecting all banks from erosion.

The spatial distribution of the induced bed level changes caused by protecting all banks from erosion is shown in Figure 4-22, while the variations along the banks are shown in Figure 4-23 and Figure 4-24.

The spatial distribution is quite complex but with some general trends, such as often increasing bed levels on bars opposite of protected banks combined with reduced bed levels in the deep channel along the bank.

The variations along the banks show general reductions of the bed levels up to 2 m, and the effect increased in the downstream direction due the cascading removal of sediment supply from bank erosion. The cascading effect leads to about twice the reduction in bed levels compared to a single protected bank.

The analysis gives a range of 1-2 m induced scour, depending on how many banks are protected.

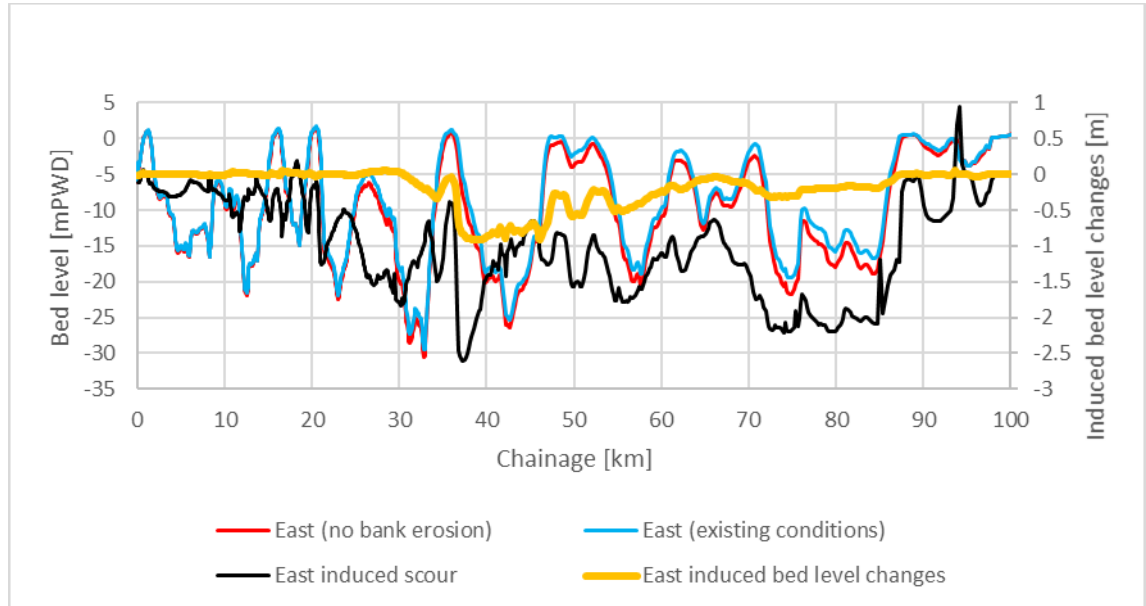


Figure 4-23 Simulated bed levels in 2034 along the east bank as well as the induced scour equal to the reduction in bed levels caused by protecting all banks from erosion. The induced bed level changes based on protecting one eroding bank are shown for reference.

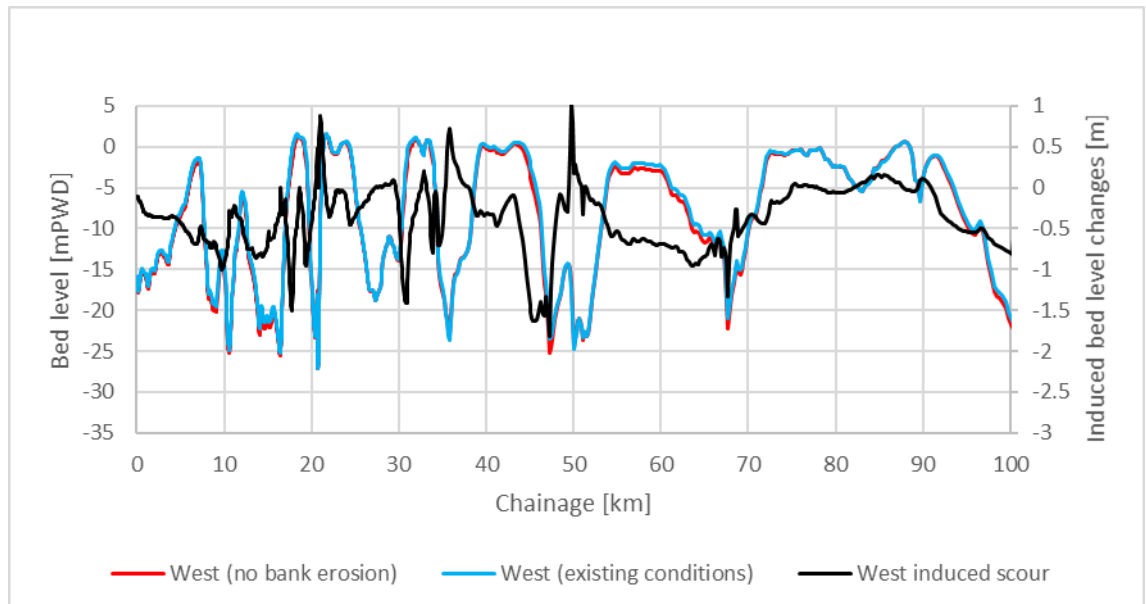


Figure 4-24 Simulated bed levels in 2034 along the west bank as well as the induced scour equal to the reduction in bed levels caused by protecting all banks from erosion.

## 4.6 Dredging of a large shoal

A good location for shoals dredging is found at the same location used for bank protection due to the large bar found opposite of the eroding bank, see Figure 4-25.

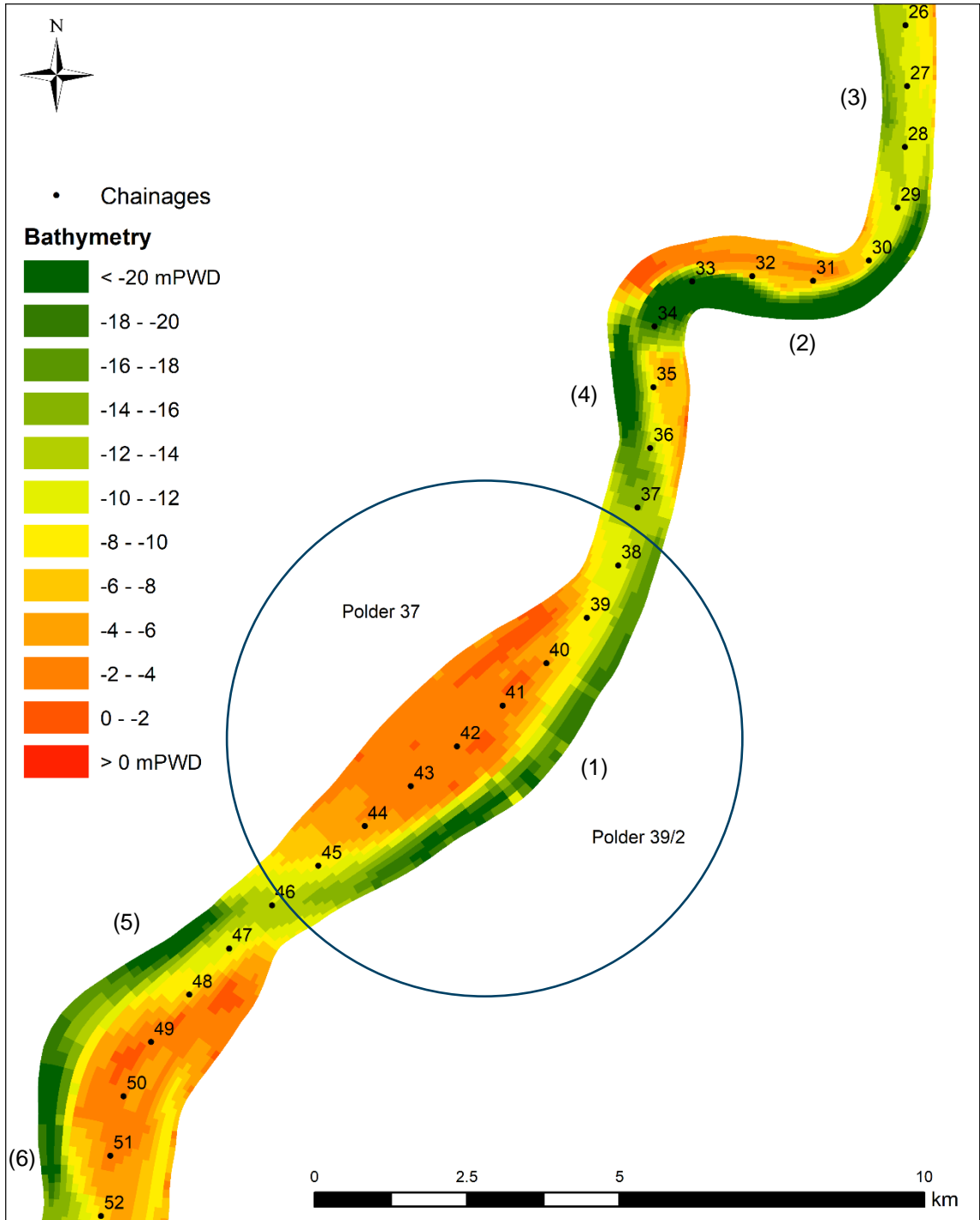


Figure 4-25 The large bar opposite of the east bank eroding Polder 39/2 was selected for dredging scenarios. Individual eroding banks in this reach are marked with numbers in brackets.

Four dredging scenarios were tested using the model:

A: Dredge the bar to -10 mPWD (54 mill m<sup>3</sup>), no backfilling of spoils

B: Same as A, but the spoils are dumped in the deeper channels in the vicinity of the bar to elevation -11.78 mPWD

C: Dredge only part of the bar and the flood channel to -10 mPWD (23.74 mill m<sup>3</sup>), dump spoils in deep channel east to elevation -10.58 mPWD

D: More dredging of the bar (22.46 mill m<sup>3</sup>), no flood channel dredging, dump spoils in outer deep channel to elevation -10.89 mPWD

When backfilling, the fixed backfilling elevation was determined to match the dredged volume.

A baseline simulation was conducted as reference for the analysis of the results.

The simulation results show the following, refer to Figure 4-26 to Figure 4-29.

The local dredging operation is beneficial also to the upstream and downstream eroding banks. This appears to be caused by the tendency of the flow to erode the upstream and downstream bars.

It is very important to dump spoils in the outer deep channel to 1) attract flow to the deeper part of the cross-section at the edge of the bar, 2) deflect flow away from the outer channel. Part of the reason for this could be that the bank erosion formula involves the near-bank depth, so reducing this depth has a large impact.

The system recovers very slowly from this dredging operation, which could be more pronounced for an eroding bank of this character for which the outer bend is already having an unfavourable flow path, and due to the relatively low curvature of the flow cutting through the bar, the secondary flow effect on the bar recovery is relatively weak.

The bar grows back over time due to 1) helical flow, 2) flow deflection from the bar, 3) flow attraction to the deep channel. The impact of helical flow on the silt transport is relatively small, which can be seen in the simulation results as the deep channel is not migrating towards the outer bank.

Scenarios C and D show that the bar located east upstream of the eroding bank will extend into the existing deep channel due to dredging. C and D are similar.

The only thing that really matters is to bring silt the short distance from the outer edge of the existing bar to the deep channel. This realigns the flow, and it appears to last for a long time.

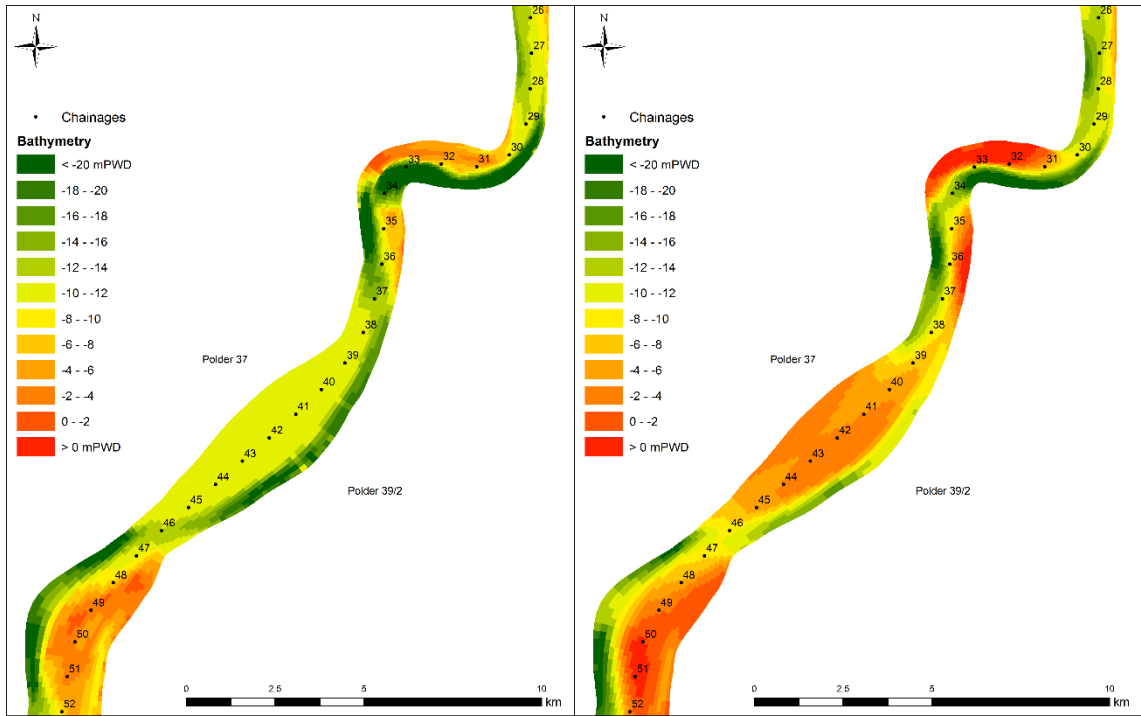


Figure 4-26 Scenario A initial (2019) bathymetry (left) and simulated bathymetry after 15 years (right).

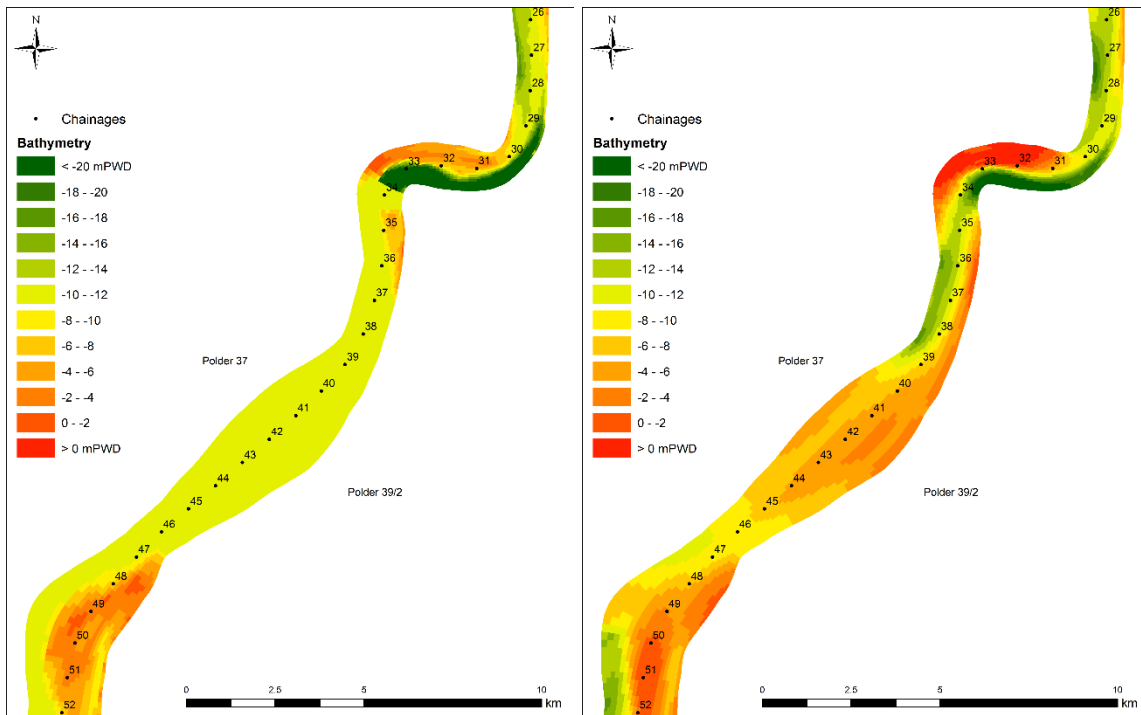


Figure 4-27 Scenario B initial (2019) bathymetry (left) and simulated bathymetry after 15 years (right).

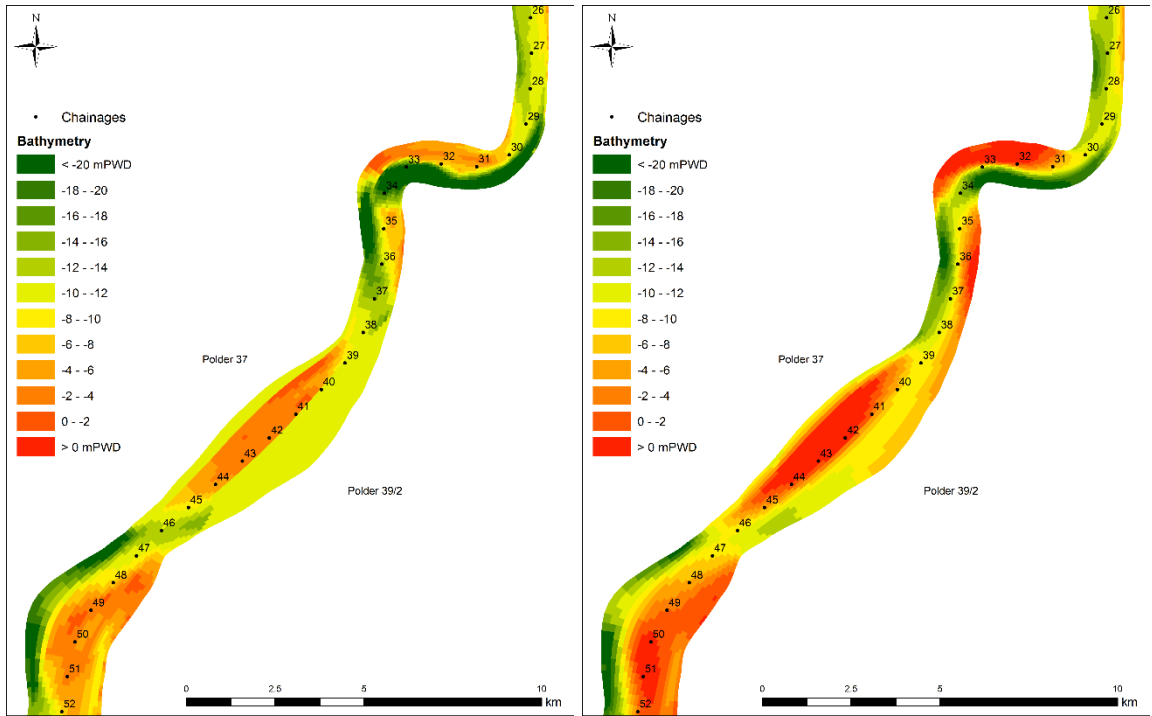


Figure 4-28 Scenario C initial (2019) bathymetry (left) and simulated bathymetry after 15 years (right).

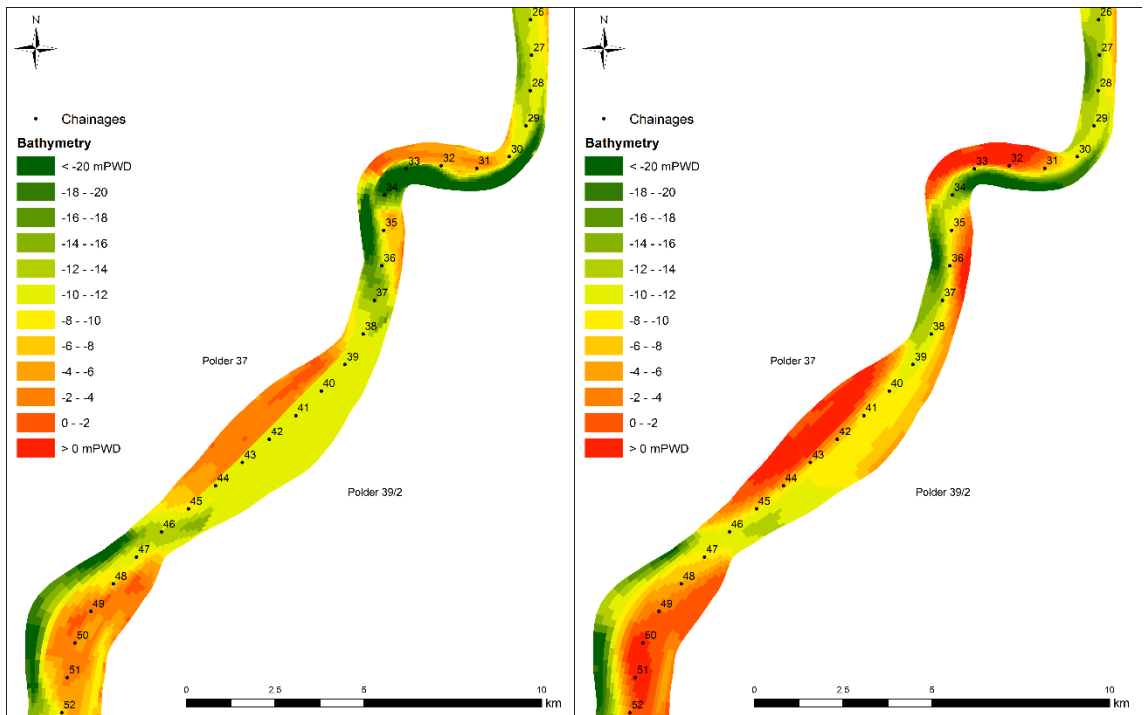


Figure 4-29 Scenario D initial (2019) bathymetry (left) and simulated bathymetry after 15 years (right).



In the following it is reconsidered whether dumping spoils into the deep channels is a realistic option. It is clear from the analysis that this process is very important, but it might not work that well in reality. Firstly, there could be practical problems getting silt dropped at the water surface to deposit in the deep channels. Secondly, the silt will be freshly deposited in the deep channel, which may make the silt easier to resuspend. The deposition can be assessed by using the traditional deposition length scale:

$$L = h * U/w_s$$

Where L is the length over which deposition takes place, h the water depth, U flow velocity and  $w_s$  sediment (silt 1 mm/s) fall velocity. Typical values give:

$$L = 20 \text{ m} * 1 \text{ m/s} / 0.001 \text{ m/s} = 20,000 \text{ m}$$

Unfortunately, this is much longer than the longitudinal extent of the outer channel. Hence it is not practical to simply dump the spoils into the outer channel. The model results show that dumping of spoils is critical in terms of ensuring that the flow does not concentrate in the channel, and instead develops what looks like a bend cut through the outer bar.

The tidal flow length also matters and can be estimated from the flow velocity and the tidal period:

$$L_{\text{tide}} = U * T$$

With the tide going in the same direction for 6 hours with 1 m/s, the sediment particles will move around 20 km before the flow reverses, i.e. same length scale as for deposition of the material.

The results show that the simple method of just dumping the spoils is not practical. The spoils need to be deposited in the outer channel by other means, such as filling textile bags (e.g. jute) with spoils before dumping in the other channel. This also protects the outer channel bed from scouring and acts essentially to prevent bend scour from reemerging, which is known as an effective, but also expensive methodology for preventing bank erosion and ensuring navigation (albeit not relevant here).

The impacts of the dredging scenarios on bank erosion are illustrated in Figure 4-30 and Figure 4-31.

The biggest difference is obviously along the target eroding bank marked as (1), where all four dredging scenarios lead to reduced erosion but with Scenario A only reducing erosion by around 50%, while Scenario B almost eliminates erosion and Scenario C and Scenario D significantly reduce erosion.

It is also clear that Scenario B reduces erosion along the upstream and downstream western banks. This is caused by the dumping of spoils in Scenario B in the deep channels along these banks. Scenarios C and D still cause a reduction of bank erosion along the downstream bank due to more water flowing over the bar east of the eroding bank.

All scenarios except D tend to make the west bank erode (downstream of the (4) mark). This is caused by flow concentration along the west bank. In Scenario C a flood channel was added to take flow away from the eastern channel, which gives a slight increase in bank erosion to the west. This suggests that Scenario C is not recommendable, while Scenario D is the best choice.

It must be understood when reading these reports that the mechanics of bank erosion is embedded in the bank erosion formula. The adopted formula has a strong influence on the near-bank water depth, which is also manifested in reductions of the near-bank water depth yielding strong reductions in bank erosion. The bank erosion formula also adopts the near-bank velocity, which is used for estimating the excess velocity. Hence, scenarios that push flow away from the bank and

reduces the near-bank water depth will be evaluated as highly effective for reducing bank erosion. Many bank erosion models were considered during the model development phase, e.g. Mosselman (1995) postulated a formula based solely on the near-bank height, which is equivalent to the near-bank water depth. If that formula had been used in the study (and it should be noted that it had the best calibration for the 2011-2019 observed bank erosion), scenarios aimed at reducing bank erosion would also be evaluated as positive if the near-bank water depth was reduced. It is not a given that the adopted bank erosion formula represents the bank erosion mechanics correctly, but the observations show that the bank height from the bathymetry to the bank elevation is very important.

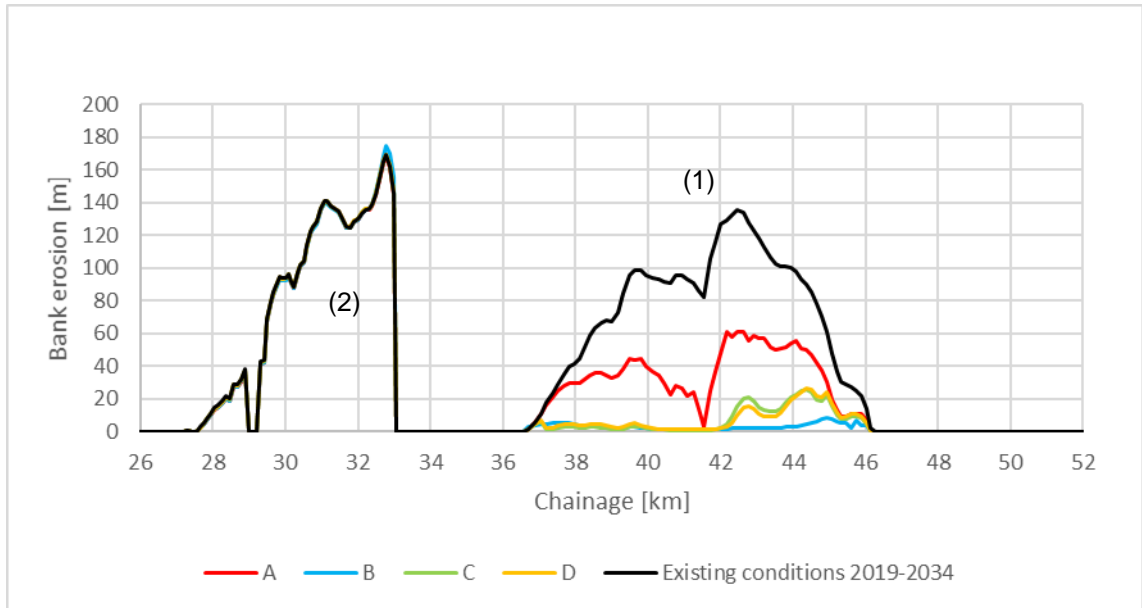


Figure 4-30 Simulated bank erosion along eastern bank 2019-2034 for existing conditions and dredging scenarios A, B, C, D. The numbers in brackets refer to the specific eroding banks shown in Figure 4-25.

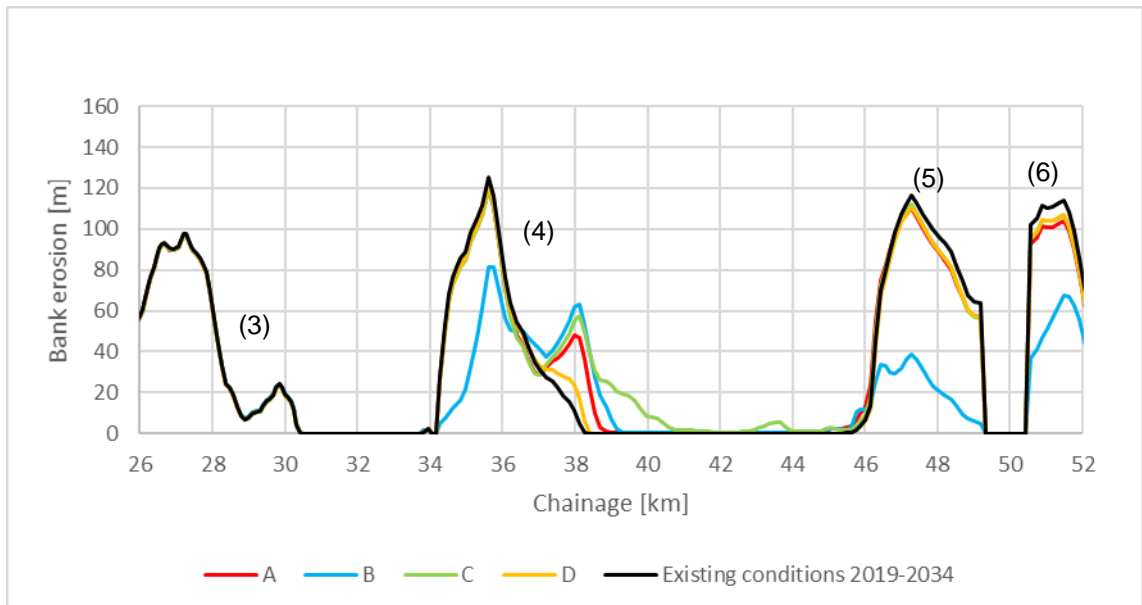


Figure 4-31 Simulated bank erosion along western bank 2019-2034 for existing conditions and dredging scenarios A, B, C, D. The numbers in brackets refer to the specific eroding banks shown in Figure 4-25.

## 5 Conclusions

The present report documents the development of the MIKE 21C model of the Baleswar River.

Several historical bathymetry datasets exist for the Baleswar River, namely 2009, 2011, 2015 and 2019. The 2009 bathymetry data was too sparse for 2D contouring, and there was a gap in the 2015 coverage, while the 2011 and 2019 datasets had similar coverage and resolution. The available bathymetry data was suitable for 2011-2019 hindcasting, while the 2015 data can be used as an intermediate between the 2011 and 2019 bathymetries, although the gap does not allow using the bathymetry in a model (but it can be compared to). This makes Baleswar River the best bathymetry data covered river in the project (most rivers have 2011 and 2019 bathymetry data).

Hydrometric data in the shape of water levels and discharges was used for calibrating the hydrodynamic model. A lot of data was available for the Baleswar River, which has been studied many times.

Several (21) bed samples were available from the Baleswar River. One single bed sample located furthest downstream shows dominating sand, while the bed samples in general show consistently that the riverbed is silty with a small amount of sand, typically below 10%. There is a lack of bed samples upstream of the very sharp bend (located just upstream of Charkhali), and the resistance calibration implies that the upstream reach could be sandy, but there are no bed samples to confirm this. Based on the available bed samples, a 1-fraction silt model was selected as the most appropriate formulation.

The Baleswar River is also well covered with respect to suspended sediment samples downstream of the very sharp bend. The suspended samples show some correlation between discharge and sediment concentration, especially for ebb conditions, even though the suspended sediment samples are from different locations. The Baleswar River also has particle size distribution data for the suspended sediment, which show that the sediment in suspension is generally finer than the bed samples. The suspended sediment fall velocity is an order of magnitude smaller than the fall velocity for the bed samples. This implies that it is difficult to model the sediment in the Baleswar River with a single representative fall velocity (single fraction model) and match both bed level changes and concentrations. In such cases matching bed levels should be the focus, while less emphasis should be on the sediment concentrations, which include wash-load.

Bank erosion was processed from Landsat images from 1988-2019. The historical bank lines show very consistent and systematic bank erosion for the whole period. For most banks along the Baleswar River it was observed that bank lines, which were eroding in 1988 also eroded in 2019, and the annual bank erosion rates are similar for the banks, both spatially and temporally. The bank lines were processed into erosion as a function of chainage along the west and east banks, and it was demonstrated that bank erosion correlates extremely well with bed levels in the way that essentially all eroding banks have deep water and are in outer bends. The sediment volumes associated with bank erosion are not insignificant compared to volumes associated with bed levels, but bank erosion clearly is not a significant contributor to the sediment budget.

A curvilinear grid was generated for the Baleswar River with 792x20 grid points. The 2011 bathymetry data was contoured on this grid. A separate 2019 grid with the same number of grid points was developed from the 2019 bank lines with the 2019 bathymetry interpolated.

The boundary conditions consisted of upstream discharge, several side channels and downstream water level time-series. At the time of model development, no continuous time-series of water level and flow boundary conditions were available for the period 2011-2019. Instead, the time-series from 2011 were repeated 8 times and used in the model to represent the 8 years of the period 2011-2019.

The hydrodynamic model calibration and validation show that the Baleswar River model performs satisfactorily. There are some issues, such as discrepancies between the MIKE 21C and SWRM when comparing 2016. However, the model calibration is generally very satisfactory.

Calibration was initially explored with the suspended sediment concentration as the main target, but this was later deemphasized because a significant part of the measured concentration is wash-load that is not included in the modelling. Comparisons to observed suspended sediment concentrations show underprediction, which was also expected because the observations show that suspended sediment has significantly smaller fall velocity compared to the bed samples, while the bed samples define the adopted fall velocity.

The cornerstone of the morphological calibration is a morphological hindcast from 2011-2019. Bathymetry data was also available for 2015 for Baleswar River, which was used as additional check of the model calibration. The comparison to observed bed levels shows reasonable agreement for both 2015 and 2019. The period 2011-2019 was characterized by significant sedimentation, while 2009-2011 was characterized by scouring. The Baleswar River is clearly very dynamic and changing all the time. The changes to the river are driven by boundary conditions.

Bank erosion was simulated using almost the same formula used for other rivers in the project. Bank erosion hindcasting from 2011-2019 showed good agreement with the observations, with the correct banks eroding and the magnitude correctly reproduced. However, some banks are poorly reproduced, notably one of the most important eroding banks along the Baleswar River, namely the west bank along Polder 35/1. For this important bank it is suspected that the velocity distribution has a lot of influence, but no ADCP data available for the model calibration.

## 5.1 Recommended future data collection

The following data is generally missing for the Baleswar River:

- Bed samples should be collected upstream of the very sharp bend at the Baleswar River confluence. Currently there are no bed samples at all upstream. It can be speculated from the flow resistance that the upstream is mixed sand/silt, which require many bed samples for determining the spatial pattern.
- Suspended sediment samples should be collected at the upstream end (Swarupkati), including particle size distribution data.
- Suspended sediment samples collected in the Baleswar River should generally include particle size distributions.
- ADCP data should be measured in riverbends to improve understanding of the velocity distributions. The data should be processed into velocity profiles and not just discharges.
- Bank material samples, including particle sizes and porosities, should be collected for the Baleswar River. At present no observations are available.

It is noted that IWM regularly collect ADCP data in the rivers. However, for convenience, the ADCP profiles are usually collected in straight reaches and processed into discharges. Hence the capability and expertise within ADCP data collection is already available, while the suggestion made in this report is to use the capability in a slightly different way by collecting the ADCP data in specific sharp bends and post-process the ADCP data into discharges (as usual) and depth-integrated velocity fields.

It can be speculated that the anticipated sandy riverbed upstream of the very sharp bend is partially dune covered. Traditional single beam echo-sounder is normally adopted in the rivers, and single beam is sufficient for the full bathymetries. However, local multibeam echo-sounder data is very valuable (especially for identifying dune fields, which cannot be done from single beam data perpendicular to the flow direction), and the capability is readily available at IWM.

## 5.2 Recommended model improvements

Some of the eroding banks in Baleswar River are poorly predicted by the model. There is currently no good explanation for this, but some of those banks are of high importance for polders, and model improvement are hence valuable.

It is possible that the upstream end is sandy, which should be accounted for. If the upstream end is sandy, a dune model should be applied to correctly capture flow deflection from the sandy bars.

## 5.3 Conclusions from the scenario simulations

The developed model was applied for the following scenario simulations:

- Scenario simulations conducted before the final model was ready
- Bank erosion projection 30 years into the future
- Impact of climate change 30 years into the future
- Impact of bank protection on bed levels
- Dredging of a shoal to reduce bank erosion

The older scenario simulations were reported for the sake of completeness. The simulations showed that dredging of a shoal could reduce bank erosion along the opposite bank, and backfilling was surprisingly slow.

Bank projection 30 years into the future showed no qualitative changes to the river bathymetry, except at the Bogi channel where a bend cut is predicted to develop. This particular location has been discussed with the CEIP DTL. Future bank erosion patterns are generally similar in the Baleswar River.

The impact of climate change was quantified using the MIKE 21C model over the period 2019-2049. The SWRM shows that climate change leads to increased tidal amplitude in the Baleswar River, especially during the monsoon. Climate change clearly causes increased bank erosion, and the reason is that the tidal discharges increase along the river. The integrated areas show that climate change causes the eroded area to increase by 9% along the western bank and 13% along the eastern bank.

Bank protection will always lead to scouring due to the removal of eroded bank material from the sediment budget. The spatial distribution of the induced scour is quite complex, but with some general trends, such as often increasing bed levels on bars opposite of protected banks combined with reduced bed levels in the deep channel along the bank. The analysis gives a range of 1-2 m induced scour, depending on how many banks are protected.

The most important scenario for the Baleswar River was the conceptual test of dredging of a shoal to reduce bank erosion. The conceptual test was conducted for a long eroding eastern bank at Polder 39/2. The results showed that dredging of the shoal can effectively eliminate bank erosion along this eastern bank. The by far strongest bank erosion reduction is achieved by dumping spoils in the outer (eroding) channel. However, this is practically problematic due to the settling length scale of the silt being longer than the longitudinal extent of the channel. The recovery of the system back to the outer channel eroding the bank appears to be very slow. The settling length issue must be addressed if the method is to work, and one proposal is to use textile bags made out of e.g. locally abundant jute, which can be filled and dumped into the outer channel. This resembles traditional methods used in outer bends to suppress bend scour.

The model results are very encouraging, but the predictions could be a bit too optimistic. During the model development, two distinctly different silt deposition models were explored: 1) critical shear stress limit (which was adopted) and 2) always deposition. The adopted critical shear stress for deposition is more traditional, while the always deposition approach is considered modern. The critical deposition limit ( $0.1 \text{ N/m}^2$ ) was found to work best in the hindcast simulations 2011-2019, while in those simulations the always deposition approach gave rise to a lot of bar activity, which eventually caused the hindcast to yield less satisfactory results, typically with bars growing too big and channels too deep.

In the case where a bar is partly dredged away, it can be speculated that the always deposition approach will lead to faster recovery of the bar elevations.

The analysis suggests that the bar regrowth in the model simulations is uncertain. This can be tested by adjusting the model to the alternative calibration. However, this is a sizeable task, as it is not enough to just switch to always deposition; the erosion rates and inflow concentrations also need to be readjusted.

Flow deflection from bars also plays a major role in regrowing the bars after dredging. In the Baleswar it was found that a constant Manning  $M$  worked better than a model involving higher resistance on bars, which would lead to too much bar formation. Hence, the model behaviour does suggest that the obtained results are realistic, at least in terms of bar formation, but the calibration of the model using a hindcast can be done in different ways, i.e. varying flow deflection and silt deposition model leading to similar hindcast results, but potentially different bar regrowth.

## 6 References

Hasegawa, K. (1989). *Universal bank erosion coefficient for meandering rivers*. Journal of Hydraulic Engineering, 115(6), 744-765.

Krumbein, W. C. (1934). *Size frequency distributions of sediments*. Journal of Sedimentary Petrology. 2 (4).

Mehta, A. J., Hayter, E. J., Parker, W. R., Krone, R. B., & Teeter, A. M. (1989). *Cohesive sediment transport*. I: Process description. Journal of Hydraulic Engineering, 115(8), 1076-1093.

Mosselman, E. (1995). *A review of mathematical models of river planform changes*. Earth Surface Processes and Landforms, 20(7), 661-670.

